CONSTRUCTION WITH HOLLOW STEEL SECTIONS

1

DESIGN GUIDE

FOR CIRCULAR HOLLOW SECTION (CHS) JOINTS UNDER PREDOMINANTLY STATIC LOADING

J. Wardenier, Y. Kurobane, J.A. Packer, G.J. van der Vegte and X.-L. Zhao

Second Edition

LSS Verlag

CONSTRUCTION WITH HOLLOW STEEL SECTIONS

1

DESIGN GUIDE

FOR CIRCULAR HOLLOW SECTION (CHS) JOINTS UNDER PREDOMINANTLY STATIC LOADING

J. Wardenier, Y. Kurobane, J.A. Packer, G.J. van der Vegte and X.-L. Zhao

Second Edition

DESIGN GUIDE

FOR CIRCULAR HOLLOW SECTION (CHS) JOINTS UNDER PREDOMINANTLY STATIC LOADING

CONSTRUCTION WITH HOLLOW STEEL SECTIONS

Edited by: Comité International pour Ie Développement et l'Étude de la Construction Tubulaire

Authors: Jaap Wardenier, Delft University of Technology, The Netherlands and National University of Singapore, Singapore
Yoshiaki Kurobane, Kumamoto University, Japan
Jeffrey A. Packer, University of Toronto, Canada
Addie van der Vegte, Delft University of Technology, The Netherlands
Xiao-Ling Zhao, Monash University, Australia

DESIGN GUIDE

FOR CIRCULAR HOLLOW SECTION (CHS) JOINTS UNDER PREDOMINANTLY STATIC LOADING

Jaap Wardenier, Yoshiaki Kurobane, Jeffrey A. Packer,
Addie van der Vegte and Xiao-Ling Zhao

Design guide for circular hollow section (CHS) joints under predominantly static loading /
[ed. by: Comité International pour le Développement et l'Étude de la Construction Tubulaire]
Jaap Wardenier, 2008
(Construction with hollow steel sections)
ISBN 978-3-938817-03-2
NE: Wardenier, Jaap; Comité International pour le Développement et l'Étude de la Construction Tubulaire;
Design guide for circular hollow section (CHS) joints under predominantly static loading

ISBN 978-3-938817-03-2

Preface

The objective of this 2nd edition of the Design Guide No. 1 for circular hollow section (CHS) joints under predominantly static loading is to present the most up-to-date information to designers, teachers and researchers.

Since the first publication of this Design Guide in 1991 additional research results became available and, based on these and additional analyses, the design strength formulae in the recommendations of the International Institute of Welding (IIW) have recently been modified. These recommendations are the basis for the new ISO standard in this field and also for this Design Guide.

However, these new IIW recommendations have not yet been implemented in the various national and international codes, which are still based on the previous 1989 edition of the IIW rules. Therefore, the recommendations in the previous version of (this Design Guide and) the IIW 1989 rules, which are moreover incorporated in Eurocode 3, are also given. Further, the new IIW formulae, the previous IIW (1989) recommended formulae and those in the API (2007) are compared with each other.

Under the general series heading "Construction with Hollow Steel Sections", CIDECT has published the following nine Design Guides, all of which are available in English, French, German and Spanish:

1. Design guide for circular hollow section (CHS) joints under predominantly static loading (1st edition 1991, 2nd edition 2008)

2. Structural stability of hollow sections (1992, reprinted 1996)

3. Design guide for rectangular hollow section (RHS) joints under predominantly static loading (1st edition 1992, 2nd edition 2009)

4. Design guide for structural hollow section columns exposed to fire (1995, reprinted 1996)

5. Design guide for concrete filled hollow section columns under static and seismic loading (1995)

6. Design guide for structural hollow sections in mechanical applications (1995)

7. Design guide for fabrication, assembly and erection of hollow section structures (1998)

8. Design guide for circular and rectangular hollow section welded joints under fatigue loading (2000)

9. Design guide for structural hollow section column connections (2004)

Further, the following books have been published:

"Tubular Structures in Architecture" by Prof. Mick Eekhout (1996) and "Hollow Sections in Structural Applications" by Prof. Jaap Wardenier (2002).

CIDECT wishes to express its sincere thanks to the internationally well-known authors of this Design Guide, Prof. Jaap Wardenier of Delft University of Technology, The Netherlands and National University of Singapore, Singapore, the late Prof. Yoshiaki Kurobane of Kumamoto University, Japan, Prof. Jeffrey Packer of University of Toronto, Canada, Dr. Addie van der Vegte of Delft University of Technology, The Netherlands and Prof. Xiao-Ling Zhao of Monash University, Australia for their willingness to write the 2nd edition of this Design Guide.

CIDECT, 2008

Airport hall with roof structure and columns of CHS

Halls for the Athens Olympic Games (2004) with CHS arches and plate to CHS joints for the cables

CONTENTS

1 Introduction

Many examples in nature demonstrate the excellent properties of the circular hollow section as a structural element in resisting compression, tension, bending and torsion. Further, the circular hollow section has proved to be the best shape for elements subjected to wind-, water- or wave-loading. The circular hollow section combines these characteristics with an architecturally attractive shape. Structures made of hollow sections have a smaller surface area than comparable structures of open sections. This, in combination with the absence of sharp corners, results in better corrosion protection.

These excellent properties should result in light “open” designs with a small number of simple joints in which gussets or stiffening plates can often be eliminated. Since the joint strength is influenced by the geometric properties of the members, optimum design can only be obtained if the designer understands the joint behaviour and takes it into account in the conceptual design. Although the unit material cost of hollow sections is higher than that of open sections, this can be compensated by the lower weight of the construction, smaller painting area for corrosion protection and reduction of fabrication cost by the application of simple joints without stiffening elements. Many examples of structural applications of hollow sections show that tubular structures can economically compete with designs in open sections, see chapter 2.

Over the last thirty five years CIDECT has initiated many research programmes in the field of tubular structures: e.g. in the field of stability, fire protection, wind loading, composite construction, and the static and fatigue behaviour of joints. The results of these investigations are available in extensive reports and have been incorporated into many national and international design recommendations with background information in CIDECT Monographs. Initially, many of these research programmes were a combination of experimental and analytical research. Nowadays, many problems can be solved in a numerical way and the use of the computer opens up new possibilities for developing the understanding of structural behaviour. It is important that the designer understands this behaviour and is aware of the influence of various parameters on structural performance.

This practical Design Guide shows how tubular structures under predominantly static loading should be designed in an optimum way, taking account of the various influencing factors. This Design Guide concentrates on the ultimate limit states design of lattice girders or trusses. Joint resistance formulae are given and also presented in a graphical format, to give the designer a quick insight during conceptual design. The graphical format also allows a quick check of computer calculations afterwards. The design rules for the uniplanar joints satisfy the safety procedures used in the European Community, North America, Australia, Japan and China.

This Design Guide is a 2nd edition and supersedes the 1st edition, with the same title, published by CIDECT in 1991. Where there is overlap in scope, the design recommendations presented herein are in accord with the most recent procedures recommended by the International Institute of Welding (IIW) Sub-commission XV-E (IIW, 2008).

Since the first publication of this Design Guide in 1991 (Wardenier et al., 1991), additional research results became available and, based on these and additional analyses, the design strength formulae in the IIW recommendations (2008) have been modified. These modifications have not yet been included in the various national and international codes, e.g. Eurocode 3. The design strength formulae in these national and international codes are still based on the previous, 1989 edition of the IIW rules.

Generally, the designers have to meet the design rules in the codes. On the other hand, researchers and teachers like to follow the latest developments. In this CIDECT Design Guide No. 1, the formulae and examples given in chapters 1 to 9 are in agreement with the newest formulae of the IIW (2008) rules. However, those of the previous version of (this Design Guide and) the IIW 1989 rules are given in chapter 10. The differences with the previous formulae, as used in the 1st

edition of this Design Guide and adopted in Eurocode 3 and many other codes, are described by Zhao et al. (2008).

Further, in Appendix A, a comparison is given between the new IIW recommended formulae and the previous IIW (1989) design rules, and in Appendix B with the API (2007) design equations.

1.1 Design philosophy and limit states

In designing tubular structures, it is important that the designer considers the joint behaviour right from the beginning. Designing members, e.g. of a girder, based on member loads only may result in undesirable stiffening of joints afterwards. This does not mean that the joints have to be designed in detail at the conceptual design phase. It only means that chord and brace members have to be chosen in such a way that the main governing joint parameters provide an adequate joint strength and an economical fabrication.

Since the design is always a compromise between various requirements, such as static strength, stability, economy in material use, fabrication and maintenance, which are sometimes in conflict with each other, the designer should be aware of the implications of a particular choice.

In common lattice structures (e.g. trusses), about 50% of the material weight is used for the chords in compression, roughly 30% for the chord in tension and about 20% for the web members or braces. This means that with respect to material weight, the chords in compression should likely be optimised to result in thin-walled sections. However, for corrosion protection (painting), the outer surface area should be minimized. Furthermore, joint strength increases with decreasing chord diameter to thickness ratio d_0/t_0 and increasing chord thickness to brace thickness ratio t_0/t_i. As a result, the final diameter to thickness ratio d_0/t_0 for the chord in compression will be a compromise between joint strength and buckling strength of the member and relatively stocky sections will usually be chosen.

For the chord in tension, the diameter to thickness ratio d_0/t_0 should be chosen to be as small as possible. In designing tubular structures the designer should keep in mind that the costs of the structure are significantly influenced by the fabrication costs. This means that cutting, end preparation and welding costs should be minimized. The end profile cutting of tubular members which have to fit other tubular members, is normally done by automatic flame cutting. However, if such equipment is not available, especially for small sized tubular members, other methods do exist, such as single, double or triple plane cuttings as described in the CIDECT Design Guide No. 7 (Dutta et al., 1998).

This Design Guide is written in a limit states design format (also known as LRFD or Load and Resistance Factor Design in the USA). This means that the effect of the factored loads (the specified or unfactored loads multiplied by the appropriate load factors) should not exceed the factored resistance of the joint, which is termed N^* or M^* in this Design Guide. The joint factored resistance expressions, in general, already include appropriate material and joint partial safety factors (γ_M) or joint resistance (or capacity) factors (ϕ). This has been done to avoid interpretation errors, since some international structural steelwork specifications use γ_M values ≥ 1.0 as dividers (e.g. Eurocode 3 (CEN, 2005a, 2005b)), whereas others use ϕ values ≤ 1.0 as multipliers (e.g. in North America, Australasia and Southern Africa). In general, the value of $1/\gamma_M$ is almost equal to ϕ.

Some connection elements which arise in this Design Guide, which are not specific to hollow sections, such as plate material, bolts and welds, need to be designed in accordance with local or regional structural steel specifications. Thus, *additional safety or resistance factors should only be used where indicated.*

If allowable stress design (ASD) or working stress design is used, the joint factored resistance expressions provided herein should, in addition, be divided by an appropriate load factor. A value of 1.5 is recommended by the American Institute of Steel Construction (AISC, 2005).

Joint design in this Design Guide is based on the ultimate limit state (or states), corresponding to the "maximum load carrying capacity". The latter is defined by criteria adopted by the IIW Sub-commission XV-E, namely the lower of:

(a) the ultimate strength of the joint, and
(b) the load corresponding to an ultimate deformation limit.

An out-of-plane deformation of the connecting CHS face, equal to 3% of the CHS connecting face diameter ($0.03d_0$), is generally used as the ultimate deformation limit (Lu et al., 1994) in (b) above. This serves to control joint deformations at both the factored and service load levels, which is often necessary because of the high flexibility of some CHS joints. In general, this ultimate deformation limit also restricts joint service load deformations to $\leq 0.01d_0$. Some design provisions for CHS joints in this Design Guide are based on experiments undertaken in the 1970s, prior to the introduction of this deformation limit and where ultimate deformations may have exceeded $0.03d_0$, although such design formulae have proved to be satisfactory in practice.

1.2 Scope and range of applicability

1.2.1 Limitations on materials

This Design Guide is applicable to both hot-finished and cold-formed steel hollow sections, as well as cold-formed stress-relieved hollow sections. The nominal specified yield strength of hollow sections should not exceed 460 N/mm^2 (MPa). This nominal yield strength refers to the finished tube product and should not be taken larger than $0.8f_u$.

The joint resistances given in this Design Guide are for hollow sections with a nominal yield strength up to 355 N/mm^2. For nominal yield strengths greater than this value, the joint resistances given in this Design Guide should be multiplied by 0.9. On one hand, this provision considers the relatively larger deformations that take place in joints with nominal yield strengths around 450 to 460 N/mm^2, when plastification of the CHS cross section occurs (for large β ratios, it may be conservative); on the other hand, for other joints the deformation/rotation capacity may be lower with yield strengths exceeding 355 N/mm^2. Furthermore, for any formula, the "design yield stress" used for computations should not be taken higher than 0.8 of the nominal ultimate tensile strength. This provision allows for ample connection ductility in cases where punching shear failure or "local yielding of brace or plate" failure govern, since strength formulae for these failure modes are based on the yield stress. For S460 steel hollow sections, the reduction factor of 0.9, combined with the limitation on f_y to $0.8f_u$, results in a total reduction in joint resistance of about 15%, relative to just directly using a yield stress of 460 N/mm^2 (Liu and Wardenier, 2004).

Some codes, e.g. Eurocode 3 (CEN, 2005b) give additional rules for the use of steel S690. These rules prescribe an elastic global analysis for structures with partial-strength joints. Further, a reduction factor of 0.8 to the joint capacity equations has to be used instead of the 0.9 factor which is used for S460.

Hot-dip galvanising of tubes or welded parts of tubular structures provides partial but sudden stress relief of the member or fabricated part. Besides potentially causing deformation of the element, which must be considered and compensated for before galvanising, the selected steel should be suitable for galvanizing (only steels with limited Si contents).

1.2.2 Limitations on geometric parameters

Most of the joint resistance formulae in this Design Guide are subject to a particular "range of validity". This often represents the range of the parameters or variables for which the formulae have been validated, by either experimental or numerical research. In some cases, it represents the bounds within which a particular failure mode will control, thereby making the design process simpler. These restricted ranges are given for each joint type where appropriate in this Design Guide, and several geometric constraints are discussed further in this section. Joints with parameters outside these specified ranges of validity are allowed, but they may result in lower joint efficiencies and generally require considerable engineering judgement and verification.

The minimum nominal wall thickness of hollow sections is 2.5 mm. Designers should be aware that some tube manufacturing specifications allow such a liberal tolerance on wall thickness (e.g. ASTM A500 (ASTM, 2007a)) that a special "design thickness" is advocated for use in structural design calculations. For CHS with nominal chord wall thicknesses exceeding 25 mm, special measures have to be taken to ensure that the through-thickness properties of the material are adequate.

Where CHS brace (web) members are welded to a CHS chord member, the included angle between a brace and chord (θ) should be $\geq 30°$. This is to ensure that proper welds can be made. In some circumstances, this requirement can be waived but only in consultation with the fabricator and the design strength should not be taken larger than that for 30°. In gapped K joints, to ensure that there is adequate clearance to form satisfactory welds, the gap between adjacent brace members should be at least equal to the sum of the brace member thicknesses (i.e. $g \geq t_1 + t_2$).

In overlapped K joints, the in-plane overlap should be large enough to ensure that the interconnection of the brace members is sufficient for adequate shear transfer from one brace to the other. This can be achieved by ensuring that the overlap, which is defined in figure 1.1, is at least 25%. Where overlapping brace members are of different widths, the narrower member should overlap the wider one. Where overlapping brace members with the same diameter have different thicknesses and/or different strength grades, the member with the lowest $t_i f_{yi}$ value should overlap the other member.

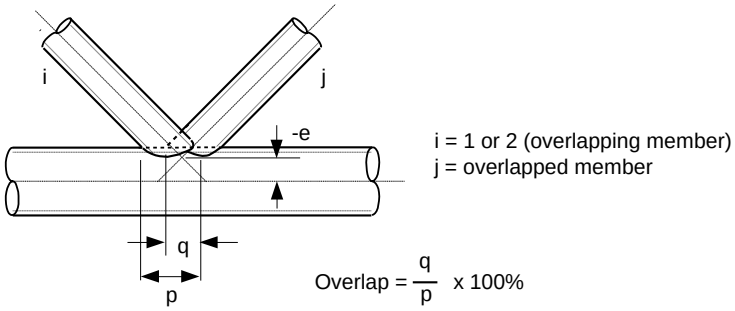

Figure 1.1 – Definition of overlap

In gapped and overlapped K joints, restrictions are placed on the noding eccentricity e, shown in figures 1.1 and 1.2, with a positive value of e representing an offset from the chord centreline towards the outside of the truss. This noding eccentricity restriction in the new IIW (2008) recommendations is $e \leq 0.25d_0$. The effect of the eccentricity is taken into account in the chord stress function. If the eccentricity exceeds $0.25d_0$, the effect of bending moments on the joint capacity should also be considered for the brace members.

The previous IIW (1989) recommendations used in the 1st edition of this Design Guide and discussed in chapter 10 give an eccentricity restriction of $-0.55d_0 \leq e \leq 0.25d_0$ for which the effect of the joint eccentricity can be ignored for *joint* design, since the effect on joint capacity had already been included in empirical or semi-empirical formulae given in chapter 10. The bending moment

produced by *any* eccentricity e should always be considered in member design by designing the chords as beam-columns.

With reference to figure 1.2, the gap g or overlap q, as well as the eccentricity e, may be calculated by equations 1.1 and 1.2 (Packer et al., 1992; Packer and Henderson, 1997):

$$g = \left(e + \frac{d_0}{2} \right) \frac{\sin(\theta_1 + \theta_2)}{\sin\theta_1 \sin\theta_2} - \frac{d_1}{2\sin\theta_1} - \frac{d_2}{2\sin\theta_2} \qquad 1.1$$

Note that a negative value of the gap g in equation 1.1 corresponds to an overlap q.

$$e = \left(\frac{d_1}{2\sin\theta_1} + \frac{d_2}{2\sin\theta_2} + g \right) \frac{\sin\theta_1 \sin\theta_2}{\sin(\theta_1 + \theta_2)} - \frac{d_0}{2} \qquad 1.2$$

Note that g above will be negative for an overlap.

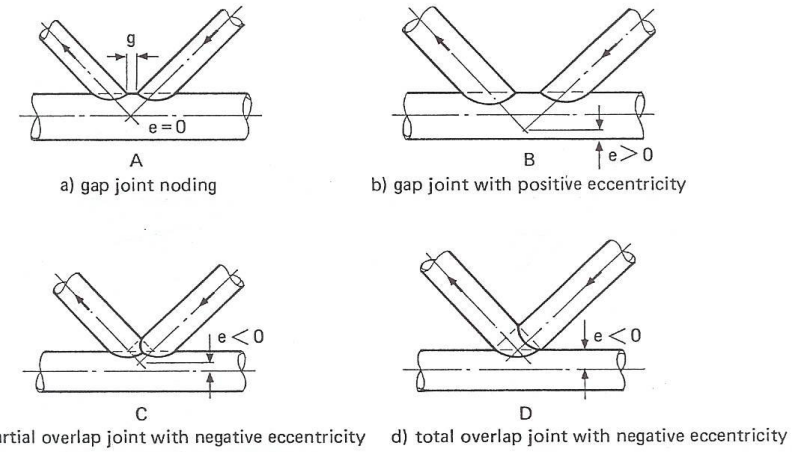

Figure 1.2 – Noding eccentricity

1.2.3 Section class limitations

The section class gives the extent to which the resistance and rotation capacity of a cross section are limited by its local buckling resistance. For example, four classes are given in Eurocode 3 (CEN, 2005a) together with three limits on the diameter to thickness ratio for CHS. For structures of hollow sections or combinations of hollow sections and open sections, the design rules for the joints are restricted to class 1 and 2 sections; therefore only these limits (according to Eurocode 3) are given in table 1.1. In other standards, slightly different values are used.

1.3 Terminology and notation

This Design Guide uses terminology adopted by CIDECT and IIW to define joint parameters, wherever possible. The term “joint” is used to represent the zone where two or more *members* are interconnected, whereas “connection” is used to represent the location at which two or more *elements* meet. The “through member” of a joint is termed the “chord” and attached members are termed braces (although the latter are also often termed bracings, branch members or web members). Such terminology for joints, connections and braces follows Eurocode 3 (CEN, 2005b).

Table 1.1 – Section class limitations according to Eurocode 3 (CEN, 2005a)

$\varepsilon = \sqrt{235/f_y}$ and f_y in N/mm^2					
Limits	CHS in compression: d_i/t_i	RHS in compression (hot-finished and cold-formed): $(b_i - 2r_o)/t_i$ (*)		I sections in compression	
				Flange: $(b_i - t_w - 2r)/t_i$	Web: $(h_i - 2t_i - 2r)/t_w$
Class 1	$50\varepsilon^2$	33ε		18ε	33ε
Class 2	$70\varepsilon^2$	38ε		20ε	38ε
Reduction factor ε for various steel grades					
f_y (N/mm^2)	235	275	355	420	460
ε	1.00	0.92	0.81	0.75	0.71

(*) For all hot-finished and cold-formed RHS, it is conservative to assume $(b_i - 2r_o)/t_i = (b_i/t_i) - 3$ (as done by AISC (2005) and Sedlacek et al. (2006)).

Figure 1.3 shows some of the common joint notation for gapped and overlapped uniplanar K joints. Definitions of all symbols and abbreviations are given in chapter 12. The numerical subscripts (i = 0, 1, 2) to symbols shown in figure 1.3 are used to denote the member of a hollow section joint. The subscript i = 0 designates the chord (or "through member"); i = 1 refers in general to the brace for T, Y and X joints, or it refers to the compression brace member for K and N joints; i = 2 refers to the tension brace member for K and N joints. For K and N overlap joints, the subscript i is used to denote the overlapping brace member (see figure 1.1).

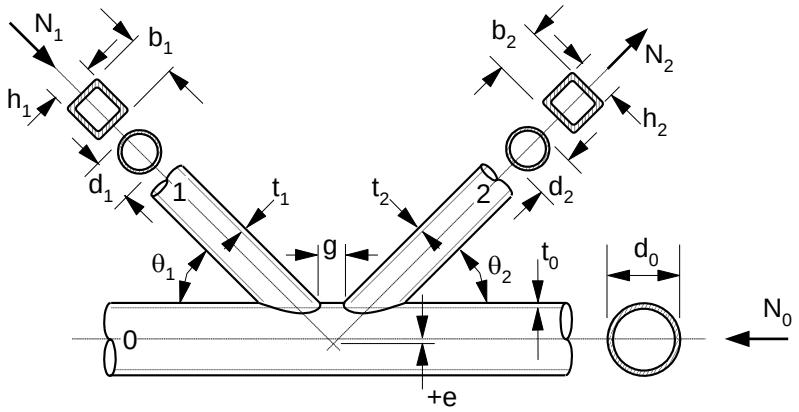

Figure 1.3 – Common notation for hollow structural section joints

1.4 Effect of geometric and mechanical tolerances on joint design strength

1.4.1 Determination of the design strength

In the analyses for the determination of the design strengths, the mean values and coefficients of variation as shown in table 1.2 have been assumed for the dimensional, geometric and mechanical properties (IIW, 2008).

In case hollow sections are used with mean values or tolerances significantly different from these values, it is important to note that the resulting design value may be affected.

Table 1.2 – Effect of geometric and mechanical tolerances on joint design strength

Parameter	Mean value	CoV	Effect
CHS or RHS thickness t_i	1.0	0.05	Important
CHS diameter d_i or RHS width b_i or depth h_i	1.0	0.005	Negligible
Angle θ_i	1.0	1°	Negligible
Relative gap $g' = g/t_0$	1.0	0.06	Important
Relative chord stress parameter n	1.0	0.05	Important
Yield stress f_y	1.18	0.075	Important

1.4.2 Delivery standards

The delivery standards in various countries deviate considerably with respect to the thickness and mass tolerances (Packer, 2007). In most countries besides the thickness tolerance, a mass tolerance is given, which limits extreme deviations. However, in some production standards the thickness tolerance is not compensated by a mass tolerance – see ASTM A500 (ASTM, 2007a). This has resulted in associated design specifications which account for this by designating a "design wall thickness" of 0.93 times the nominal thickness t (AISC, 2005) and in Canada even a design wall thickness of 0.90t is used for ASTM A500 hollow sections. However, the ASTM A501 (ASTM, 2007b) for hot-formed hollow sections has tightened its mass tolerance up to -3.5% with no thickness tolerance, resulting in small minus deviations from the nominal thickness.

The Canadian cold-formed product standard, CAN/CSA G40.20/G40.21 (CSA, 2004) has a -5% thickness tolerance throughout the thickness range and a -3.5% mass tolerance.

In Australia, the AS 1163 (Standards Australia, 1991) gives a thickness tolerance of +/- 10% and a lower mass tolerance of -4%.

In Europe, where nominal thicknesses are used in design, see EN 1993-1-1 (CEN, 2005a), the thickness tolerances are (partly) compensated by the mass tolerance. For example, table 1.3 shows the tolerances for hot-finished hollow sections according to EN 10210 (CEN, 2006a) and for cold-formed hollow sections according to EN 10219 (CEN, 2006b).

Table 1.3 – Tolerances for hot-finished and cold-formed hollow sections

<table>
<tr><td rowspan="2">Thickness (mm)</td><td rowspan="2">Thickness tolerance Cold-formed (EN 10219)</td><td rowspan="2">Thickness tolerance Hot-finished (EN 10210)</td><td rowspan="2">Mass tolerance (EN 10210) (EN 10219)</td><td colspan="2">Governing (minimum)</td></tr>
<tr><td>(EN 10219)</td><td>(EN 10210)</td></tr>
<tr><td>$t \leq 5$</td><td>+/- 10%</td><td rowspan="3">-10%</td><td rowspan="3">+/- 6%</td><td rowspan="2">-6%</td><td rowspan="3">-6%</td></tr>
<tr><td>$5 < t \leq 8.33$</td><td rowspan="2">+/- 0.5 mm</td></tr>
<tr><td>$8.33 < t$</td><td>-0.5 mm</td></tr>
</table>

These thickness tolerances have not only an effect on the capacity of the sections but also on the joint capacity. Considering that the joint capacity criteria are a function of t^{α} with $1 \leq \alpha \leq 2$, a large tolerance (as for example according to ASTM A500) can have a considerable effect on the joint capacity. Thus, in these cases a lower design thickness or an additional γ_M factor may have to be taken into account, for example as used in the USA.

In case the thickness tolerance is limited by a mass tolerance, the actual limits determine whether the nominal thickness can be used as the design thickness. Furthermore, if these tolerances are similar or smaller than those for other comparable steel sections, the same procedure can be used.

In Australia and Canada (for CSA) the tolerances on thickness and mass are such that the nominal thickness can be assumed as the design thickness. The same applies to hot-formed hollow sections according to ASTM A501.

The tolerances in Europe could, especially for the lower thicknesses, result in an effect on the joint capacity. On the other hand, the joints with a smaller thickness generally have a larger mean value for the yield strength and relatively larger welds, resulting in larger capacities for small size specimens as shown in figure 1.4 (van der Vegte et al., 2008b), which (partly) compensates the effect of the minus thickness tolerance.

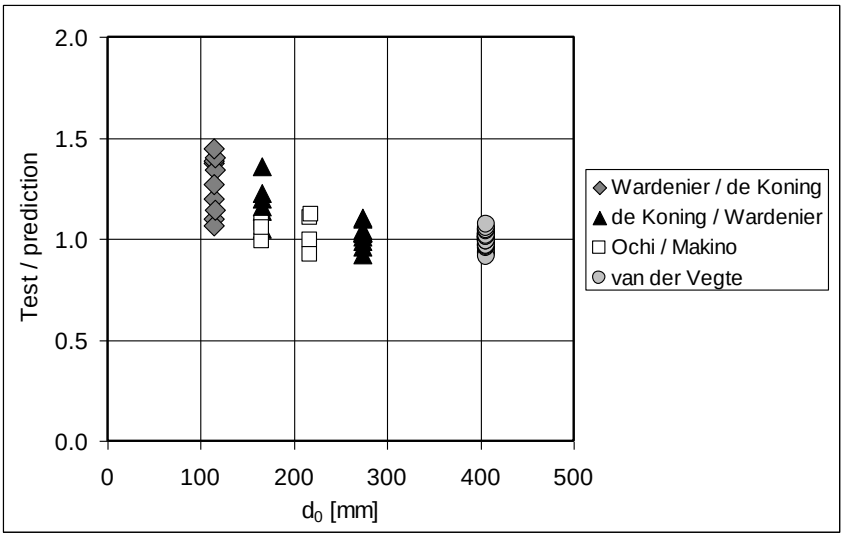

Figure 1.4 – Size effect in tubular joints due to relatively larger welds in small sized specimens (van der Vegte et al., 2008b)

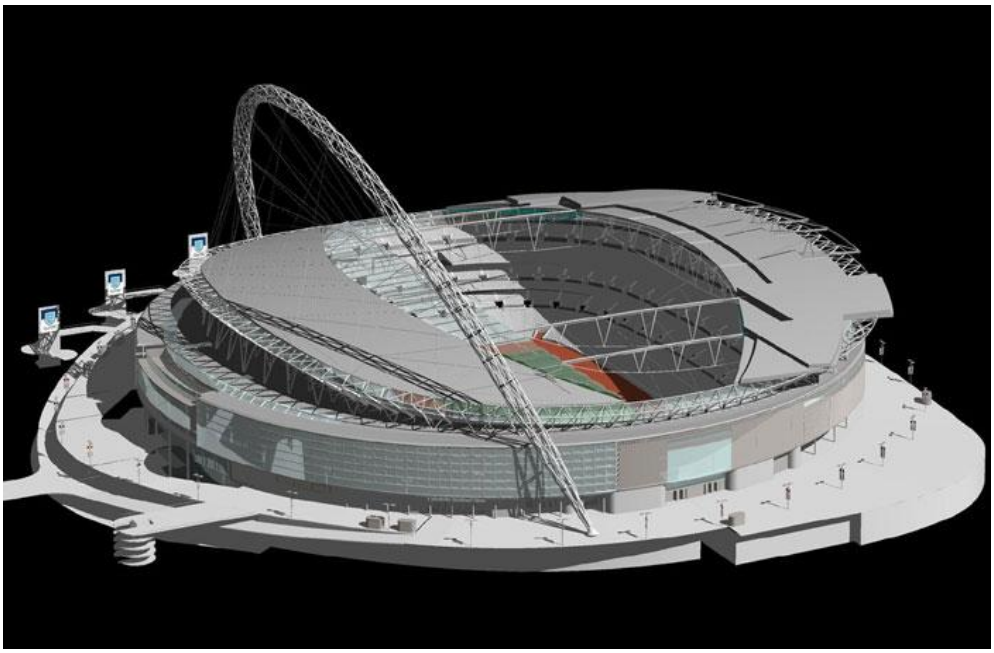

Model of the roof of a football stadium with an arch support

2 Applications of circular hollow sections

As already stated in the introduction, the circular hollow section combines excellent structural properties with an architecturally attractive shape. This has resulted in many applications in buildings, halls, bridges, barriers, masts, towers, offshore and special applications, such as glass houses, radio telescopes, sign gantries, parapets, cranes, jibs, sculptures, etc. (Eekhout, 1996; Wardenier, 2002). For indication, some examples are given in figures 2.1 to 2.4.

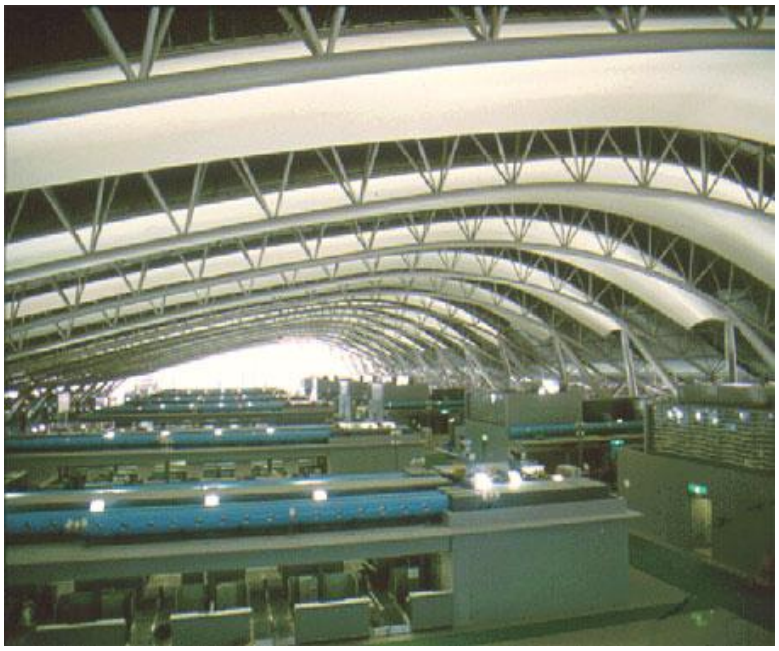

Figure 2.1 – Circular hollow sections used in halls

Figure 2.2 – Circular hollow sections used in a bridge

Figure 2.3 – Circular hollow sections used in a barrier

Figure 2.4 – Circular hollow sections used in offshore structures

3 Design of tubular trusses

3.1 Truss configurations

Some of the common truss types are shown in figure 3.1. Warren trusses will generally provide the most economical solution since their long compression brace members can take advantage of the fact that CHS are very efficient in compression. They have about half the number of brace members and half the number of joints compared to Pratt trusses, resulting in considerable labour and cost savings. The panel points of a Warren truss can be located at the load application points on the chord, if necessary with an irregular truss geometry, or even away from the panel points (thereby loading the chord in bending). If support is required at all load points to a chord (for example, to reduce the unbraced length), a modified Warren truss could be used rather than a Pratt truss by adding vertical members as shown in figure 3.1(a).

Warren trusses provide greater opportunities to use gap joints, the preferred arrangement at panel points. Also, when possible, a regular Warren truss achieves a more "open" truss suitable for practical placement of mechanical, electrical and other services. Truss depth is determined in relation to the span, loads, maximum deflection, etc., with increased truss depth reducing the loads in the chord members and increasing the lengths of the brace members. The ideal span to depth ratio is usually found to be between 10 and 15. If the total costs of the building are considered, a ratio nearer 15 will represent optimum value.

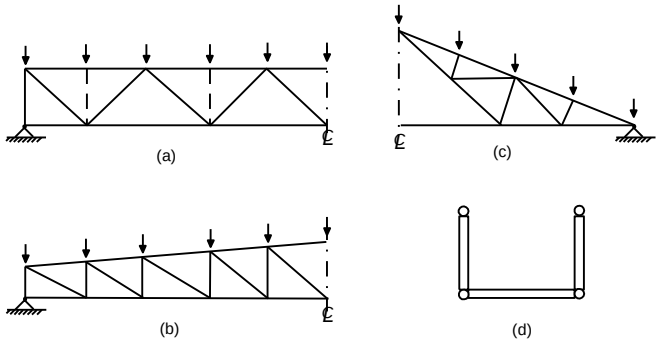

Figure 3.1 – Common CHS uniplanar trusses
(a) Warren trusses (modified Warren with verticals)
(b) Pratt truss (shown with a sloped roof, but may have parallel chords)
(c) Fink truss
(d) U-framed truss

3.2 Truss analysis

Elastic analysis of CHS trusses is frequently performed by assuming that all members are pin connected. Nodal eccentricities between the centre lines of intersecting members at panel points should preferably be kept to $e \leq 0.25d_0$. These eccentricities produce primary bending moments which, for a pinned joint analysis, need to be taken into account in chord member design e.g. by treating it as a beam-column. This is done by distributing the panel point moment (sum of the horizontal components of the brace member forces multiplied by the nodal eccentricity) to the chord on the basis of relative chord stiffness on either side of the joint (i.e. in proportion to the values of moment of inertia divided by chord length to the next panel point, on either side of the joint).

For the capacity formulae of chapter 10 (the formulae of the previous, 1st edition of this Design Guide), the eccentricity moments can be ignored for the design of the joints provided that the eccentricities are within the limits $-0.55d_0 \leq e \leq 0.25d_0$.

If these eccentricity limits are violated, the eccentricity moment may have a detrimental effect on joint strength and the eccentricity moment must be distributed between the members of a joint. If moments are distributed to the brace members, the joint capacity must then be checked for the interaction between axial load and bending moment, for each brace member.

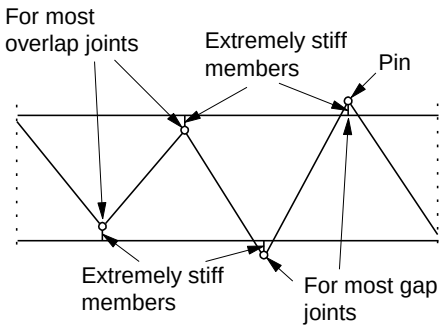

Figure 3.2 – Plane frame joint modelling assumptions to obtain realistic forces for member design

A rigid joint frame analysis is not recommended for most planar, triangulated, single-chord, directly-welded trusses, as it generally tends to exaggerate brace member moments, and the axial force distribution will still be similar to that for a pin-jointed analysis.

Transverse loads applied to either chord away from the panel points produce primary moments which must always be taken into account when designing the chords.

Computer plane frame programs are regularly used for truss analysis. In this case, the truss can be modelled by considering a continuous chord with brace members pin connected to it at distances of +e or -e from it (e being the distance from the chord centreline to the intersection of the brace member centrelines). The links to the pins are treated as being extremely stiff as indicated in figure 3.2. The advantage of this model is that a sensible distribution of bending moments is automatically generated throughout the truss, for cases in which bending moments need to be taken into account in the design of the chords.

Table 3.1 – Moments to be considered for CHS truss design

Type of moment	**Primary**	**Primary**	**Secondary**
Moments due to	Nodal eccentricity ($e \leq 0.25d_0$)	Transverse member loading	Secondary effects such as local deformations
Chord design	Yes	Yes	No
Design of other members	No	Yes	No
Design of joints	Yes, for Q_f only; for formulae of chapter 10 only if the eccentricity limits are exceeded	Yes, influences Q_f	No, provided parametric limits of validity are met

Secondary moments, resulting from end fixity of the brace members to a flexible chord wall, can generally be ignored for both members and joints, provided that there is deformation and rotation capacity adequate to redistribute stresses after some local yielding at the connections. This is the case when the prescribed geometric limits of validity for design formulae given in chapter 4 are followed. Welds in particular need to have potential for adequate stress redistribution without premature failure, and this will be achieved with the recommendations given in section 3.9. Table 3.1 summarizes when moments need to be considered for designing a CHS truss.

Plastic design could be used to proportion the chords of a truss by considering them as continuous beams with pin supports from the brace members. In such a design, the plastically designed members must be plastic design sections and the welds must be sized to develop the capacity of the connected brace members.

3.3 Effective lengths for compression members

To determine the effective length KL for a compression member in a truss, the effective length factor K can always be conservatively taken as 1.0. However, considerable end restraint is generally present for compression members in a CHS truss, and it has been shown that K is generally appreciably less than 1.0 (Mouty, 1981; Rondal et al., 1996). This restraint offered by members framing into a joint could disappear, or be greatly reduced, if all members were designed optimally for minimum mass, thereby achieving ultimate capacity simultaneously under static loading (Galambos, 1998). In practice, design for optimal or minimum mass will rarely coincide with minimum cost; the brace members are usually standardized to a few selected dimensions (perhaps even two) to minimize the number of section sizes for the truss. In the unlikely situation that all compression brace members are proportioned on the basis of a single load combination, and all reach their compressive resistances at approximately the same truss loading, an effective length factor of 1.0 is recommended. CIDECT has sponsored and coordinated extensive research work to specifically address the determination of effective lengths in hollow section trusses, resulting in reports from CIDECT Programmes 3E-3G and Monograph No. 4 (Mouty, 1981). A re-evaluation of all test results has been undertaken to produce recommendations for Eurocode 3. This has resulted in the following effective length recommendations.

3.3.1 Simplified rules

For CHS chord members:

In the plane of the truss:

KL = 0.9 L where L is the distance between chord panel points 3.1

In the plane perpendicular to the truss:

KL = 0.9 L where L is the distance between points of lateral support for the chord 3.2

For CHS brace members:

In either plane:

KL = 0.75 L where L is the panel point to panel point length of the member 3.3

These values of K are only valid for CHS members which are connected around the full perimeter of the member, without cropping or flattening of the members. Compliance with the joint design requirements of chapter 4 will likely place even more restrictive control on the member dimensions. More detailed recommendations, resulting in lower K values are given in CIDECT Design Guide No. 2 (Rondal et al., 1996).

3.3.2 Long, laterally unsupported compression chords

Long, laterally unsupported compression chords can exist in pedestrian bridges such as U-framed trusses and in roof trusses subjected to large wind uplift. The effective length of such laterally unsupported truss chords can be considerably less than the unsupported length. For example, the actual effective length of a bottom chord, loaded in compression by uplift, depends on the loading in the chord, the stiffness of the brace members, the torsional rigidity of the chords, the purlin to truss joints and the bending stiffness of the purlins. The brace members act as local elastic supports at each panel point. When the stiffness of these elastic supports is known, the effective length of the compression chord can be calculated. A detailed method for effective length factor calculation has been given by CIDECT Monograph No. 4 (Mouty, 1981).

3.4 Truss deflections

For the purpose of checking the serviceability condition of overall truss deflection under specified (unfactored) loads, an analysis with all members being pin-jointed will provide a conservative (over)estimate of truss deflections when all the joints are overlapped. A better assumption for overlap conditions is to assume continuous chord members and pin-jointed brace members. However, for gap-connected trusses, a pin-jointed analysis still generally underestimates overall truss deflections, because of the flexibility of the joints. At the service load level, gap-connected CHS truss deflections are underestimated by around 5-10%. Thus, a conservative approach for gap-connected CHS trusses is to estimate the maximum truss deflection by 1.1 times that calculated from a pin-jointed analysis.

3.5 General joint considerations

It is essential that the designer has an appreciation of factors which make it possible for CHS members to be connected together at truss panel points without extensive (and expensive) reinforcement. Apparent economies from minimum-mass member selection will quickly vanish at the joints if a designer does not have knowledge of the critical considerations which influence joint efficiency.

1. Chords should generally have thick walls rather than thin walls. The stiffer walls resist loads from the brace members more effectively, and the joint resistance thereby increases as the diameter to thickness ratios decrease. For the compression chord, however, a large thin section is more efficient in providing buckling resistance, so for this member the final CHS wall slenderness will be a compromise between joint strength and buckling strength, and relatively stocky sections will usually be chosen.

2. Brace members should have thin walls rather than thick walls (except overlap joints), as joint efficiency increases as the ratio of chord wall thickness to brace wall thickness increases. In addition, thin brace member walls will require smaller fillet welds for a pre-qualified joint (weld volume is proportional to t^2).

3. Ideally, CHS brace members should have a smaller width than CHS chord members, as this gives an easier weld situation for the joint at the saddle of the chord section.

4. Gap joints (K and N) are preferred to overlap joints because the members are easier to prepare, fit and to weld. In good designs, a minimum gap $g \geq t_1 + t_2$ should be provided such that the welds do not overlap each other.

5. When overlap joints are used, at least a quarter of the diameter (in the plane of the truss) of the overlapping member needs to be engaged in the overlap; however 50% is preferable.

6. An angle of less than 30° between a brace member and a chord creates serious welding difficulties at the crown heel location and is not covered by the scope of these recommendations

(see section 3.9). However, angles less than 30° may be possible if the design is based on an angle of 30° and it is shown by the fabricator that a satisfactory weld can be made.

3.6 Truss design procedure

In summary, the design of a CHS truss should be approached in the following way to obtain an efficient and economical structure.

I. Determine the truss layout, span, depth, panel lengths, truss and lateral bracing by the usual methods, but keep the number of joints to a minimum.

II. Determine loads at joints and on members; simplify these to equivalent loads at the panel points if performing manual analysis.

Ill. Determine axial forces in all members by assuming that joints are either: (a) pinned and that all member centre lines are noding, or (b) that the chord is continuous with pin-connected braces.

IV. Determine chord member sizes by considering axial loading, corrosion protection and tube wall slenderness. (Usual diameter to thickness ratios are 20 to 30.) An effective length factor of K = 0.9 can be used for the design of the compression chord. Taking account of the standard mill lengths in design may reduce the end-to-end joints within chords. For large projects, it may be agreed that special lengths are delivered. Since the joint strength depends on the yield stress of the chord, the use of higher strength steel for chords (when available and practical) may offer economical possibilities. The delivery time of the required sections has to be checked.

V. Determine brace member sizes based on axial loading, preferably with thicknesses smaller than the chord thickness. The effective length factor for the compression brace members can initially be assumed to be 0.75 (see section 3.3.1).

VI. Standardize the brace members to a few selected dimensions (perhaps even two), to minimize the number of section sizes for the structure. Consider availability of all sections when making member selections. For aesthetic reasons, a constant outside member width may be preferred for all brace members, with wall thicknesses varying; but this will require special quality control procedures in the fabrication shop.

VII. Layout the joints; from a fabrication point of view, try gap joints first. Check that the joint geometry and member dimensions satisfy the validity ranges for the dimensional parameters given in chapter 4, with particular attention to the eccentricity limit. Consider the fabrication procedure when deciding on a joint layout.

VIII. If the joint resistances (efficiencies) are not adequate, modify the joint layout (for example, overlap rather than gap) or modify the brace or chord members as appropriate, and recheck the joint capacities. Generally, only a few joints will need checking.

IX. Check the effect of primary moments on the design of the chords. For example, use the proper load positions (rather than equivalent panel point loading that may have been assumed if performing manual analysis); determine the bending moments in the chords by assuming either: (a) pinned joints everywhere or (b) continuous chords with pin ended brace members. For the compression chord, also determine the bending moments produced by any noding eccentricities, by using either of the above analysis assumptions. Then check that the factored resistance of all chord members is still adequate, under the influence of both axial loads and primary bending moments.

X. Check truss deflections (see section 3.4) at the specified (unfactored) load level, using the proper load positions.

XI. Design welds.

3.7 Arched trusses

The joints of arched trusses can be designed in a similar way to those of straight chord trusses. If the arched chords are made by bending at the joint location only, as shown in figure 3.3(a), the chord members can also be treated in a similar way to those of straight chord trusses provided that the bending radius remains within the limits to avoid distortion of the cross section (Dutta, 2002). If the arched chords are made by continuous bending, the chord members have a curved shape between the joint locations, as shown in figure 3.3(b). In this case, the curvature should be taken into account in the member design by treating the chord as a beam-column. (Moment = axial force x eccentricity.)

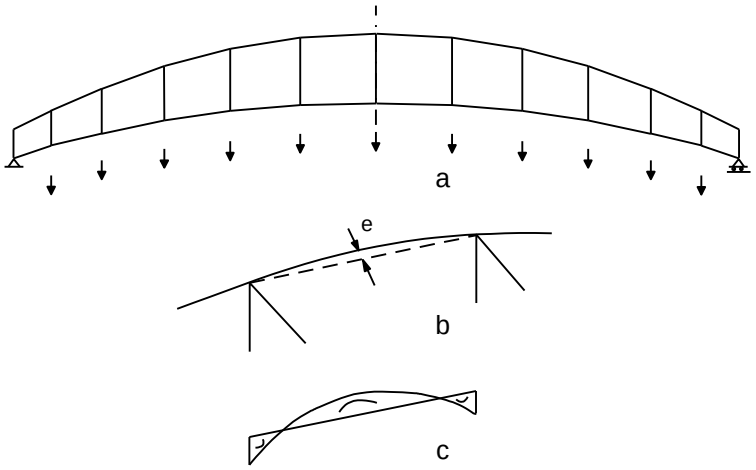

Figure 3.3 – Arched truss

3.8 Guidelines for earthquake design

In seismic design, the joints should meet additional requirements with regard to overstrength resulting in members being critical. For sufficient rotation capacity, the members should meet at least the class 1 requirements of table 1.1. For detailed information, reference is given to the CIDECT Design Guide No. 9 (Kurobane et al., 2004).

3.9 Design of welds

Except for certain K and N joints with partially overlapped brace members (as noted below), a welded connection should be established around the entire perimeter of a brace member by means of a butt weld, a fillet weld, or a combination of the two. Fillet welds which are automatically prequalified for any brace member loads should be designed to give a resistance that is not less than the brace member capacity. According to Eurocode 3 (CEN, 2005b), this results in the following minimum throat thickness ''a'' for fillet welds around brace members, assuming matched electrodes and ISO steel grades (IIW, 2008):

$a \geq 0.92\ t$, for S235 ($f_{yi} = 235\ N/mm^2$)
$a \geq 0.96\ t$, for S275 ($f_{yi} = 275\ N/mm^2$)
$a \geq 1.10\ t$, for S355 ($f_{yi} = 355\ N/mm^2$)
$a \geq 1.42\ t$, for S420 ($f_{yi} = 420\ N/mm^2$)
$a \geq 1.48\ t$, for S460 ($f_{yi} = 460\ N/mm^2$)

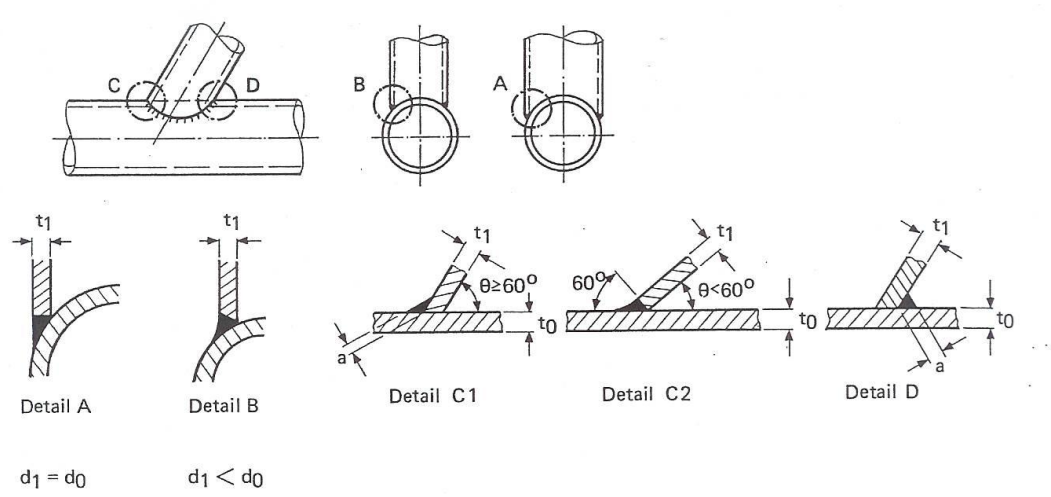

Figure 3.4 – Weld details

With overlapped K and N joints, welding of the toe of the overlapped member to the chord is particularly important for 100% overlap situations. For partial overlaps, the toe of the overlapped member need not be welded, providing the components, normal to the chord, of the bracing member forces do not differ by more than about 20%. The larger diameter brace member should be the “through member”. If both braces are of the same diameter then the thicker brace should be the overlapped (through) brace and pass uninterrupted through to the chord. If both braces are of the same size (outside dimension and thickness) then the more heavily loaded brace member should be the “through member”. When the brace member force components normal to the chord member differ by more than 20%, the full circumference of the through brace should be welded to the chord.

Generally, the weaker member (defined by wall thickness times yield strength) should be attached to the stronger member, regardless of the load type, and smaller members sit on larger members.

It is more economical to use fillet welds than butt (groove) welds. However, the upper limit on throat or leg size for fillet welds will depend on the fabricator. Most welding specifications only allow fillet welding at the toe of a brace member if $\theta_i \geq 60°$. Because of the difficulty of welding at the heel of a brace member at low θ values, a lower limit for the applicability of the joint design rules given herein has been set at $\theta_i = 30°$. Some recommended weld details (IIW, 2008) are illustrated in figure 3.4.

4 Welded uniplanar truss joints between CHS chords and CHS brace members

4.1 Joint classification

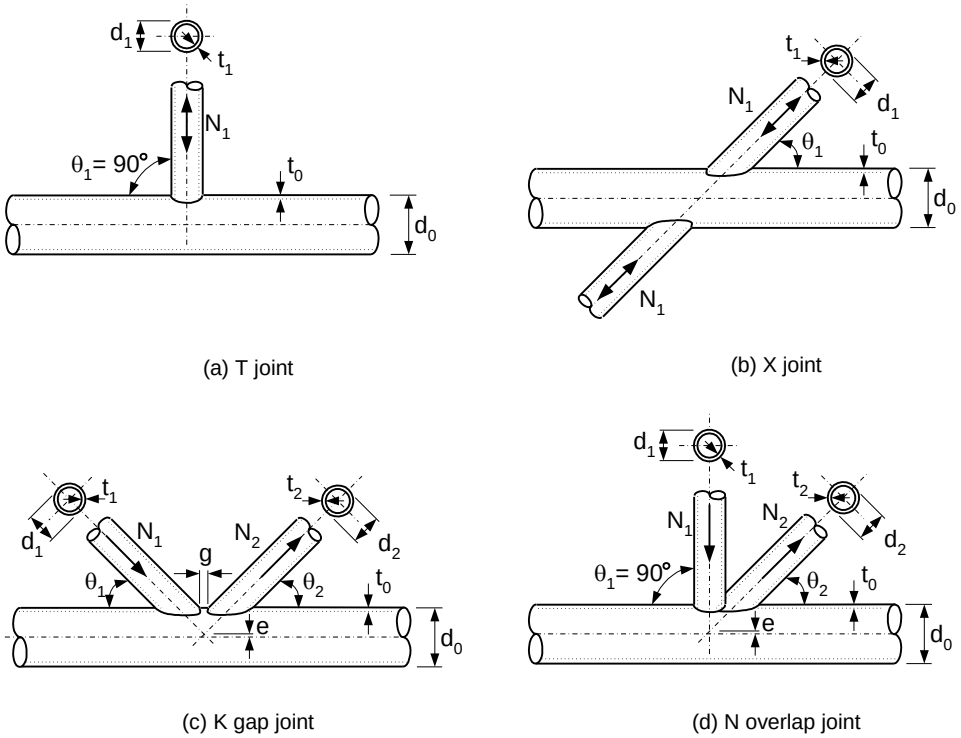

Figure 4.1 – Basic joint configurations i.e. T, X and K joints

Figure 4.1 shows the basic types of joint configurations i.e. T, X and K or N joints. However, the classification of hollow section truss-type joints as T (which includes Y), X, or K (which includes N) is based on the method of force transfer in the joint, not on the physical appearance of the joint. Examples of such classification are shown in figure 4.2, and definitions follow.

(a) When the normal component of a brace member force is equilibrated by beam shear (and bending) in the chord member, the joint is classified as a T joint when the brace is perpendicular to the chord, and a Y joint otherwise.

(b) When the normal component of a brace member force is essentially equilibrated (within 20%) by the normal force component of another brace member (or members), on the same side of the joint, the joint is classified as a K joint. The relevant gap is between the primary brace members whose loads equilibrate. An N joint can be considered as a special type of K joint.

(c) When the normal force component is transmitted through the chord member and is equilibrated by a brace member (or members) on the opposite side, the joint is classified as an X joint.

(d) When a joint has brace members in more than one plane, the joint is classified as a multiplanar joint (see chapter 6).

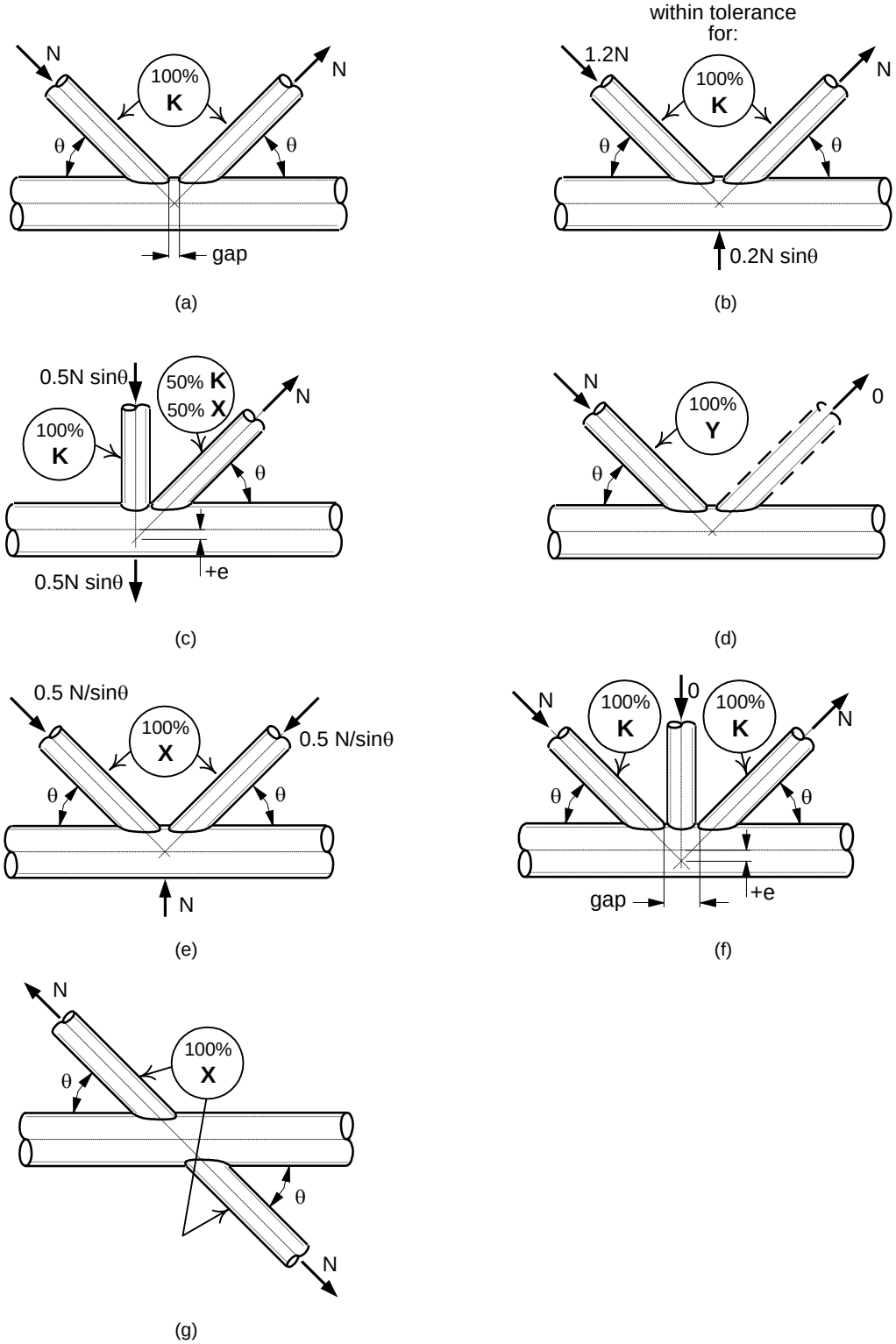

Figure 4.2 – Examples of hollow section joint classification

When brace members transmit part of their load as K joints and part of their load as T, Y, or X joints, the adequacy of each brace needs to be determined by linear interaction of the proportion of the brace load involved in each type of load transfer. However, the effect of the chord preloading should be added to the joint type with the most unfavourable chord load function.

One K joint, in figure 4.2(b), illustrates that the brace force components normal to the chord member may differ by as much as 20% and still be deemed to exhibit K joint behaviour. This is to accommodate slight variations in brace member forces along a typical truss, caused by a series of panel point loads.

The N joint in figure 4.2(c), however, has a ratio of brace force components normal to the chord member of 2:1. In this case, that particular joint needs to be analysed as both a "pure" K joint (with balanced brace forces) and an X joint (because the remainder of the diagonal brace load is being transferred through the joint), as shown in figure 4.3. For the diagonal tension brace in that particular joint, one would need to check that:

$$\frac{0.5N}{\text{K joint resistance}} + \frac{0.5N}{\text{X joint resistance}} \leq 1.0$$

If the gap size in a gapped K (or N) joint (e.g. figure 4.2(a)) becomes large and exceeds the value permitted by the gap/eccentricity limit, then the "K joint" should also be checked as two independent Y joints.

In X joints such as figure 4.2(e) where the braces are close or overlapping, the joint should be checked as an X joint, considering both brace load components perpendicular to the chord.

In K joints such as figure 4.2(d), where a brace has very little or no loading, the joint can be treated as a Y joint, as shown.

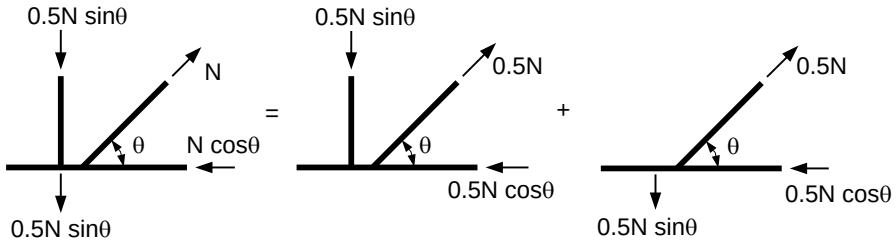

Figure 4.3 – Checking of a K joint with imbalanced brace loads

Some special uniplanar joints with braces on both sides of the chord where the brace forces act in various ways, are dealt with in table 4.4.

4.2 Joint capacity equations

The joint strength is generally governed by two criteria, i.e. plastification of the chord cross section or punching shear, shown in figure 4.4. For T, Y and X joints, the resistance is based on the strength under brace compression loading, although this can also be used for brace tensile loading. The ultimate resistance under tensile loading is usually higher than that under compressive loading. However, it is not always possible to take advantage of this additional strength due to larger deformations or premature cracking.

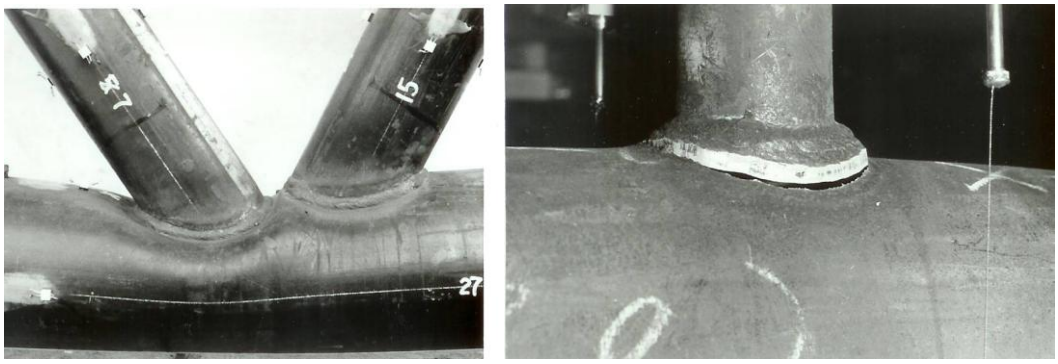

(a) Chord plastification (b) Chord punching shear

Figure 4.4 – Chord plastification and punching shear failure modes

Recently, Sub-commission XV-E of the International Institute of Welding has reanalysed all joint strength formulae. Based on rigorous examinations in combination with multiple additional finite element (FE) studies, new design strength functions have been established (IIW, 2008). Nowadays, with well calibrated FE models, reliable parameter studies can be performed, especially for chord plastification failures. In these reanalyses, it is shown that the experimental databases have to be used with care.

The new joint strength equations for chord plastification are, in principle, based on the ring model approach (Togo, 1967). However, the influence functions for β, γ, expressed by Q_u, and n, expressed by Q_f, have been determined using multi-regression analyses of the FE results. After simplifications, the formulae have been compared with the experimental database compiled by Makino et al. (1996) and the FE database of Qian et al. (2008). Finally, design strength formulae have been developed (van der Vegte et al., 2008a, 2008b).

For distinction with the formulae in the previous edition, which are incorporated in many national and international codes, a slightly different presentation is used, shown in table 4.1. This format is similar to that in the API recommendations (API, 2007):

$$N_i^* = Q_u\, Q_f\, \frac{f_{y0}\, t_0^2}{\sin\theta_i} \qquad 4.1$$

The parameter Q_u gives the influence function for the parameters β and γ, while the parameter Q_f accounts for the influence of the chord stress on the joint capacity.

For chord punching shear, the formula is similar to that in previous editions, although the presentation is slightly different.

$$N_i^* = 0.58\, f_{y0}\, \pi\, d_i\, t_0\, \frac{k_a}{\sin\theta_i} \qquad 4.2$$

where k_a is a parameter for the connection perimeter in relation to the brace perimeter as function of θ_i:

$$k_a = \frac{1+\sin\theta_i}{2\sin\theta_i} \qquad 4.3$$

For indication, the Q_u functions for X, T and K gap joints with $2\gamma = 25$ are illustrated in figure 4.5. For each of the three joint types, the capacity increases with increasing β ratio. Further, Q_u is lowest for X joints and highest for K gap joints with a small gap. The Q_u for T joints is the same as that for K joints with a large gap. These relations are in good agreement with the expected physical behaviour.

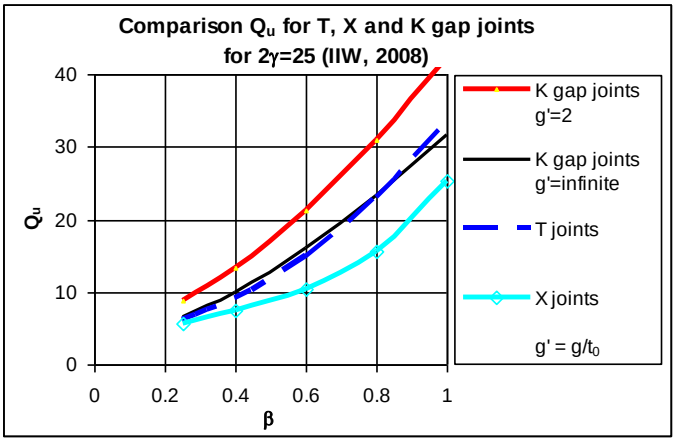

Figure 4.5 – Comparison of Q_u for T, X and K gap joints ($2\gamma = 25$)

One of the main differences with the joint strength formulae given in the previous edition of the Design Guide, here also recorded in chapter 10, is that the chord stress function Q_f is now related to the maximum chord stress, whereas previously, the chord stress function f(n') was based on the so-called prestress. Further, the reanalyses also showed that for large tensile chord load, a reduction of the joint resistance has to be taken into account.

In table 4.1, the total (normal) stress ratio, n, in the chord connecting face, due to axial load plus bending moment, is computed and its effect on joint resistance determined. It should be noted that the most punitive stress effect, Q_f, in the chord on either side of the joint is to be used.

The Q_f functions are graphically presented in figures 4.6 to 4.8 for the individual effects of chord axial loading on T, Y, and X joints, chord moment loading on T, Y, and X joints, and chord axial loading on K gap joints. As shown in figures 4.6 and 4.7, the chord bending compression stress effect for T, Y and X joints is the same as that for chord axial compression loading.

The range of validity of the formulae, given in table 4.1, is about the same as in the previous edition of the Design Guide, recorded in table 10.1 of chapter 10. Although for particular cases the γ validity range could be larger, Sub-commission IIW-XV-E has limited the 2γ ratio to 50 (or class 2) because for ratios exceeding this limit, the deformations may govern, while in other cases the deformation capacity may not be sufficient to redistribute secondary bending moments.

4.3 T, Y and X joints

In the new joint strength formulae for T and Y joints, summarized in table 4.1, the effect of chord bending due to the brace load is now fully included in the chord stress function Q_f, giving a better presentation of the capacity (van der Vegte et al., 2006). The previous chord plastification formula (chapter 10) was only based on experimental results which were, due to the test set up, influenced by chord bending.

The previous formula for X joints gave, for very low β values, a higher capacity than for T joints, which is not correct. The new formulae give for low γ ratios, slightly lower values than the previous strength equations, which agrees with the work on thick-walled joints by Qian (2005). It was further shown by Qian (2005) that for X joints with small angles θ_1, chord shear failure could occur when $\cos\theta_1 > \beta$.

4.4 K and N joints

In the previous edition of the Design Guide, one formula was given for gap and overlap K joints (chapter 10). However, overlap and gap joints behave differently, with other influencing parameters. Therefore, rigorous reanalyses have been carried out on K gap joints (van der Vegte et al., 2007) and overlap joints. For overlap joints, it was found that these could be approached in the same way as overlap joints between RHS sections (Wardenier, 2007).

4.4.1 K and N joints with gap

The new equation for chord plastification is significantly simpler with respect to the gap function. The new design equation gives for low γ values, lower strengths than the previous equations (chapter 10), which agrees with the work of Qian (2005) on joints with thick-walled sections. Further, for low β values, the new functions give lower results. The database used previously included many small scale specimens with low β ratios and relatively large welds, which increased the mean ultimate strength value of joints with low β values with small gaps. The new strength equations are based on sections with larger dimensions and smaller welds.

Triangular girders with CHS members and bolted joints with plates

Table 4.1 – Limit states criteria for axially loaded CHS joints

Criterion to be checked	**Axially loaded joints with CHS braces and chord**
Design strength: chord plastification	$N_i^* = Q_u\, Q_f\, \frac{f_{y0}\, t_0^2}{\sin\theta_i}$ eq. 4.1
Design strength: chord punching shear (only for $d_i \le d_0 - 2t_0$)	$N_i^* = 0.58\, f_{y0}\, \pi\, d_i\, t_0\, \frac{k_a}{\sin\theta_i}$ eq. 4.2
	$k_a = \frac{1+\sin\theta_i}{2\sin\theta_i}$ eq. 4.3

Function Q_u	
X joints (*) 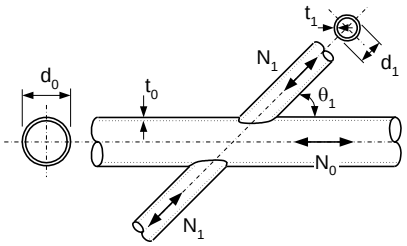	$Q_u = 2.6\left(\frac{1+\beta}{1-0.7\beta}\right)\gamma^{0.15}$ eq. 4.4
T and Y joints 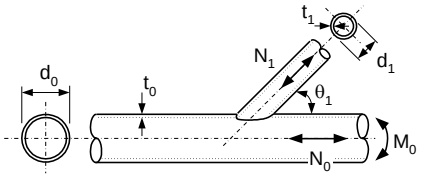	$Q_u = 2.6\left(1+6.8\beta^2\right)\gamma^{0.2}$ eq. 4.5
K gap joints 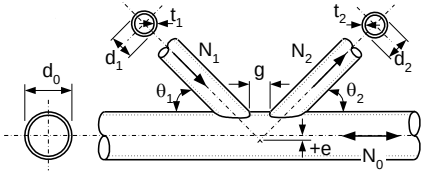	$Q_u = 1.65\,(1+8\beta^{1.6})\,\gamma^{0.3}\,[1+\frac{1}{1.2+(\frac{g}{t_0})^{0.8}}]$ eq. 4.6

(*) For X joints with $\cos\theta_1 > \beta$, check also for chord shear failure (see equation 6.2 in table 6.1).

Function Q_f		
	$Q_f = \left(1-\lvert n\rvert\right)^{C_1}$ with $n = \frac{N_0}{N_{pl,0}} + \frac{M_0}{M_{pl,0}}$ in connecting face	eq. 4.7
	Chord compression stress (n < 0)	**Chord tension stress (n ≥ 0)**
T, Y, X joints	$C_1 = 0.45 - 0.25\beta$	$C_1 = 0.20$
K gap joints	$C_1 = 0.25$	

Table 4.1 – Limit states criteria for axially loaded CHS joints (continued)

Range of validity			
General	$0.2 \le \frac{d_i}{d_0} \le 1.0$	$t_i \le t_0$	$\frac{e}{d_0} \le 0.25$
	$\theta_i \ge 30°$	$g \ge t_1+t_2$	$f_{yi} \le f_{y0}$ $f_y \le 0.8f_u$ $f_y \le 460$ N/mm^2 (**)
Chord	**Compression**	class 1 or 2 (***) and $2\gamma \le 50$ (for X joints: $2\gamma \le 40$)	
	Tension	$2\gamma \le 50$ (for X joints: $2\gamma \le 40$)	
Braces	**Compression**	class 1 or 2 (***) and $d_i/t_i \le 50$	
	Tension	$d_i/t_i \le 50$	

(**) For $f_{y0} > 355$ N/mm^2, see section 1.2.1
(***) Limits for d_i/t_i are given in table 4.2

Table 4.2 – Maximum d_i/t_i ratios for CHS in compression (CEN, 2005a)

	Maximum d_i/t_i ratios			
Steel grade	S235	S275	S355	S460
Yield stress f_y	235 N/mm^2	275 N/mm^2	355 N/mm^2	460 N/mm^2
Class 1	50	42	33	25
Class 2	70	59	46	35

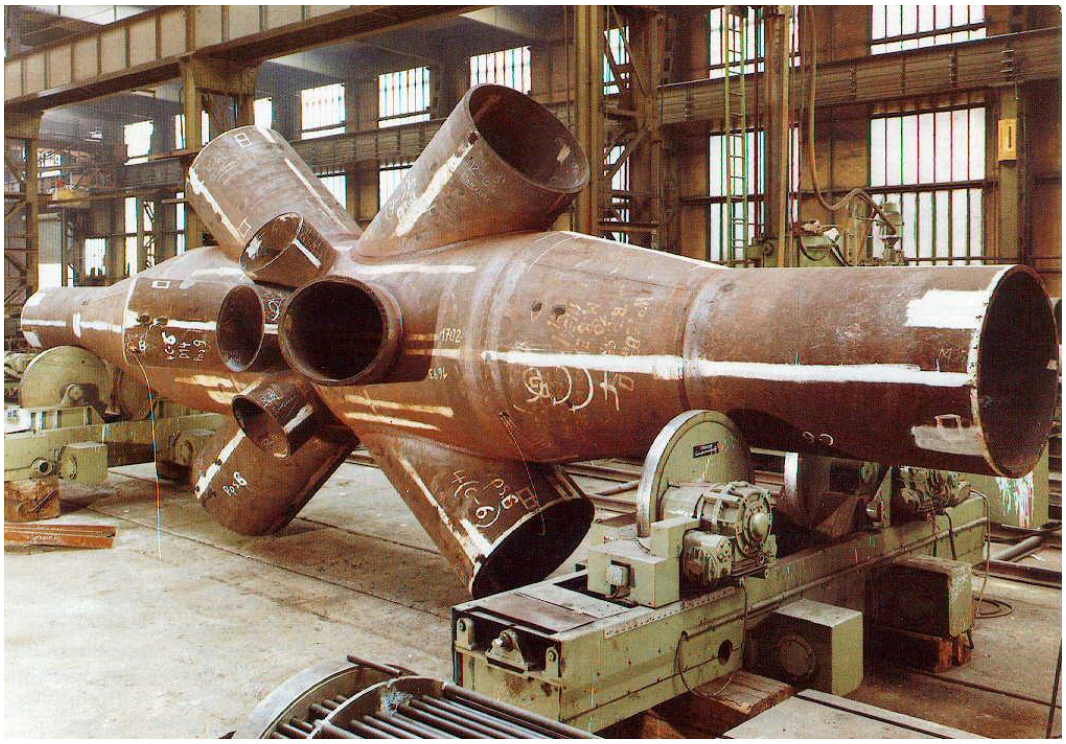

Complex multiplanar welded joint

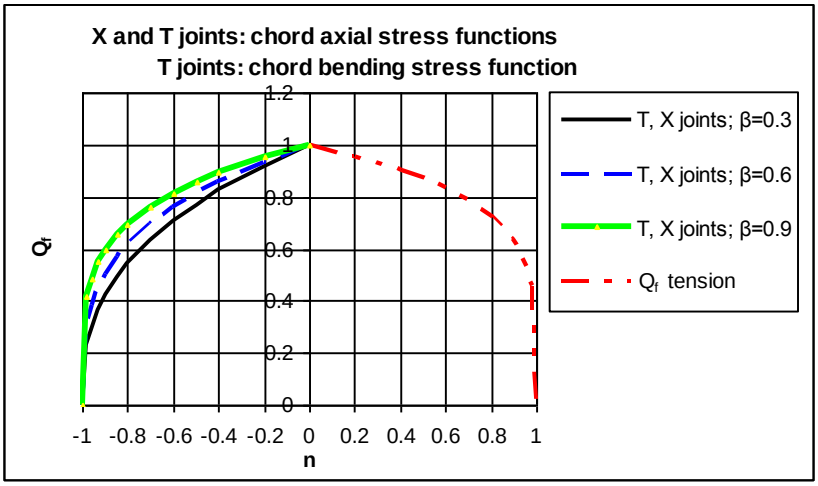

Figure 4.6 – Chord axial stress function Q_f for T and X joints and chord bending stress function Q_f for T joints

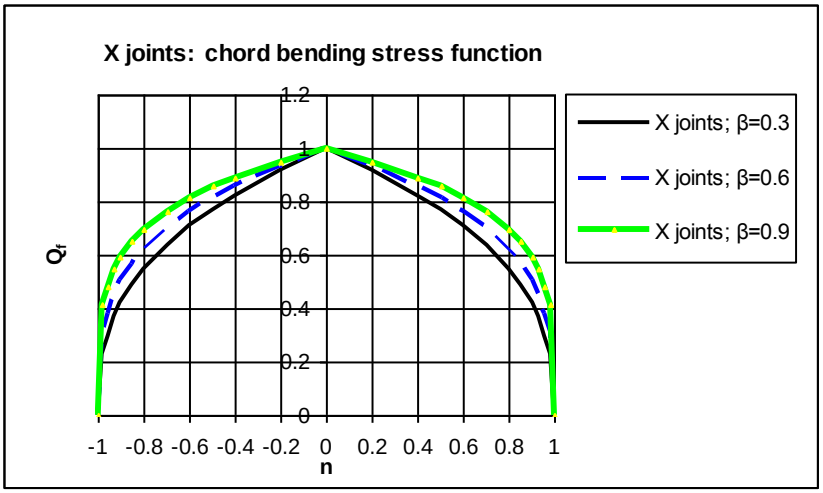

Figure 4.7 – Chord bending stress function Q_f for X joints

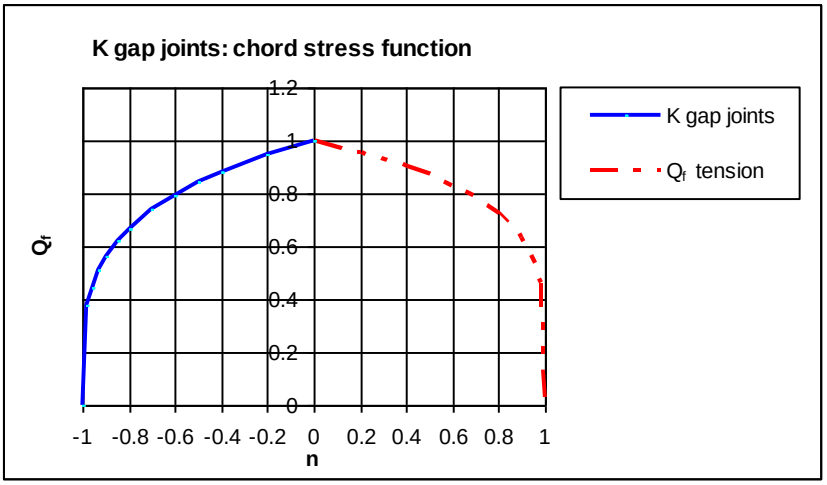

Figure 4.8 – Chord axial stress function Q_f for K gap joints

4.4.2 K and N joints with overlap

As stated before, for overlap joints the same approach is now adopted for all types of overlap joints, regardless whether circular or rectangular braces are used in combination with a circular, rectangular or an open section chord (Wardenier, 2007). Only the effective width parameters depend on the type of section. The resistance of overlap joints between circular hollow sections with 25% ≤ Ov ≤ 100% overlap is based on the following criteria:

(1) Local yielding of the overlapping brace, equations 4.8 and 4.9
(2) Local chord member yielding at the joint location based on interaction between axial load and bending moment, equation 4.10
(3) Shear of the connection between the brace(s) and the chord, equation 4.11

Figure 4.9 shows the overlap joint configuration with the cross sections to be examined for these criteria. For K and N overlap joints, the subscript i is used to denote the overlapping brace member, while the subscript j refers to the overlapped brace member.

Local yielding of the overlapping brace (criterion 1) should always be verified, although shear between the braces and the chord (criterion 3) may only become critical for larger overlaps, i.e. larger than 60% or 80%, respectively, depending on whether the hidden toe location of the overlapped brace is welded to the chord. The check for local chord member yielding (criterion 2) is, in principle, a member check and may become critical for larger overlaps and/or larger β ratios.

For 100% overlap joints, similar criteria (equations 4.9, 4.10 and 4.12) have to be verified. Only here, as shown by Qian et al. (2007), overlapping brace shear (equation 4.12) and chord member yielding (equation 4.10) will generally be the governing criteria. Although an overlap of 100% is given in the recommendations, the overlap will generally be slightly larger to allow proper welding of the overlapping brace to the overlapped brace.

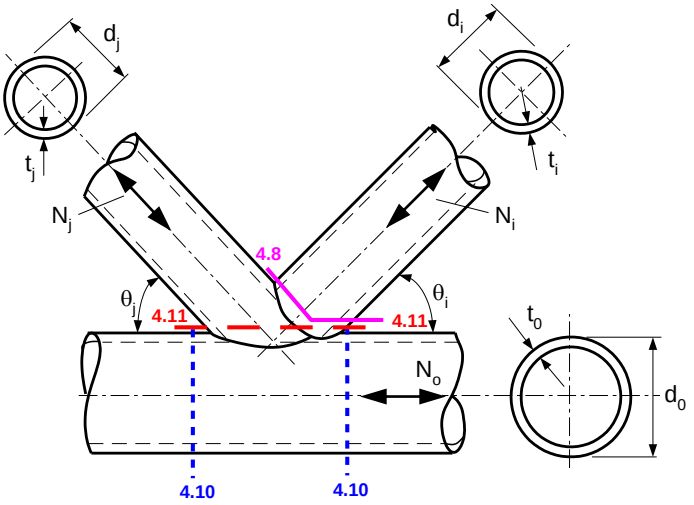

Figure 4.9 – Overlap joint configuration with cross sections to be checked

Joints with overlaps between 0% and 25% should be avoided because in those cases, the stiffness of the connection between the overlapping brace and the overlapped brace is much larger than that of the overlapping brace to chord connection, which may lead to premature cracking and lower capacities (Wardenier, 2007).

Table 4.3 – K overlap joints

$$Ov = overlap = \frac{q}{p} \times 100\%$$

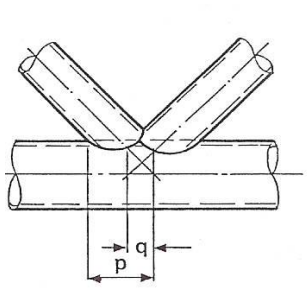

Local yielding of overlapping brace

25% ≤ Ov < 100%

$$N_i^* = f_{yi}\, t_i \frac{\pi}{4}\left[2d_i + d_{ei} + d_{e,ov} - 4t_i\right] \qquad \text{eq. 4.8}$$

Ov = 100%

$$N_i^* = f_{yi}\, t_i \frac{\pi}{4}\left[2d_i + 2d_{e,ov} - 4t_i\right] \qquad \text{eq. 4.9}$$

Local chord member yielding

$$\left(\frac{N_0}{N_{pl,0}}\right)^{1.7} + \frac{M_0}{M_{pl,0}} \le 1.0 \quad (*) \qquad \text{eq. 4.10}$$

Brace shear (only to be checked for Ov > Ov_{limit})

Ov_{limit} < Ov < 100% (**)

$$N_i \cos\theta_i + N_j \cos\theta_j \le \frac{\pi}{4}\left[0.58 f_{ui} \frac{\left[\left(\frac{100 - Ov}{100}\right) 2d_i + d_{ei}\right] t_i}{\sin\theta_i} + 0.58 f_{uj} \frac{(2d_j + c_s\, d_{ej})\, t_j}{\sin\theta_j}\right] \qquad \text{eq. 4.11}$$

Ov = 100%

$$N_i \cos\theta_i + N_j \cos\theta_j \le 0.58 f_{uj} \frac{\pi}{4} \frac{(3d_j + d_{ej})\, t_j}{\sin\theta_j} \qquad \text{eq. 4.12}$$

(*) Where N_0 and M_0 are to be selected at a common location (left or right from the joint) that produces the greatest summation; M_0 includes the moment due to noding eccentricity.
(**) If hidden toe of overlapped brace is not welded: Ov_{limit} = 60% and c_s = 1
If hidden toe of overlapped brace is welded: Ov_{limit} = 80% and c_s = 2

Effective width factors

$$d_{ei} = \frac{12}{d_0/t_0} \frac{f_{y0}\, t_0}{f_{yi}\, t_i} d_i \text{ but} \le d_i \qquad d_{ej} = \frac{12}{d_0/t_0} \frac{f_{y0}\, t_0}{f_{yj}\, t_j} d_j \text{ but} \le d_j \qquad d_{e,ov} = \frac{12}{d_j/t_j} \frac{f_{yj}\, t_j}{f_{yi}\, t_i} d_i \text{ but} \le d_i$$

General note	The efficiency (i.e. design resistance divided by brace squash load) of the overlapped brace j shall not exceed that of the overlapping brace i.

Range of validity			
General	$\frac{d_i}{d_0}$ and $\frac{d_j}{d_0} \ge 0.2$ $\quad \frac{d_i}{d_j} \ge 0.75$		t_i and $t_j \le t_0$ $\quad t_i \le t_j$
	θ_i and $\theta_j \ge 30°$	Ov ≥ 25%	f_{yi} and $f_{yj} \le f_{y0}$ $\quad f_y \le 0.8 f_u$ $f_y \le 460$ N/mm^2 (***)
Chord	**Compression**	class 1 or 2 (****) and $2\gamma \le 50$	
	Tension	$2\gamma \le 50$	
Braces	**Compression**	class 1 or 2 (****) and $d_1/t_1 \le 50$	
	Tension	$d_2/t_2 \le 50$	

(***) For f_{y0} > 355 N/mm^2, see section 1.2.1
(****) Limits for d_0/t_0 and d_1/t_1 are given in table 4.2

4.5 Special types of joints

In tubular structures, various other joint configurations exist which have not been dealt with in the previous chapters. However, the strength of several types of joints can be directly related to the basic types presented in sections 4.3 and 4.4.

Table 4.4 shows some special types of CHS uniplanar joints with braces directly welded to the chord.

Table 4.4 – Special types of uniplanar joints

Type of joint	Relationship to the formulae of tables 4.1 and 4.3
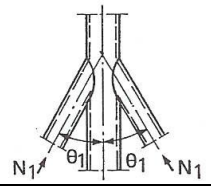	$N_1 \le N_1^*$ eq. 4.13 with N_1^* from X joint
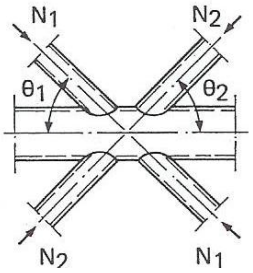	$N_1 \sin\theta_1 + N_2 \sin\theta_2 \le N_i^* \sin\theta_i$ eq. 4.14 with N_i^* (i = 1 or 2) from X joint where $N_i^* \sin\theta_i$ is the larger of $N_1^* \sin\theta_1$ and $N_2^* \sin\theta_2$
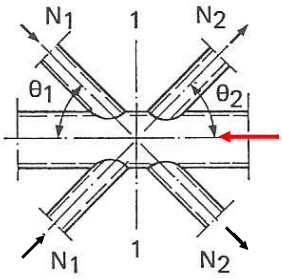	$N_i \le N_i^*$ (i = 1 or 2) with N_i^* (i = 1 or 2) from K joint, but with the actual chord force
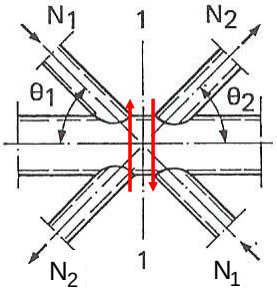	$N_i \le N_i^*$ (i = 1 or 2) with N_i^* (i = 1 or 2) from K joint Note: Check cross section 1-1 for shear failure in the gap: $\left(\frac{N_{gap,0}}{N_{pl,0}}\right)^2 + \left(\frac{V_{gap,0}}{V_{pl,0}}\right)^2 \le 1.0$ eq. 4.15 where: $N_{gap,0}$ = axial force in gap $N_{pl,0} = A_0 f_{y0}$ $V_{gap,0}$ = shear force in gap $V_{pl,0} = 0.58 f_{y0} \frac{2A_0}{\pi}$

4.6 Joints with cans

Large diameter CHS sections are built up from cans with a maximum length equal to the maximum plate width from which they are made. In structures with these large size tubular sections, it is easy to use a larger can thickness at the joint locations. This is, for example, commonly used in offshore structures. However, it can also be used for other heavily loaded structures, for example bridges and large span structures.

X Joints with short can lengths have been numerically investigated by van der Vegte (1995). For X joints, it was shown that the can should have a minimum length of $2.5d_0$ in order to obtain a joint capacity based on the can thickness. For smaller can lengths, a linear interpolation can be used between the resistance of the joint with and without a can. For this case, API (2007) gives the following equation:

$$N_1^* = \left[r + (1-r)\left(\frac{t_0}{t_{can}}\right)^2 \right] N_{can}^* \qquad 4.16$$

$$\text{with } r = \frac{l_{can}}{2.5d_0} \le 1.0 \text{ and } t_{can} > t_0 \qquad 4.17$$

Because of the dominant load transfer through membrane action, API allows for X joints with $\beta > 0.9$, a smaller can length down to $1.5d_0$ for $\beta = 1.0$. However, compared to the numerical data, this recommendation is somewhat too optimistic in the opinion of the authors of this Design Guide.

The interpolation function for can lengths (equation 4.16) can also be used for T and Y joints. For balanced K joints, a lower can length can be used due to the compensating ovalizing effects of the two braces. No experimental or numerical data are available for K joints, but API (2007) recommends an extension of $0.25d_0$ with a minimum of 300 mm from the footprint of the braces at both sides of the joint to obtain a capacity based on the can thickness.

4.7 Graphical design charts with examples

In the diagrams in tables 4.5 to 4.8, the joint design strength is expressed in terms of the efficiency of the connected braces, i.e. the joint design strength for axially loaded joints N_i^* is divided by the yield load $A_i f_{yi}$ of the connected brace. This results in efficiency formulae of the following type:

$$\frac{N_i^*}{A_i f_{yi}} = C_e \frac{f_{y0}\, t_0}{f_{yi}\, t_i} \frac{Q_f}{\sin\theta_i} \qquad 4.18$$

For each type of joint, the efficiency parameter C_e given in the diagrams, is a function of the diameter ratio β and the chord diameter to thickness ratio $2\gamma = d_0/t_0$.

In case $d_1 \neq d_2$ for K joints, equation 4.18 has to be multiplied by $\frac{d_1 + d_2}{2d_i}$, in which d_i is the diameter of the considered brace.

The value of the parameter C_e in equation 4.18 gives the efficiency for the brace of a joint with $Q_f = 1.0$, a brace angle $\theta_i = 90°$ and the same wall thickness and design yield stress for chord and brace.

From the efficiency equation, it can be easily observed that yield stress and thickness ratio between chord and brace are extremely important for an efficient material use of the brace. Decreasing the angle θ_i increases the efficiency. The function Q_f depends on the chord stress. The efficiency formula shows directly that the following measures are favourable for the joint efficiency:

- brace wall thickness as small as possible ($t_i < t_0$), but limits for local buckling are to be satisfied
- higher strength steel for chords than for braces ($f_{y0} > f_{yi}$)
- angle $\theta_i << 90°$; hence, prefer K joints to N joints

Table 4.5 – Efficiency design chart for CHS T and Y joints

T and Y joints of circular hollow sections

Symbols	**Geometric range of validity**
$\beta = \frac{d_1}{d_0}$ $2\gamma = \frac{d_0}{t_0}$ 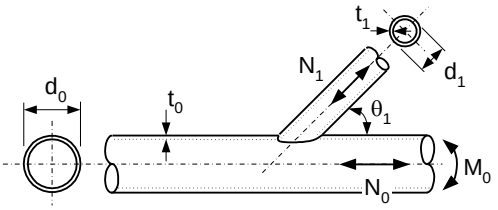	$0.2 \le \beta \le 1.0$ compression chord: class 1 or 2 and $2\gamma \le 50$ tension chord: $2\gamma \le 50$ compression brace: class 1 or 2 and $d_1/t_1 \le 50$ tension brace: $d_1/t_1 \le 50$ $t_1 \le t_0$ $\theta_1 \ge 30°$

Design chart

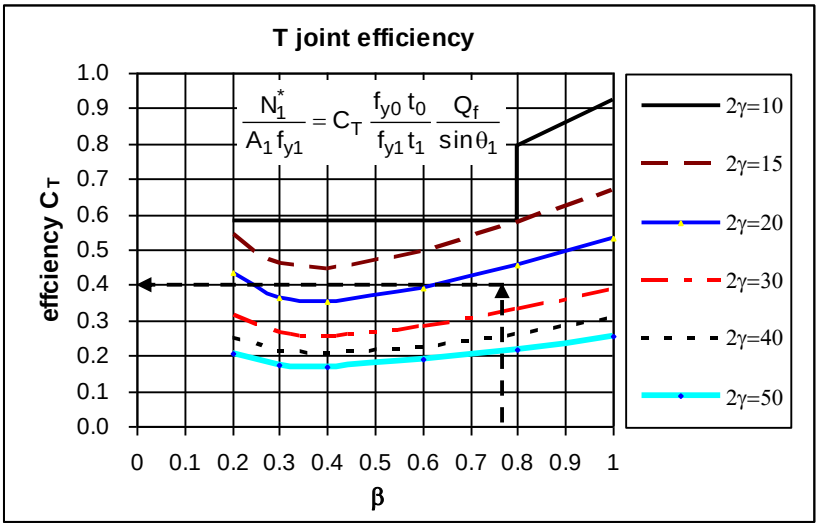

Calculation example

chord: Φ 219.1 x 10.0 $d_0/t_0 = 21.9$ $f_{y0} = f_{y1}$

brace: Φ 168.3 x 4.5 $d_1/t_1 = 37.4$ $\theta_1 = 90°$ $\sin\theta_1 = 1.0$

S355 $\beta = \frac{d_1}{d_0} = \frac{168.3}{219.1} = 0.77$

C_T = 0.40 and for n = -0.48 due to bending: $Q_f = 0.83$ (see figure 4.7)

$$\frac{N_1^*}{A_1 f_{y1}} = 0.40 \times \frac{10}{4.5} \times 0.83 = 0.74$$

Table 4.6 – Efficiency design chart for CHS X joints

X joints of circular hollow sections

Symbols	**Geometric range of validity**
$\beta = \frac{d_1}{d_0}$ $2\gamma = \frac{d_0}{t_0}$ 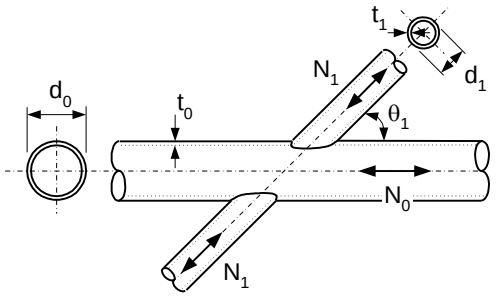	$0.2 \le \beta \le 1.0$ compression chord: class 1 or 2 and $2\gamma \le 40$ tension chord: $2\gamma \le 40$ compression brace: class 1 or 2 and $d_1/t_1 \le 50$ tension brace: $d_1/t_1 \le 50$ $t_1 \le t_0$ $\theta_1 \ge 30°$

Design chart

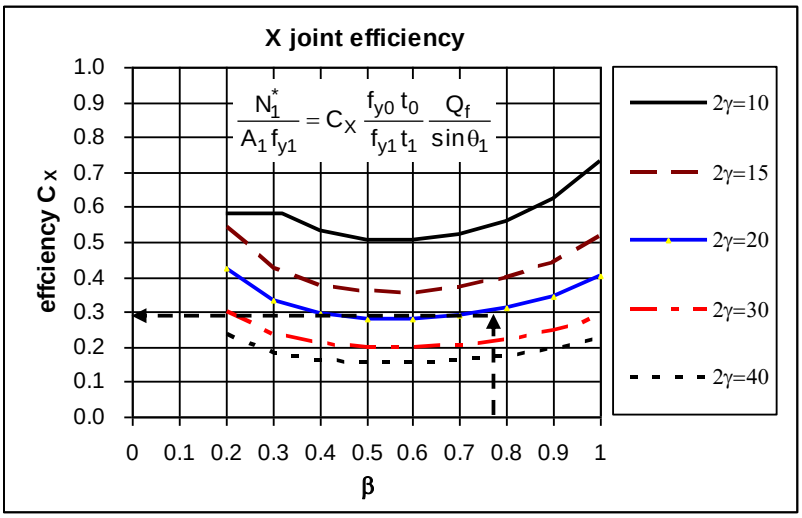

Calculation example

chord: Φ 219.1 x 10.0 $d_0/t_0 = 21.9$ $f_{y0} = f_{y1}$

brace: Φ 168.3 x 5.6 $d_1/t_1 = 30.0$ $\theta_1 = 90°$ $\sin\theta_1 = 1.0$

S355 $\beta = \frac{d_1}{d_0} = \frac{168.3}{219.1} = 0.77$

$C_X = 0.29$ and for n = -0.5 due to axial compression: $Q_f = 0.82$ (see figure 4.6)

$$\frac{N_1^*}{A_1 f_{y1}} = 0.29 \times \frac{10}{5.6} \times 0.82 = 0.42$$

Table 4.7 – Efficiency design charts for CHS K gap joints

K and N gap joints of circular hollow sections

Symbols	Geometric range of validity
$\beta = \frac{d_1 + d_2}{2d_0}$ $2\gamma = \frac{d_0}{t_0}$ $g' = \frac{g}{t_0}$ 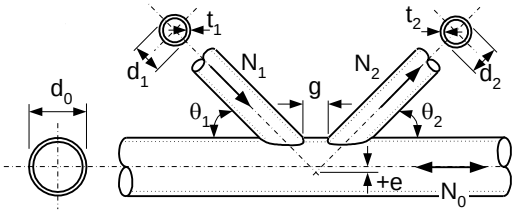	$0.2 \le \beta \le 1.0$ compression chord: class 1 or 2 and $2\gamma \le 50$ tension chord: $2\gamma \le 50$ compression brace: class 1 or 2 and $d_1/t_1 \le 50$ tension brace: $d_2/t_2 \le 50$ $t_i \le t_0$ $g \ge t_1 + t_2$ $\theta_i \ge 30°$ $\frac{e}{d_0} \le 0.25$

Design chart

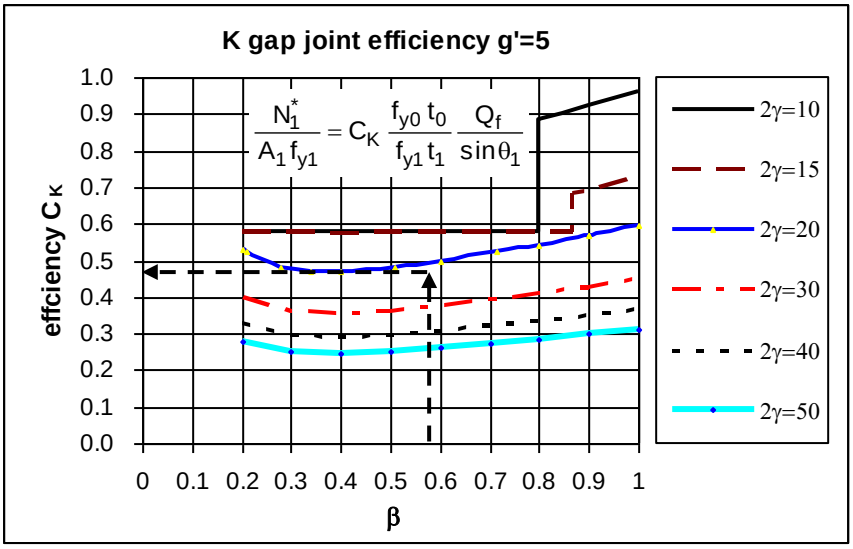

Calculation example

chord : Φ 219.1 x 10.0 — $d_0/t_0 = 21.9$ — $f_{y0} = f_{y1} = f_{y2}$

brace 1: Φ 139.7 x 6.3 — $d_1/t_1 = 22.2$ — e = 0 — g = 63 mm

brace 2: Φ 114.5 x 5.0 — $d_2/t_2 = 22.9$ — n = -0.7

$\theta_1 = \theta_2 = 40°$ — $\sin\theta_1 = \sin\theta_2 = 0.643$

n = -0.7 — $Q_f = 0.75$ (see figure 4.8) — g = 63 mm, thus $g' = \frac{63}{10} = 6.3$

$\beta = \frac{139.7 + 114.5}{2 \times 219.1} = 0.58$ with $\frac{d_1 + d_2}{2d_i} = 0.91$ for brace 1, and 1.11 for brace 2

C_K = 0.46

$\frac{N_1^*}{A_1 f_{y1}} = 0.46 \times \frac{10}{6.3} \times \frac{1}{0.643} \times 0.75 \times 0.91 = 0.77$ $\frac{N_2^*}{A_2 f_{y2}} = 0.46 \times \frac{10}{5} \times \frac{1}{0.643} \times 0.75 \times 1.11 > 1.0$

Table 4.7 – Efficiency design charts for CHS K gap joints (continued)

K and N gap joints of circular hollow sections

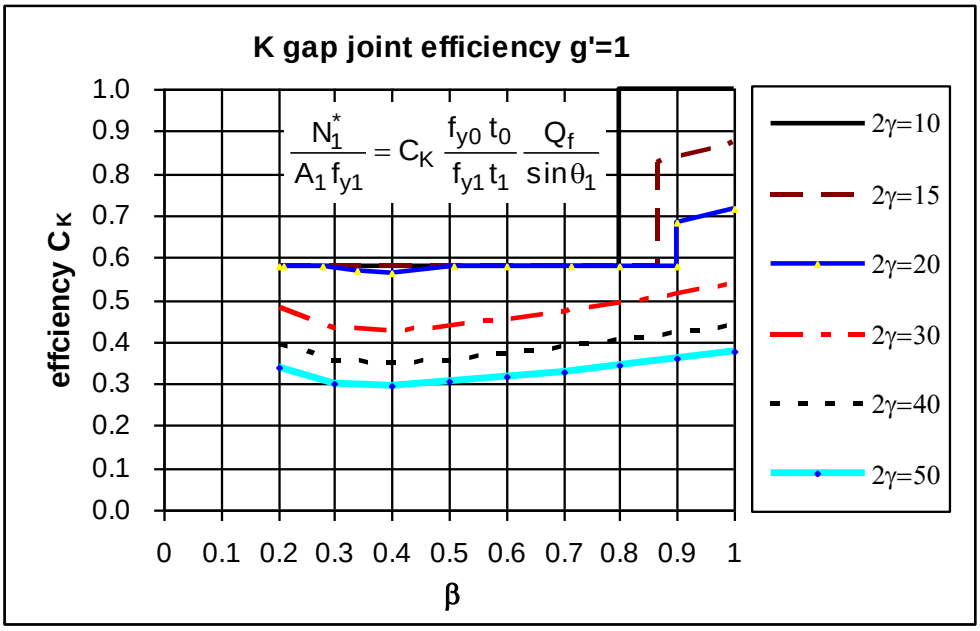

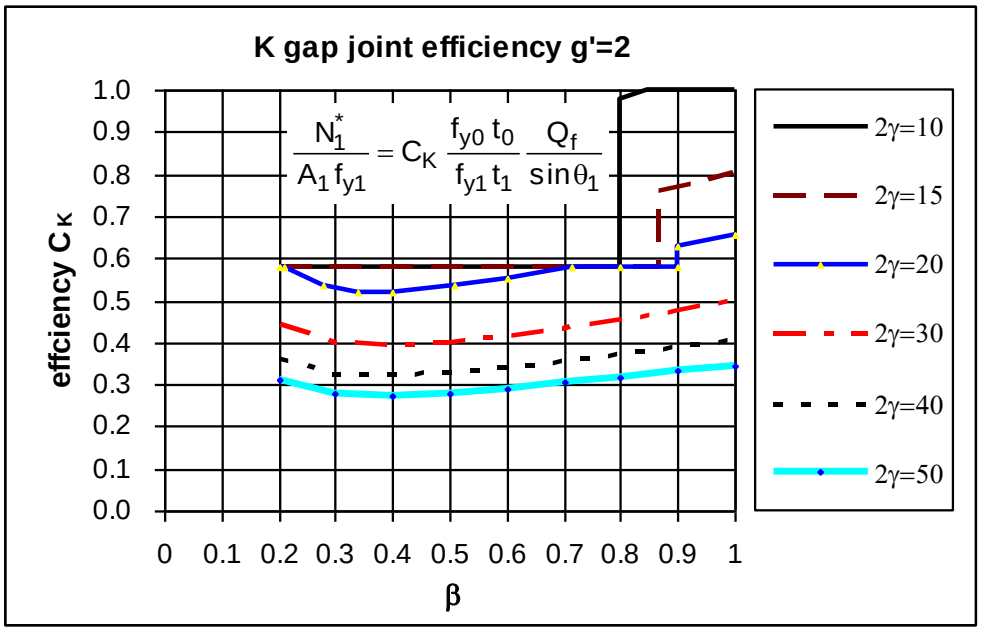

Table 4.7 – Efficiency design charts for CHS K gap joints (continued)

K and N gap joints of circular hollow sections

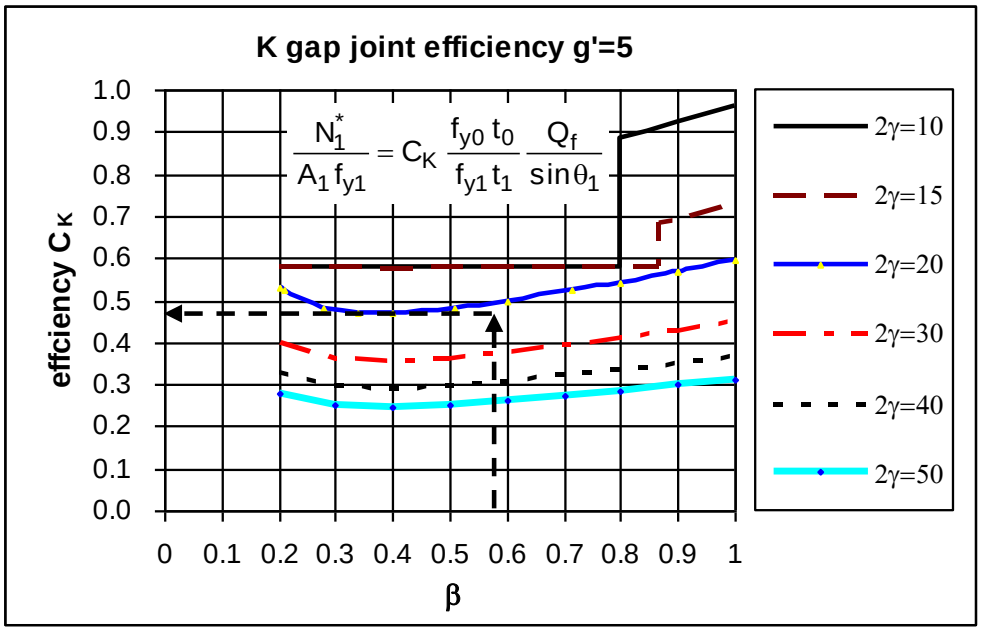

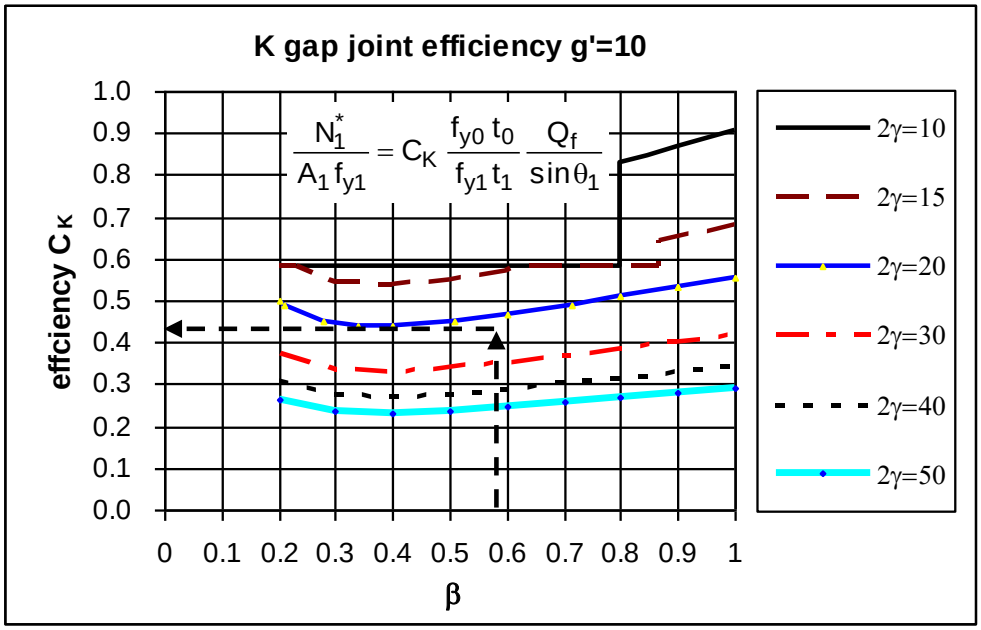

Table 4.8 – Efficiency design chart for CHS K overlap joints ($25\% \le Ov \le Ov_{limit} = 60\%$ or 80%)

K and N overlap joints of circular hollow sections

Symbols	**Geometric range of validity**
$2\gamma = \frac{d_0}{t_0}$ 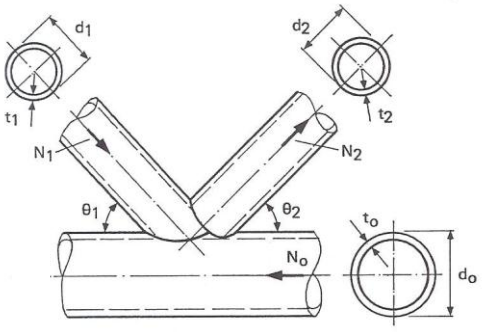 For the configuration shown: compression brace 1 = overlapped member j tension brace 2 = overlapping member i	$\frac{d_i}{d_0}$ and $\frac{d_j}{d_0} \ge 0.2$ $\quad \frac{d_i}{d_j} \ge 0.75$ $\frac{t_i}{t_0}$ and $\frac{t_j}{t_0} \le 1.0$ $\quad \frac{t_i}{t_j} \le 1.0$ compression chord: class 1 or 2 and $2\gamma \le 50$ tension chord: $2\gamma \le 50$ compression brace: class 1 or 2 and $d_1/t_1 \le 50$ tension brace: $d_2/t_2 \le 50$ θ_i and $\theta_j \ge 30°$ $25\% \le Ov \le Ov_{limit} = 60\%$ or 80%

Design chart

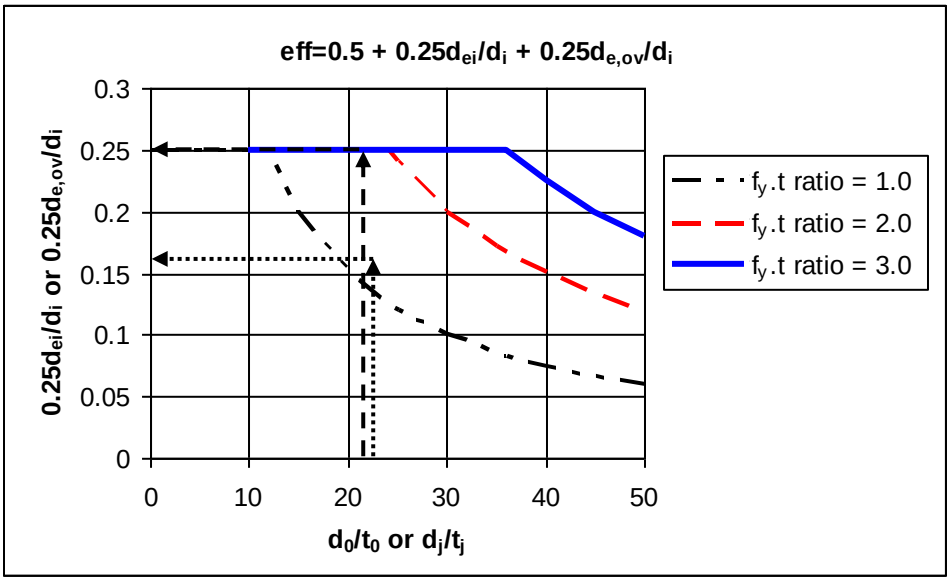

Table 4.8 – Efficiency design chart for CHS K overlap joints (25% ≤ Ov ≤ Ov_{limit} = 60% or 80%) (continued)

Calculation example		
chord : Φ 219.1 x 10.0	d_0/t_0 = 21.9	$f_{y0} = f_{y1} = f_{y2}$
brace 1: Φ 139.7 x 6.3	d_j/t_j = 22.2	
brace 2: Φ 114.5 x 5.0	d_i/t_i = 22.9	Ov = 50%

For Ov = 50%, besides member checks, only local yielding of the overlapping brace needs to be checked:

$\frac{f_{y0}\ t_0}{f_{yi}\ t_i} = \frac{10}{5.0} = 2.0$ thus, with d_0/t_0 = 21.9: $0.25d_{ei}/d_i = 0.25$

$\frac{f_{yj}\ t_j}{f_{yi}\ t_i} = \frac{6.3}{5.0} = 1.2$ thus, with d_j/t_j = 22.2: $0.25d_{e,ov}/d_i = 0.16$

Hence, the brace efficiency for both braces is:

Eff. = $0.50 + 0.25d_{ei}/d_i + 0.25d_{e,ov}/d_i$

= 0.50 + 0.25 + 0.16 = 0.91

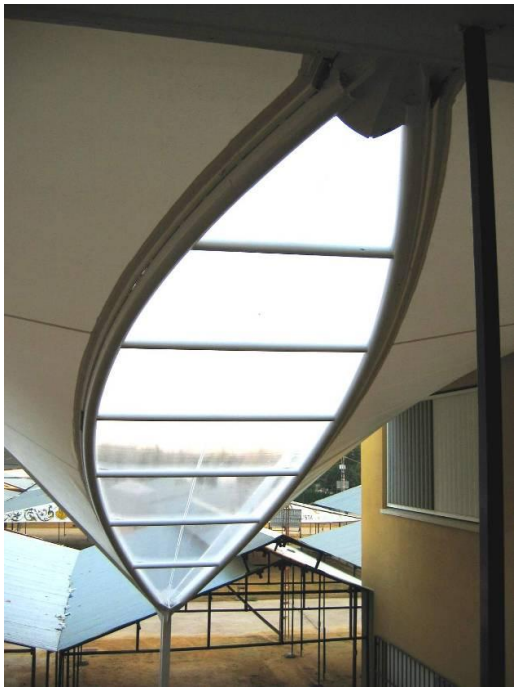

Eye shaped curved CHS roof structure

5 Welded CHS to CHS joints under moment loading

5.1 Joints with brace(s) subjected to in-plane or out-of-plane bending moment

One should distinguish between primary bending moments due to noding eccentricities (figure 1.2) needed for the equilibrium with the external loading and secondary bending moments due to end fixities of the joint members as a result of induced deformations in the structural system. In principle, the secondary moments are not needed for the equilibrium with the external loading e.g. the secondary moments in members of lattice girders. As already mentioned in chapter 1, these secondary moments do not influence the load bearing capacity of lattice girders if the joints have sufficient deformation capacity, i.e. within the parameter limits given in tables 4.1 and 4.3. The moments due to noding eccentricity in lattice girders may be assumed to be taken by the chord members.

Joints predominantly loaded by in-plane bending moments are generally of the T-type and called Vierendeel joints (figure 5.1(a)). These joints also exist in framed structures.

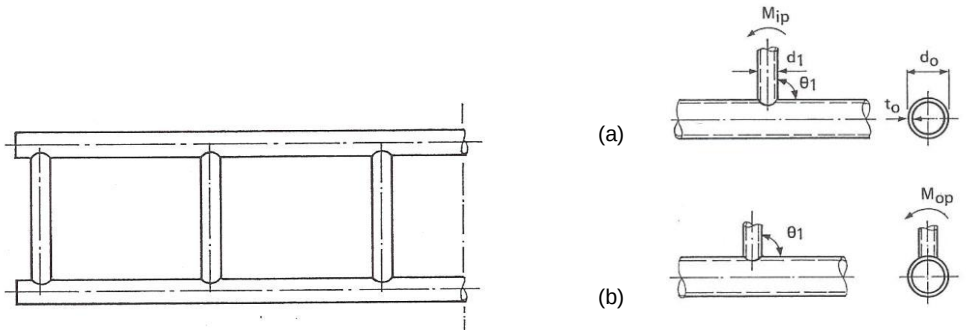

Figure 5.1 – Uniplanar Vierendeel joints

Out-of-plane bending moments (figure 5.1(b)) are not very common in uniplanar structures; this type of loading generally appears more frequently in multiplanar structures.

The formulae in table 5.1 for chord plastification and chord punching shear can be used within the range of validity given in table 4.1, except *all* braces must be class 1 or 2. These formulae have been based on the reanalyses by IIW-XV-E (van der Vegte et al., 2008a, 2008b; Qian et al., 2008).

In a similar manner to axially loaded joints, the joint moment capacity formulae are also presented in efficiency design charts (figures 5.2 and 5.3). The joint efficiencies C_{ip} or C_{op} give the joint moment design strength divided by the plastic moment capacity $W_{pl,1} f_{y1}$ of the brace. The efficiency is limited by the punching shear moment capacity which, for $\theta_1 = 90°$, results in an efficiency factor of 0.58. These diagrams show that in most cases the in-plane bending moment resistance is significantly larger than that for out-of-plane bending.

It should be noted that the joint rotational stiffness C (moment per radian) may considerably influence the moment distribution in statically indeterminate structural systems, e.g. portal frames and Vierendeel trusses. If rigid joints are required, it is recommended to choose a β ratio near 1.0 or low d_0/t_0 ratios in combination with high t_0/t_1 ratios.

Figures 5.4 and 5.5 give, based on the work of Efthymiou (1985), a graphical presentation of the rotational joint stiffness C of T joints for in-plane and out-of-plane bending moments. More detailed information about the joint flexibility for axial loading and bending moments can be found in Buitrago et al. (1993) and in Dier and Lalani (1995). This information may be especially helpful in case of fatigue design for an exact determination of the bending moments in the members.

Table 5.1 – Limit states criteria for CHS joints loaded by brace bending moments

Criterion to be checked	**Joints with CHS braces and chord loaded by brace bending moments** (*)	
Design strength: chord plastification	$M_1^* = Q_u\, Q_f\, \frac{f_{y0}\, t_0^2}{\sin\theta_1}\, d_1$ eq. 5.1	
Design strength: chord punching shear (only for $d_1 \le d_0 - 2t_0$)	$M_1^* = 0.58\, f_{y0}\, d_1^2\, t_0\, \frac{k_b}{\sin\theta_1}$ eq. 5.2	
	Brace in-plane bending: $k_b = \frac{1 + 3\sin\theta_1}{4\sin\theta_1}$ eq. 5.3	Brace out-of-plane bending: $k_b = \frac{3 + \sin\theta_1}{4\sin\theta_1}$ eq. 5.4

(*) The equations in table 5.1 may also be used for K gap joints (if brace moments have to be considered, see section 1.2.2), by checking that the brace utilization due to bending plus the brace utilization due to axial load ≤ 0.8. For K overlap joints, no evidence exists.

Function Q_u		
	Brace in-plane bending	**Brace out-of-plane bending**
T, Y, X joints 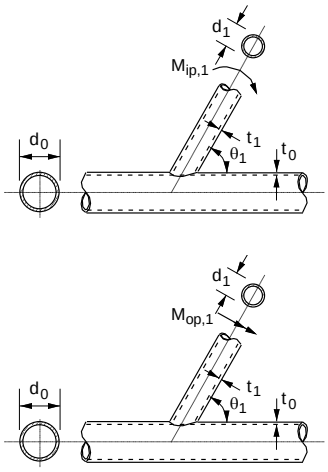	$Q_u = 4.3\,\beta\,\gamma^{0.5}$ eq. 5.5	$Q_u = 1.3\left(\frac{1+\beta}{1-0.7\beta}\right)\gamma^{0.15}$ eq. 5.6

Function Q_f		
	$Q_f = (1 - \lvert n \rvert)^{C_1}$ with eq. 4.7 $n = \frac{N_0}{N_{pl,0}} + \frac{M_0}{M_{pl,0}}$ in connecting face	
	Chord compression stress (n < 0)	**Chord tension stress (n ≥ 0)**
T, Y, X joints	$C_1 = 0.45 - 0.25\beta$	$C_1 = 0.20$

Range of validity	Same as table 4.1

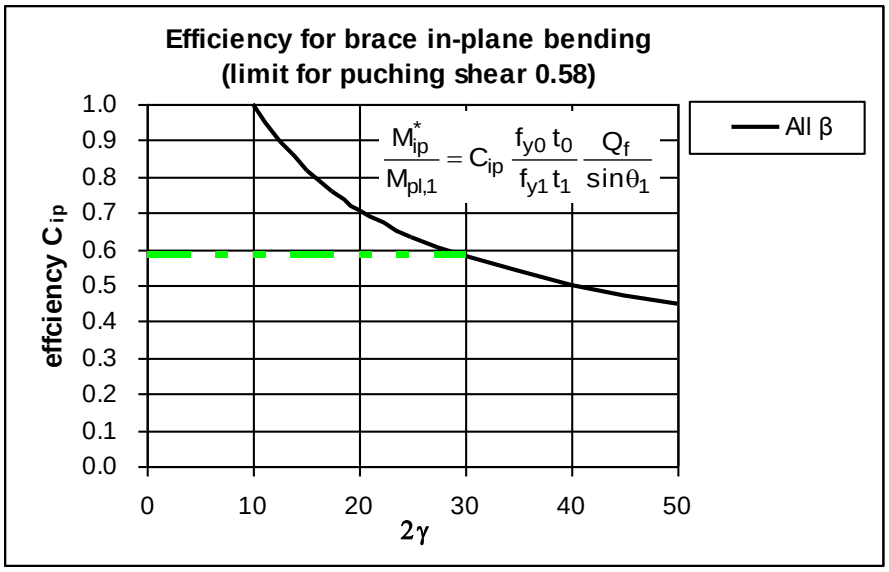

Figure 5.2 – Efficiency design chart for joints loaded by brace in-plane bending moment

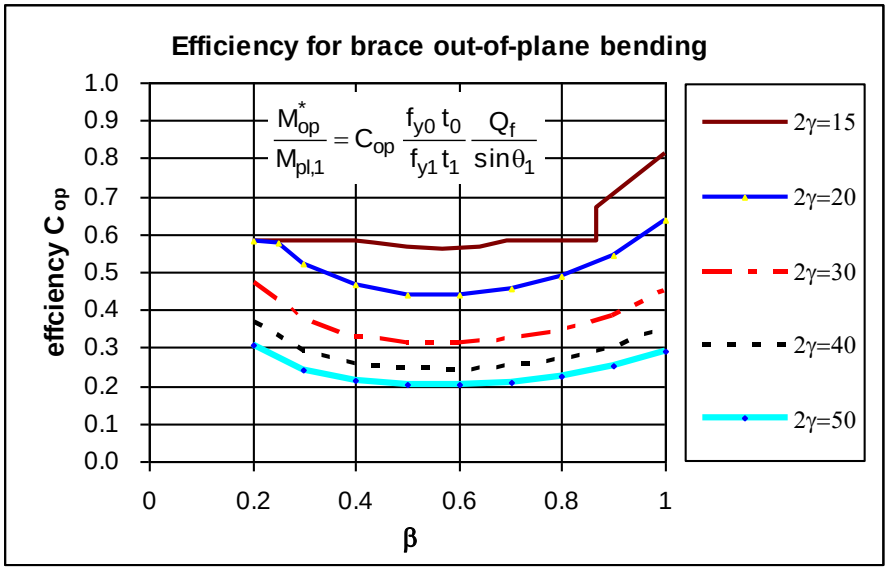

Figure 5.3 – Efficiency design chart for joints loaded by brace out-of-plane bending moment

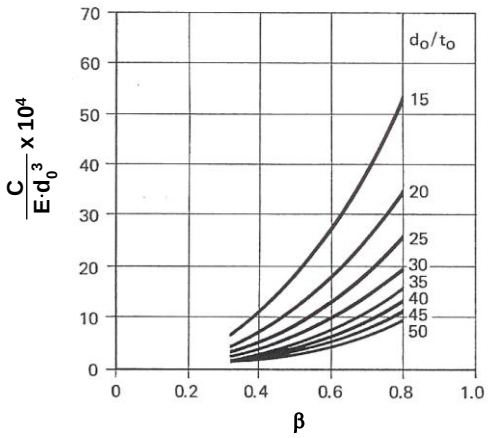

Figure 5.4 – Joint stiffness for brace in-plane bending moments of T joints

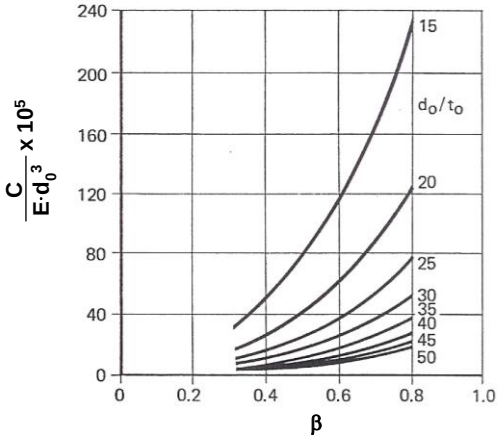

Figure 5.5 – Joint stiffness for brace out-of-plane bending moments of T joints

5.2 T and X joints with brace(s) subjected to combinations of axial load, in-plane bending and out-of-plane bending moment

Especially in three dimensional structures, the joints may be loaded by combinations of axial loading and bending moments. Investigations have shown that in-plane bending is less severe than out-of-plane bending and a reasonable simplified lower bound interaction function is based on the work of Hoadley and Yura (1985):

$$\frac{N_1}{N_1^*} + \left(\frac{M_{ip,1}}{M_{ip,1}^*} \right)^2 + \frac{M_{op,1}}{M_{op,1}^*} \leq 1.0 \qquad 5.7$$

in which N_1, $M_{ip,1}$ and $M_{op,1}$ are the (brace) loads acting, and N_1^* , $M_{ip,1}^*$ and $M_{op,1}^*$ are the design strengths. It should be noted that the joint stiffnesses given in figures 5.4 and 5.5 can be affected considerably by the presence of axial loading (Stol et al., 1985). However, insufficient test evidence is available for a more precise recommendation.

5.3 Knee joints

Some special types of joints are illustrated in figure 5.6 for frame corners. These knee joints have been investigated at the University of Karlsruhe by Karcher and Puthli (2001), who recommend these joints to be designed based on the following requirements for both members:

$$\frac{N}{N_{pl,0}} + \frac{M}{M_{pl,0}} \leq \alpha \qquad 5.8$$

$$\alpha = (0.05\, d_0/t_0 + 0.77)^{-1.2}\, (235/f_{y0})^{0.5} \qquad 5.9$$

The term α is a stress reduction factor, which can be taken as 1.0 for mitred joints with stiffening plates. For the mitred joints without stiffening plates, α is a function of the cross sectional parameters as shown in figure 5.7 and equation 5.9. The steel grade with S in figure 5.7 refers to the nominal yield stress.

Based on previous work of Mang et al. (1997), it is recommended that for joints without stiffening plates, the shear force V and the axial force N in the members should not exceed:

$$\frac{V}{V_{pl,0}} \le 0.5 \text{ and } \frac{N}{N_{pl,0}} \le 0.2 \qquad 5.10$$

For mitred knee joints with angles $\theta > 90°$, the same recommendations as for $\theta = 90°$ can be adopted (Karcher and Puthli, 2001).

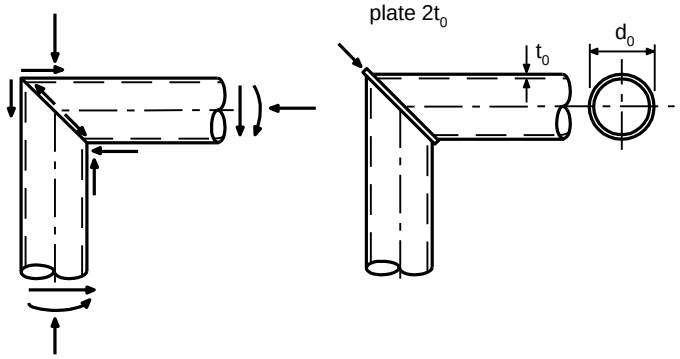

Figure 5.6 – CHS knee joints

Although the unstiffened joints have been investigated for $10 \le d_0/t_0 \le 100$, it is recommended that for structural applications, d_0/t_0 is restricted to class 1 sections.

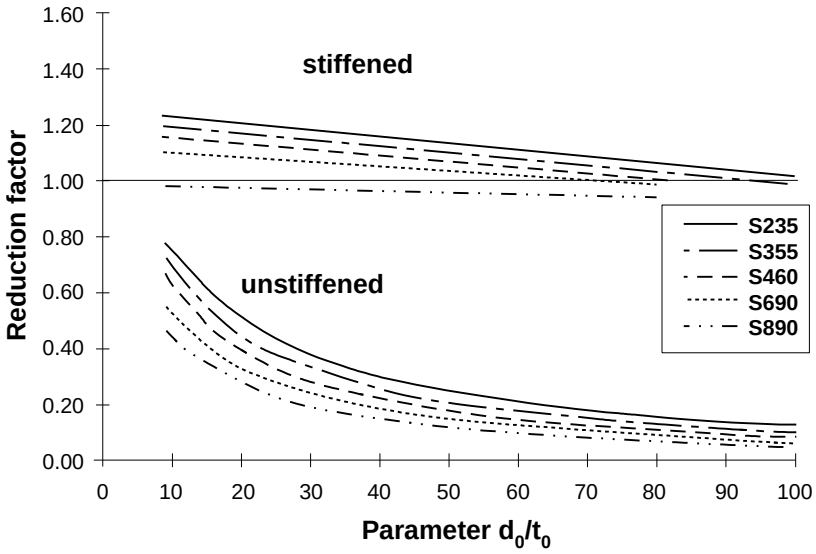

Figure 5.7 – Stress reduction factor α, for unstiffened mitred CHS knee joints

The joints with a stiffening plate can be considered to be rigid, whereas the stiffness behaviour of the unstiffened joints depends on the d_0/t_0 ratio. The unstiffened joints can only be assumed to be rigid for very low d_0/t_0 ratios. No formulae for the joint stiffness are available.

For those structural applications where a reasonable strength, stiffness and rotational capacity are required, it is recommended that a stiffened joint with class 1 sections is used. For other structural applications, it is recommended to use unstiffened joints only if the sections satisfy at least the plastic design requirements. The stiffening plate thickness should satisfy $t_p > 2t_0$ and not be taken smaller than 10 mm.

6 Multiplanar welded joints

6.1 TT and XX joints

Multiplanar joints are frequently used in tubular structures, e.g. in towers, offshore jacket structures, triangular or quadrangular girders, etc.

Tests have been carried out on double T joints (TT joints) with a 90° included angle between both braces loaded in compression (table 6.1). Compared to the strength of uniplanar joints, the multiplanar joint strength did not vary substantially, although the stiffness increased considerably (Mitri et al., 1987).

Further work in this field has been carried out by Paul et al. (1989, 1992) and van der Vegte (1995). Based on the results of these studies, simple guidelines can be given.

One can imagine that the multiplanar effects are most substantial for double X joints as shown in figure 6.1. Finite element calculations have shown that multiplanar loading has a substantial influence on the strength and stiffness as compared to a uniplanar X joint. In the case where the loads acting in one plane have the same magnitude as those in the other plane, but with an opposite sense (e.g. compression vs. tension), the joint strength may drop by about 1/3 compared to the uniplanar joint (see figure 6.1). On the other hand, for loadings with the same sense, the joint strength increases considerably. However, this increase in strength may be accompanied by a reduction in deformation and rotation capacity. A conservative assumption will be to adopt the same percentage increase in strength for loads in the same sense as the percentage reduction for opposite loads.

6.2 KK joints

For K joints in triangular girders, shown in figure 6.2, various tests have been carried out by Makino et al. (1984) and Paul (1992). The proposed interaction equation can simply be replaced by a constant of 0.9, to be applied to the strength of uniplanar joints and adopted in the previous recommendations, see table 10.3. However, the proposals were based on analyses taking account of the chord prestress. The reanalyses showed that the reduction is due to the larger chord force. Hence, in the new recommendations in table 6.1, the correction factor to be applied to the formulae in table 4.1 is 1.0 and the reduction effect is included in the Q_f function.

6.3 Design recommendations

Design rules covering multiplanar effects are given only by AWS (2006). However, the formulation is developed on elastic considerations and, depending on the configuration and loading of the joints, may be unreliable for strength predictions.

Based on the existing evidence, it is recommended to design multiplanar joints using the range of validity and formulae for uniplanar joints given in tables 4.1 and 4.3 with the correction factors in table 6.1.

Similar recommendations (table 10.3) with exception of the factor for KK joints, have also been adopted by Eurocode 3, but are related to the formulae summarized in table 10.1.

brace Φ 399 x 10 chord Φ 1006 x 25	brace Φ 599 x 10 chord Φ 1006 x 25	
β = 0.4	β = 0.6	
1 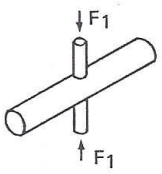	2 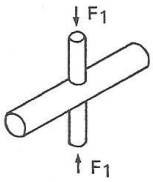	
3 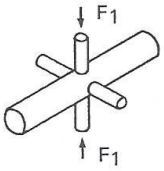	4 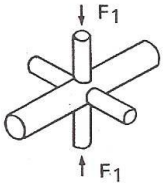	
5 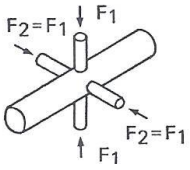	6 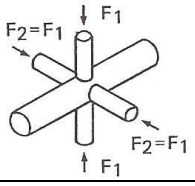	
	7 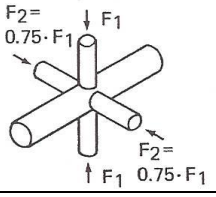	
8 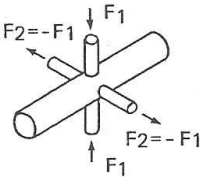	9 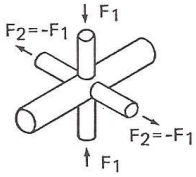	

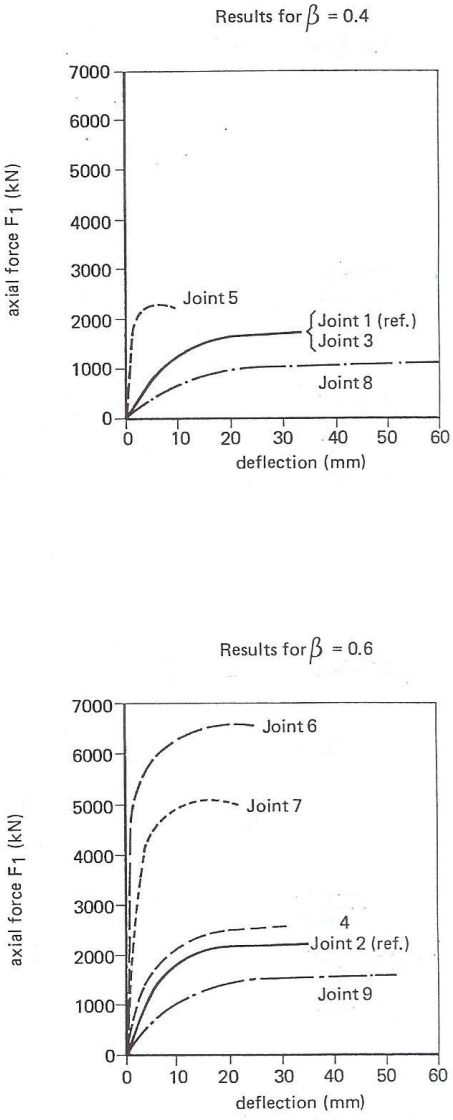

Figure 6.1 – Multiplanar X joints

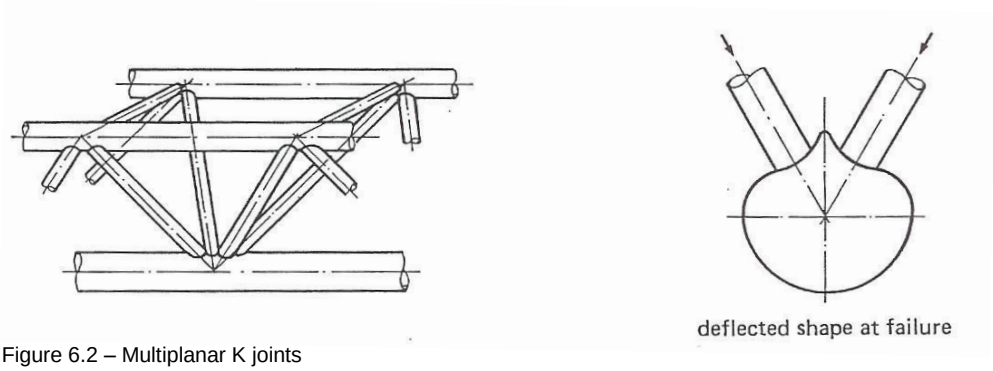

Figure 6.2 – Multiplanar K joints

Table 6.1 – Correction factors for multiplanar joints

Type of joint	**Correction factor μ to uniplanar joint strength**
TT joints 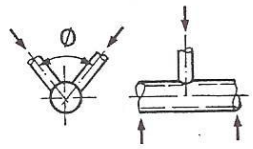	μ = 1.0
XX joints 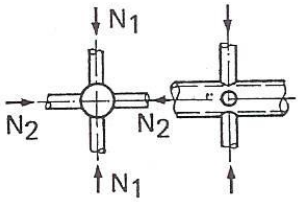	$\mu = 1 + 0.35 \frac{N_2}{N_1}$ eq. 6.1 Notes: - Take account of the sign of N_2 and N_1, with $\|N_1\| \geq \|N_2\|$ - N_2/N_1 is negative if the members in one plane are in tension and in the other plane in compression.
KK gap joints 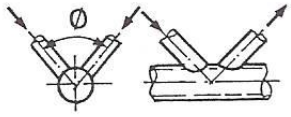	μ = 1.0 Note: In a gap joint, the cross section in the gap has to be checked for shear failure: $\left(\frac{N_{gap,0}}{N_{pl,0}}\right)^2 + \left(\frac{V_{gap,0}}{V_{pl,0}}\right)^2 \leq 1.0$ eq. 6.2 where: $N_{gap,0}$ = axial force in gap $N_{pl,0} = A_0 f_{y0}$ $V_{gap,0}$ = shear force in gap $V_{pl,0} = 0.58 f_{y0} \frac{2A_0}{\pi}$
Range of validity	Same as table 4.1 $60° \leq \phi \leq 90°$

7 Welded plate, I, H or RHS to CHS chord joints

7.1 Plate, I, H or RHS to CHS chord joints

The capacity of joints between plates, I sections and RHS sections as braces and a CHS chord, as illustrated in figure 7.1, is directly related to that of joints between CHS braces and chords. The database is mainly based on tests carried out in Japan (Kurobane, 1981; Wardenier, 1982; Makino et al., 1991).

Initially in the reanalysis by IIW-XV-E, the functions Q_u were directly related to the joints with CHS braces and chords in such a way that the resulting formulae in table 7.1 give for medium β and γ ratios, about the same capacity as the previous IIW (1989) formulae, summarized in table 10.4. However, a more detailed analysis (Wardenier et al., 2008b) revealed that large discrepancies exist between the various data sets. Therefore, the constant is reduced from 2.6 to 2.2. Further, compared to the recommendations in the 1st edition of this Design Guide, the η function has been marginally changed from $(1+0.25\eta)$ to $(1+0.4\eta)$, and a factor 0.8 is included in the Q_u function for in-plane bending of the joints with a longitudinal plate. The Q_f factors for chord compression loading are based on the work of de Winkel (1998) while for chord tensile loading, the functions for CHS joints are adopted.

The range of validity of the formulae given in table 7.1, is similar to that for CHS joints, except that the width of transverse plates is limited to $\beta \geq 0.4$ and the length of longitudinal plates to $1 \leq \eta \leq 4$.

For a plate to CHS joint, for punching shear, the chord at both sides of a plate is effective, resulting in equation 7.2. However, for an RHS or I section brace (subjected to axial loading or out-of-plane bending), the part between the flanges cannot contribute to the capacity, giving equation 7.1.

For transverse plates, the line of action of the force is in line with the plate. Hence, the angle θ_1 is equal to the angle of the force acting on the plate. For longitudinal plates, even though the plate can be at 90° to the chord, the axial force can be pulling at a different angle on the plate. Apparently this is a common situation with tension cables connected to hollow sections via plates. As a result, for longitudinal plates, the angle θ_1 should also be taken to the line of action of the force.

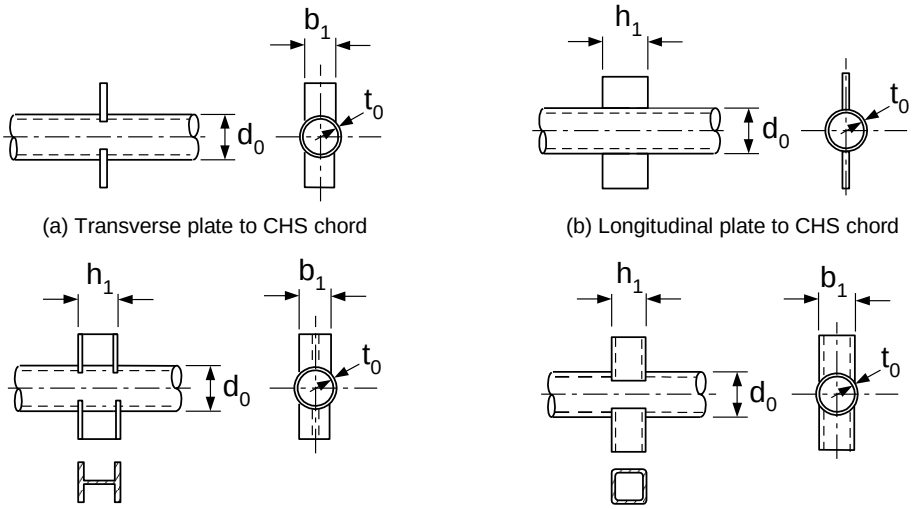

(a) Transverse plate to CHS chord

(b) Longitudinal plate to CHS chord

(c) I section to CHS chord

(d) RHS section to CHS chord

Figure 7.1 – Plate, I and RHS to CHS chord joints

Table 7.1 – Limit states criteria for joints with plate, I or RHS braces to CHS chord

Joints with plate, I or RHS braces to CHS chord		
Criterion to be checked	**Brace axial load**	**Brace bending moment**
Design strength: chord plastification	$N_1^* = Q_u\, Q_f\, \frac{f_{y0}\, t_0^2}{\sin\theta_1}$ eq. 4.1	$M_1^* = Q_{ub}\, Q_f\, f_{y0}\, t_0^2\, h_1$ eq. 5.1a
Design strength: chord punching shear (only for $b_1 \le d_0 - 2t_0$)	For I section with $\eta \le 2$ (for axial loading and brace out-of-plane bending) and RHS section: $\frac{N_1}{A_1} + \frac{M_{ip,1}}{W_{el,ip,1}} + \frac{M_{op,1}}{W_{el,op,1}} \le 0.58 f_{y0} \frac{t_0}{t_1}$ eq. 7.1	
	All other cases: $\frac{N_1}{A_1} + \frac{M_{ip,1}}{W_{el,ip,1}} + \frac{M_{op,1}}{W_{el,op,1}} \le 1.16 f_{y0} \frac{t_0}{t_1}$ eq. 7.2	

		Function Q_u	**Function Q_{ub} in terms of Q_u**	
Type of joint CHS chord with:		**Brace axial load**	**Brace in-plane bending**	**Brace out-of-plane bending**
Transverse plate (*) (**) 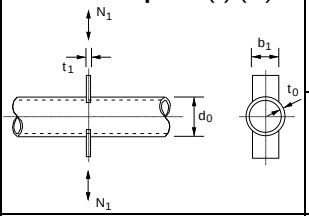	**X**	$Q_u = 2.2\left(\frac{1+\beta}{1-0.7\beta}\right)\gamma^{0.15}$ eq. 7.3	$Q_{ub} = 0$	$Q_{ub} = 0.5 Q_u \frac{b_1}{h_1}$
	T	$Q_u = 2.2\left(1+6.8\beta^2\right)\gamma^{0.2}$ eq. 7.4	$Q_{ub} = 0$	$Q_{ub} = 0.5 Q_u \frac{b_1}{h_1}$
Longitudinal plate (**) 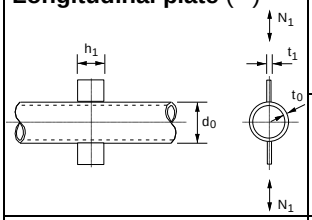	**X**	$Q_u = 5\left(1+0.4\eta\right)$ eq. 7.5	$Q_{ub} = 0.8 Q_u$	$Q_{ub} = 0$
	T			
I or RHS (*) 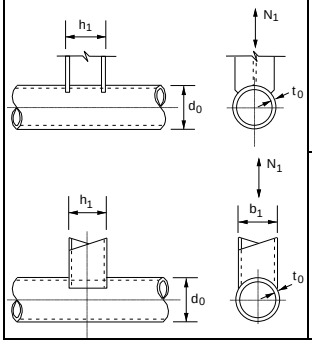	**X**	$Q_u = 2.2\left(\frac{1+\beta}{1-0.7\beta}\right)\left(1+0.4\eta\right)\gamma^{0.15}$ eq. 7.6	$Q_{ub} = \frac{Q_u}{1+0.4\eta}$	$Q_{ub} = 0.5 Q_u \frac{b_1}{h_1}$
	T	$Q_u = 2.2\left(1+6.8\beta^2\right)\left(1+0.4\eta\right)\gamma^{0.2}$ eq. 7.7	$Q_{ub} = \frac{Q_u}{1+0.4\eta}$	$Q_{ub} = 0.5 Q_u \frac{b_1}{h_1}$

(*) The chord should also be checked for shear failure for:
X joints with transverse plates and angles $\theta_1 < 90°$
X joints with RHS or I section brace members and $\cos\theta_1 > h_1/d_0$

(**) For transverse and longitudinal plates: *θ_1 = angle of the force acting on the plate*

Table 7.1 – Limit states criteria for joints with plate, I or RHS braces to CHS chord (continued)

Function Q_f		
	$Q_f = (1-\lvert n\rvert)^{C_1}$ with eq. 7.8 $n = \frac{N_0}{N_{pl,0}} + \frac{M_0}{M_{pl,0}}$ in connecting face	
	Brace axial load **Brace in-plane bending and out-of-plane bending**	
	Chord compression stress (n < 0)	**Chord tension stress (n ≥ 0)**
All joints	$C_1 = 0.25$	$C_1 = 0.20$

Range of validity			
General	$0.2 \le \frac{b_1}{d_0} \le 1.0$	$\theta_1 \ge 30°$ (**)	$f_{y1} \le f_{y0}$ $f_y \le 0.8 f_u$ $f_y \le 460$ N/mm^2 (***)
CHS chord	**Compression**	class 1 or 2 (****) and $2\gamma \le 50$ (for X joints: $2\gamma \le 40$)	
	Tension	$2\gamma \le 50$ (for X joints: $2\gamma \le 40$)	
RHS braces	**Compression**	class 1 or 2 (****) and $b_1/t_1 \le 40$ and $h_1/t_1 \le 40$	
	Tension	$b_1/t_1 \le 40$ and $h_1/t_1 \le 40$	
I section braces	**Compression**	class 1 or 2 (****)	
	Tension	none	
Transverse plate	$\beta = \frac{b_1}{d_0} \ge 0.4$		
Longitudinal plate	$1 \le \eta = \frac{h_1}{d_0} \le 4$		

(***) For $f_{y0} > 355$ N/mm^2, see section 1.2.1
(****) Section class limitations for CHS in compression are given in table 4.2
Section class limitations for RHS and I sections in compression are defined in table 1.1

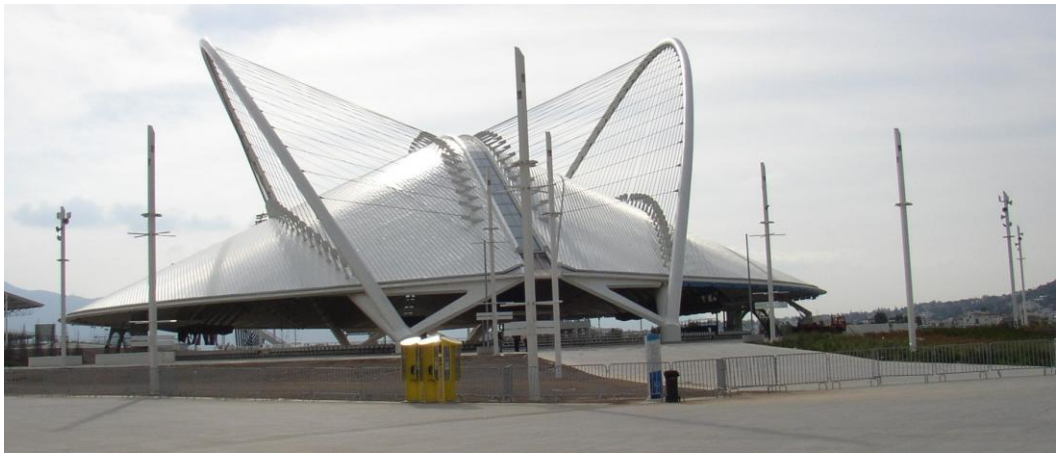

CHS arches

7.2 Longitudinal plate joints under shear loading

This type of joint is primarily found in “simple” shear joints for example to hollow section columns, where the plate is typically referred to as a “shear tab” or “fin plate”. A simple criterion to avoid a punching shear failure is to ensure that the tensile resistance of the tab (per unit plate length) is less than the shear resistance of the CHS wall along two planes (per unit plate length). This is, based on CHS columns, achieved if:

$$t_p < 1.16 \frac{f_{y0}}{f_{yp}} t_0 \qquad 7.9$$

This design check is valid for CHS members that do not have slender cross-sections (i.e. which are not thin-walled; i.e. are not class 4 according to Eurocode 3 (CEN, 2005a)). Further information regarding this detail is provided in CIDECT Design Guide No. 9 (Kurobane et al., 2004).

7.3 Gusset plate to slotted CHS joints

Single gusset plates, slotted into the ends of hollow section members and concentrically aligned with the axis of the member, as shown in figures 7.2 and 7.3, are commonly found in diagonal brace members of steel framed buildings and also in roof web-to-chord member joints.

Slotted CHS joints are noted by the presence (or lack) of an open slot at the end of the slotted CHS. An open slot allows for liberal construction and fabrication tolerances, if the longitudinal welds are performed on site. If the gusset plate bears against the end of the slot (common for shop fabrication) the ends of the gusset plate are typically welded with “end return welds”.

Two possible failure modes have been identified for gusset plate-to-slotted CHS joints loaded in tension: circumferential failure (CF) of the CHS (see figure 7.2) and tear out (TO) – or “block shear” – failure of the CHS (see figure 7.3). As a consequence of only part of the CHS cross-section being connected, an uneven stress distribution around the CHS perimeter always occurs during load transfer at the connection. This phenomenon, known as shear lag, is illustrated in figure 7.2 and is principally influenced by the weld length, L_w, or the “stick-in length”. For long weld lengths shear lag effects become negligible, while for short weld lengths ($L_w / w < 0.7$) with $w = 0.5\pi d_i - t_p$ tear out governs over circumferential fracture of the CHS.

These connection types have been studied by a number of researchers, including Ling et al. (2007a, 2007b), Packer (2006) and Martinez Saucedo and Packer (2006). For both cases illustrated in figure 7.2, Martinez Saucedo and Packer (2006) have shown that the CHS circumferential failure limit state design resistance in tension can be determined by equation 7.10.

$$N_i^* = 0.9\, A_n f_{ui} \left(1 - \frac{1}{\left[1 + \left(\frac{L_w}{w} \right)^{2.4} \right]^{5.7}} \right) \qquad \text{for } L_w / w \geq 0.7 \qquad 7.10$$

For the CHS tear out limit state (see figure 7.3), the design resistance in tension can be determined by summing the fracture resistance of the net area in tension and the resistance of the gross area in shear (Martinez Saucedo and Packer, 2006), see equation 7.11.

$$N_i^* = 0.9 \left(A_{nt} f_{ui} + 0.58 A_{gv} \left(\frac{f_{yi} + f_{ui}}{2} \right) \right) \qquad \text{for } L_w / w < 0.7 \qquad 7.11$$

Depending on the weld length, L_w, only one of these two limit states (failure modes) needs to be checked. The 0.9 factor in these equations represents a $1/\gamma_M = \phi$ term. As indicated in figure 7.2(a)

and figure 7.3(a), when there is an opening at the end of the slot, cracking starts at the end of the weld. Thus, under static loading, the cutting of the slot end does not need to be smooth, drilled or machined, and some roughness is tolerable.

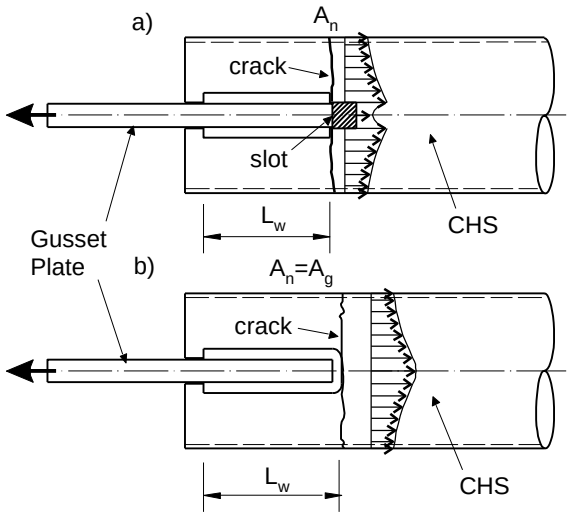

Figure 7.2 – Gusset plate-to-slotted CHS joints: Circumferential failure (CF) with a) longitudinal welds only and b) with longitudinal welds plus a weld return

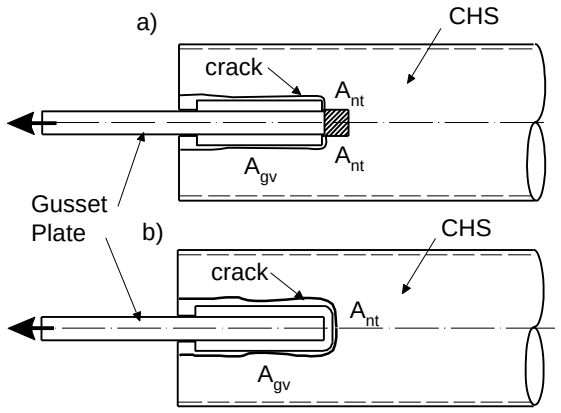

Figure 7.3 – Gusset plate-to-slotted CHS joints: Tear out (TO) failure with a) longitudinal welds only and b) with longitudinal welds plus a weld return

For the CHS circumferential failure limit state design resistance in compression, separate equations are given but for simplicity equations 7.10 and 7.11 can conservatively be used. In the case of a typical long compression member, member failure will govern.

An easy way to design these joints, for tension and compression, is to ensure that $L_w \geq 1.3d_i$ which will ensure that a capacity equal to or larger than the yield capacity of the CHS member is provided.

In Martinez Saucedo and Packer (2006), equations are also given for slotted plate to CHS joints, but these joints behave worse compared to the plate-to-slotted CHS joint.

7.4 Tee joints to the ends of CHS members

When an axial force is applied to the end of a CHS member, via a welded Tee joint as shown in figure 7.4, the possible limit state for the CHS is yielding of the walls or the Tee web (due to applied tension or compression loads). Also, the resistance of the CHS needs to be computed with consideration for shear lag. A conservative distribution slope can be assumed as 2.5:1 from each face of the Tee web (stem), which is based on Kitipornchai and Traves (1989). This produces a dispersed effective load width of ($t_w + 5t_p$), which has also been adopted by Packer and Henderson (1997). It is proposed to use conservatively this effective width around the perimeter of the CHS member. Thus the resistance of the CHS can be computed by summing the contributions of the parts of the tube cross-sectional area into which the load is distributed. Hence:

$$N_1^* = 2f_{y1}\, t_1 \left(t_w + 5t_p\right) \le A_1 f_{y1} \qquad 7.12$$

A similar load dispersion can be assumed for the capacity of the Tee web. If the web has the same width as the diameter of the cap plate, i.e. ($d_1 + 2s$), the capacity of the Tee web is:

$$N_1^* = 2f_{yw}\, t_w \left(t_1 + 2.5t_p + s\right) \qquad 7.13a$$

$$\le 2f_{yw}\, t_w \left(t_1 + 5t_p\right) \qquad 7.13b$$

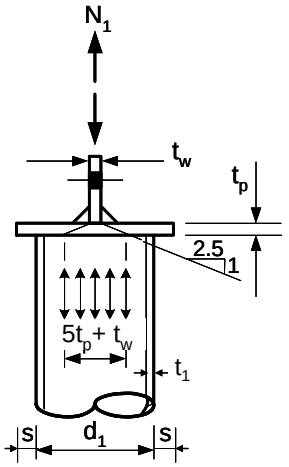

Figure 7.4 – Load dispersion for a Tee joint on the end of a CHS member

In equation 7.12, the size of any weld leg to the Tee web (stem) has been conservatively ignored. If the weld leg size is known, it is acceptable to assume load dispersion from the toes of the welds. If the applied load N_1 (figure 7.4) is compressive, then the CHS should not have a slender cross-section (i.e. not class 4).

Tee joints to the ends of CHS members usually have the web (stem) centred on the CHS member axis, but connection is then frequently made to a single gusset plate, usually by bolting. In such situations a bending moment is induced in the joint by the eccentricity between the plates which must be considered. Under compression loads, the gusset plate and the Tee web (stem) should be proportioned as beam-columns, assuming that both ends of the connection can sway laterally relative to each other. These comments also apply to the proportioning of other plates covered in chapter 7, when the plate is loaded in compression but connected by a lap splice eccentrically to another single gusset plate.

8 Bolted joints

For bolted joints, use is made of plates, forks, T sections or cut-outs of I sections welded to the CHS member as shown in figures 8.1 and 8.2. For these joints, general recommendations are not given in the codes but the bolts and the plates have to be checked in the normal way for shear, contact pressure and failure of the net cross sectional area. All national and international codes give these criteria.

Furthermore, requirements regarding minimum and maximum bolt distances have to be satisfied. For high strength friction grip bolted joints, special requirements are given for pre-tensioning of the bolts and the condition of the contact surfaces.

The calculation methods used for many types of bolted joints between or to hollow sections are not basically different from those used for any other type of joint in conventional steel construction. (Some calculation examples are given in chapter 11). Bolted joints are especially desirable on site between prefabricated sub-assemblies. Various examples of bolted joints are given in figures 8.1 to 8.4.

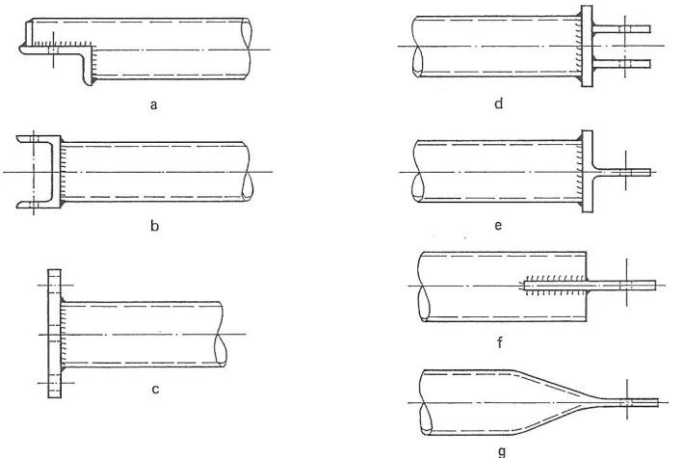

Figure 8.1 – Bolted end joints

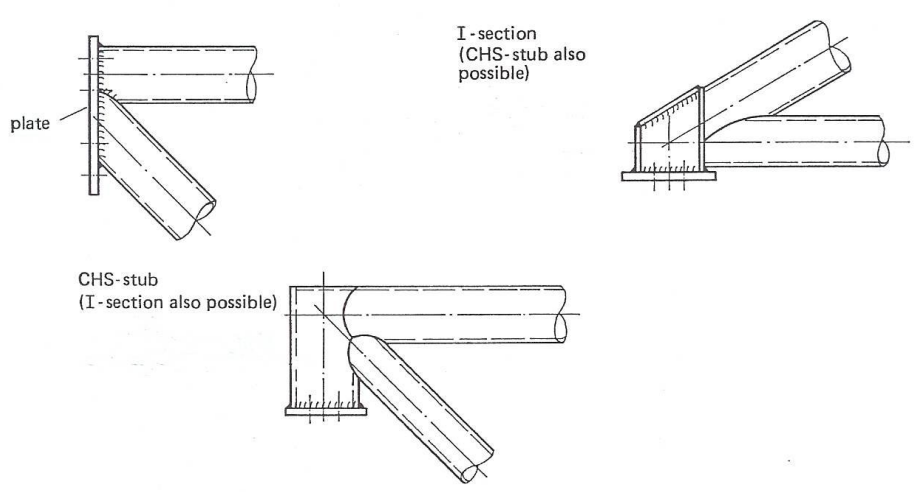

Figure 8.2 – Bolted truss support joints

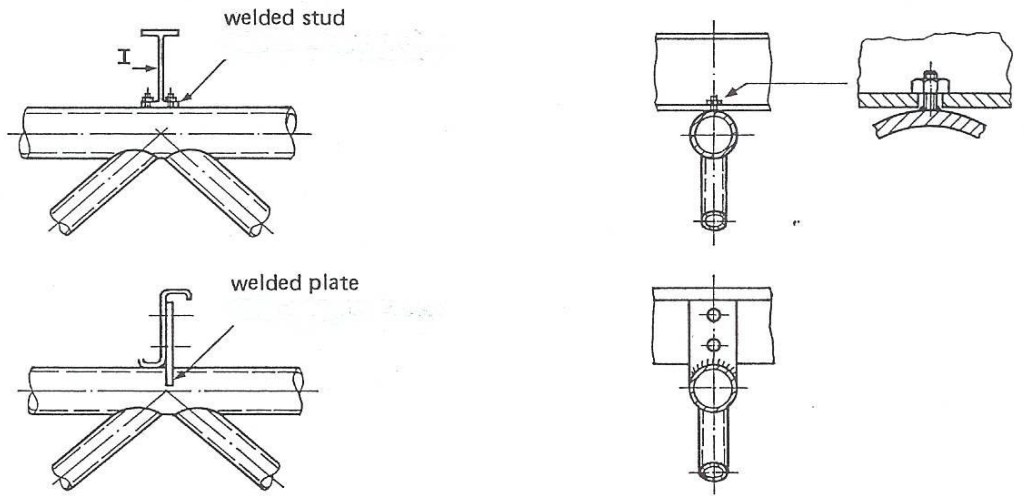

Figure 8.3 – Bolted purlin joints

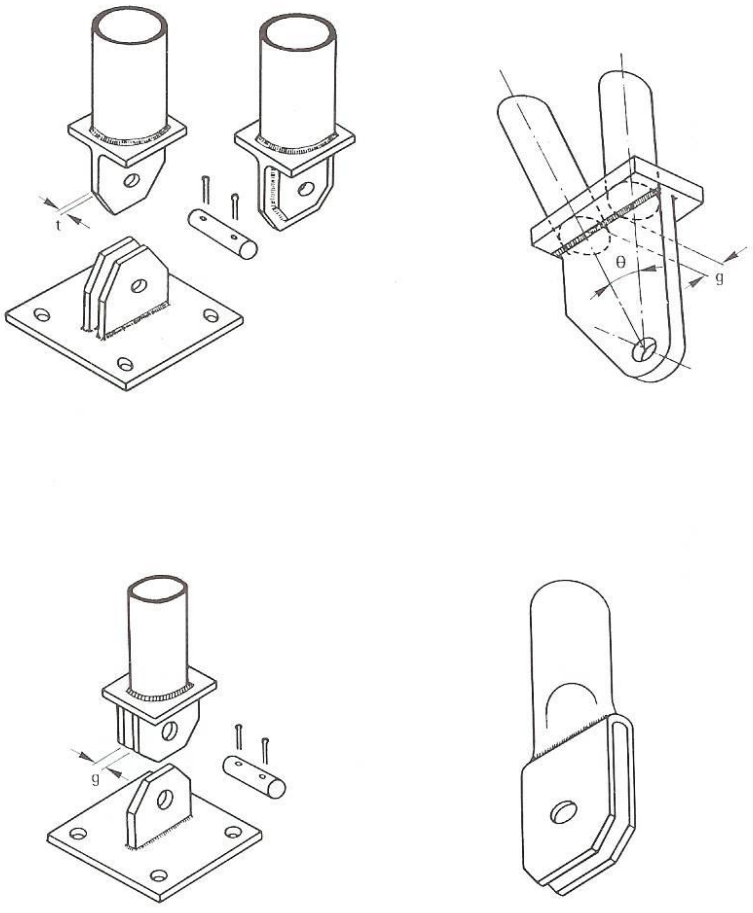

Figure 8.4 – Some other examples of bolted end joints

8.1 Flange-plate joints

For flange joints, various investigations have been carried out, e.g. by Kato and Hirose (1984) and Igarashi et al. (1985). Based on the work of Igarashi et al. (1985), recommendations are included in the Japanese Recommendations for the Design and Fabrication of Tubular Truss Structures in Steel (AIJ, 2002) which are given here in table 8.1.

Implicit in these joint details is an allowance for prying forces amounting to 1/3 of the total bolt force at the ultimate limit state and the assumption that the tube yield strength must be developed. The modes of failure assumed in determining these details are those due to plastification of flange plates and not due to tensile failure of high strength bolts. The standard details shown in table 8.1 are for STK400 tubes (specified minimum f_y = 235 N/mm^2 and minimum ultimate tensile strength of 402 N/mm^2), SS400 plates (specified minimum yield strength = 245 N/mm^2) and F10T bolts (about equal to Grade 10.9 bolts with a specified minimum ultimate tensile strength of 981 N/mm^2).

Table 8.1 – Standard details for flange full strength joints

	Maximum tube dimensions d_i x t_i (mm)	Thickness of flange plate t_f (mm)	Nominal diameter of bolt (mm)	Minimum number of bolts	Edge distance e_1 (mm)	Edge distance e_2 (mm)
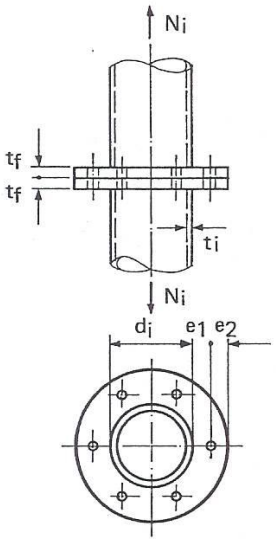	60.5 x 3.2 through 89.1 x 3.2	12	16	4	35	25
	89.1 x 4.2 through 101.6 x 3.5	16	16	4	35	25
	114.3 x 3.5	16	20	4	40	30
	139.8 x 4.0 165.2 x 4.0	16	20	6	40	30
	114.3 x 6.0 139.8 x 5.0	19	20	6	40	30
	165.2 x 5.0	19	20	8	40	30
	190.7 x 5.3 through 216.3 x 5.8	22	22	8	40	35
	216.3 x 8.2	25	22	12	40	35
	267.4 x 6.0	25	22	10	40	35
	267.4 x 6.6	28	22	10	40	35
	267.4 x 9.3	28	22	16	40	35
	318.5 x 6.0	25	24	10	45	40
	318.5 x 7.9	28	24	14	45	40
	318.5 x 10.3	28	24	18	45	40
	355.6 x 6.4	28	24	10	45	40
	355.6 x 9.5	32	24	18	45	40
	406.4 x 6.4	28	24	16	45	40
	406.4 x 9.5	32	24	22	45	40
	406.4 x 12.7	36	24	26	45	40
	457.2 x 6.4	28	24	16	45	40
	457.2 x 9.5	32	24	22	45	40
	457.2 x 12.7	36	24	32	45	40

According to Igarashi et al. (1985), the flange plate thickness t_f can be determined from:

$$t_f = \sqrt{\frac{2N_i\,\gamma_M}{f_{yp}\,\pi\,f_3}} \qquad 8.1$$

where:
N_i = tensile member force
f_{yp} = yield strength of plate
γ_M = 1.1 (partial safety factor)
f_3 = dimensionless factor to be obtained from figure 8.5
t_f = thickness of flange plate

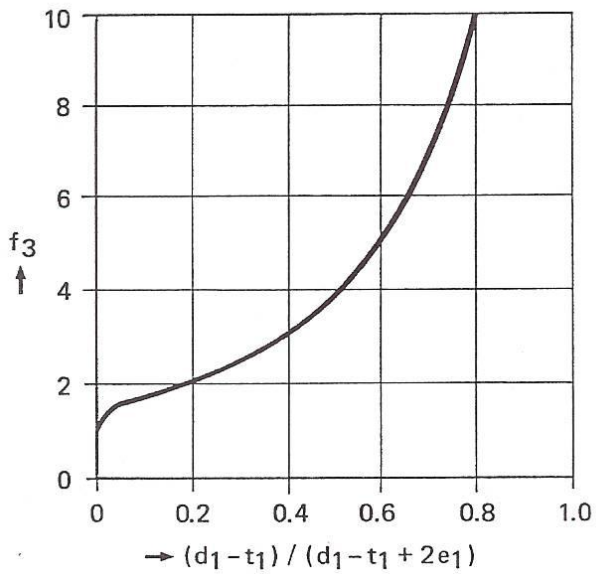

Figure 8.5 – Parameter f_3 for use in equations 8.1 and 8.2 for the design of CHS flange plate joints

The dimension e_1 (see table 8.1) should be kept as low as possible to minimize prying action (around 1.5d to 2d with d = bolt diameter), but the clearance between the nut and the weld should be at least 5 mm.

The number of bolts n can be determined from:

$$n \geq \frac{N_i\left[1-\frac{1}{f_3}+\frac{1}{f_3\,\ln(r_1/r_2)}\right]}{0.67\,T_u}\,\gamma_M \qquad 8.2$$

where
f_3 = dimensionless factor to be obtained from figure 8.5
T_u = ultimate tensile resistance of a bolt
r_1 = $0.5d_i + 2e_1$
r_2 = $0.5d_i + e_1$

For other variables, see equation 8.1.

8.2 Nailed joints

As an alternative to bolting or welding, steel circular hollow sections can be nailed together to form reliable structural joints. Up to now, this method of connection has only been verified for splice joints between two co-axial tubes (see figure 8.6). In such a joint, one tube can fit snugly inside the other, in such a way that the outside diameter of the smaller equals the inside diameter of the larger. Nails are then shot fired and driven through the two wall thicknesses and arranged symmetrically around the tube perimeter.

As an alternative, two tubes of the same outside diameter can be joined to each other by means of a tubular collar over both tube ends; in this case nails are again inserted by driving them through the two tube walls.

Research at the University of Toronto by Packer (1996) has covered a range of tube sizes with various diameter to thickness ratios, tube wall thickness and lack of fit. The observed failure modes were nail shear failure, tube bearing failure, and net section fracture of the tube. These failure modes have been identified for both static and fatigue loading. Simple design formulae, derived from bolted and riveted joints, have been verified for both these load cases.

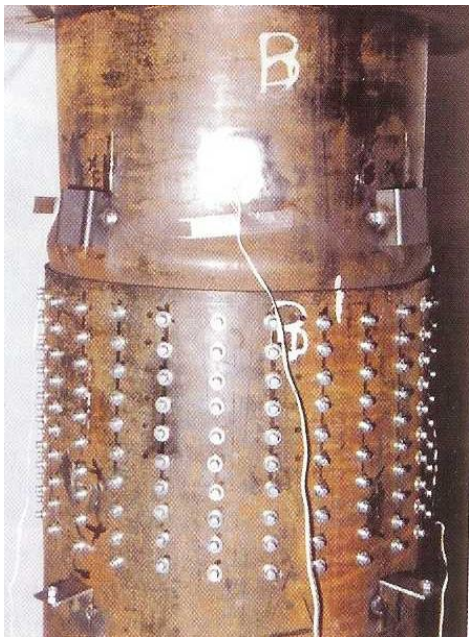

Figure 8.6 – Nailed joint

9 Other welded joints

9.1 Reinforced joints

Especially for the enhancement of under-dimensioned joints, various reinforcing methods exist, such as ring stiffeners, doubler or collar plates and grouting of the chord.

9.1.1 Joints with ring stiffeners

Although in the past several analytical, experimental and numerical investigations (e.g. Marshall, 1986) have been carried out, with the recent and improved numerical methods of the last decennium, more evidence is becoming available for the design of these joints (e.g. Lee and Llewelyn-Parry, 1998; Willibald, 2001).

Ring stiffeners can be placed internally or externally and they can consist just of a ring plate perpendicular to the chord or with a flange welded on top of it. Depending on the type of brace loading, they can be located at the brace saddle location for brace axial and out-of-plane bending loading or at the brace crown locations for brace in-plane bending.

The formulae available are generally restricted to the investigated type of joint with a defined loading and parameter range. In principle they are based on a summation of the capacity of the unstiffened joint and the plastic capacity of the ring stiffener(s) for which a part of the chord can be assumed as an effective flange. Depending on whether the ring stiffener has a flange, the effective cross section of the ring stiffener with the effective chord flange forms a T or I section. Especially at the crossing of the stiffeners and the brace wall, hard points exist and the chord material should have a good lamellar tearing resistance.

Since the strength enhancement depends on the β and γ ratios, the type of joint, the loading and the type and location of the stiffeners, reference is given to the existing literature. Generally, these stiffeners are expensive and where possible they should be avoided if other strengthening methods are feasible.

9.1.2 Joints with collar or doubler plates

For the enhancement of the strength of joints with thin-walled chords, reinforcement by collar or doubler plates (figure 9.1) may be used, as discussed by Choo et al. (2004, 2005). Doubler plates are welded to the chord with the brace welded to the doubler plate. These joints are also used for installation on site of auxiliary structures. In case of collar plates, the brace is welded to the chord and the collar, consisting of two or four parts, is welded to the chord and the brace around the brace to chord connection, as shown in figures 9.1 and 9.2.

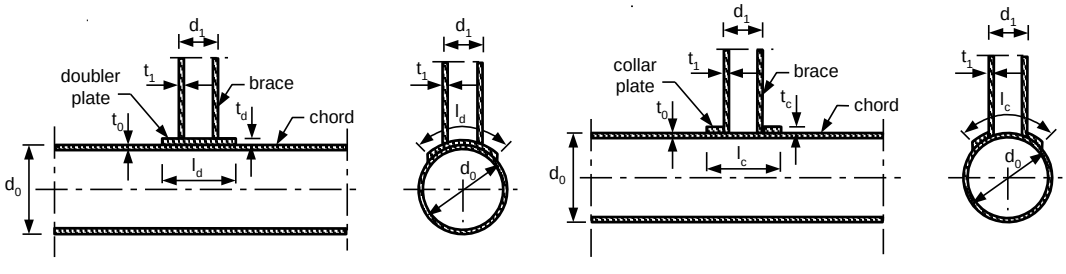

(a) Doubler plate (b) Collar plate

Figure 9.1 – Doubler and collar plate stiffened joints

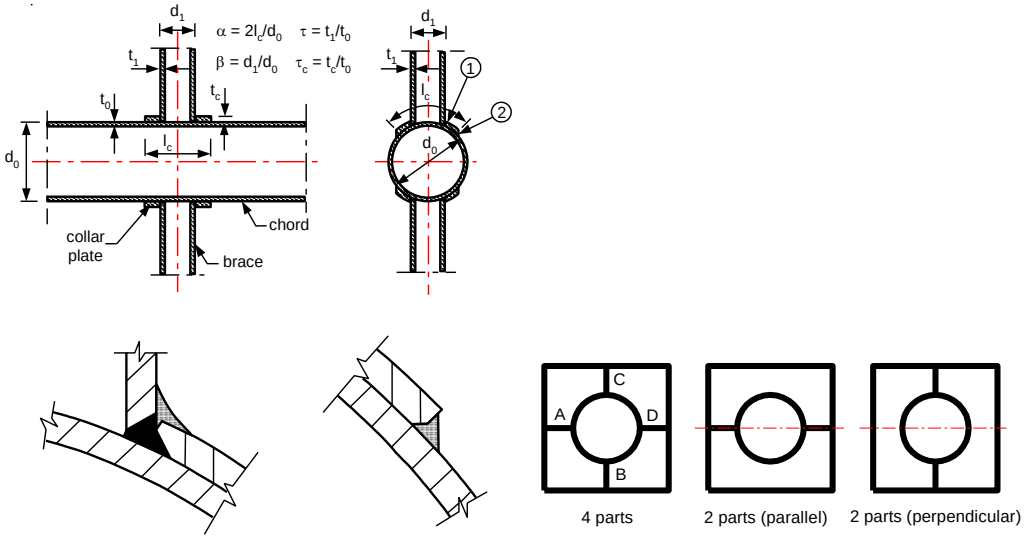

Figure 9.2 – Collar plate stiffened joints with possible weld arrangement

Collar plates provide a suitable efficient reinforcement and give generally a better enhancement than a doubler plate. For joints predominantly loaded by in-plane bending, the two parts parallel to the chord may be the preferred option whereas for out-of-plane bending, the parts perpendicular to the chord axis are preferred. If welding has to be minimised, the latter option can also be used for axial loading.

These reinforced joints have been extensively investigated at the National University of Singapore under brace axial loading and under in-plane bending moments. In all the investigations it was shown that for collar and doubler plates with a thickness equal or larger than that of the chord, the strength could be enhanced by 30% or more, depending on the dimensions of the collar and doubler plates and geometric parameters and the loading. As an example, for X joints with 2γ = 50.8 and β = 0.25, figure 9.3 shows the ratio of the strength ($F_{u,c}$, $M_{i,u,c}$, $M_{o,u,c}$) of the collar plate reinforced joint with respect to the strength ($F_{u,u}$, $M_{i,u,u}$, $M_{o,u,u}$) of referenced un-reinforced joints, as a function of the relative plate-to-chord wall thickness ratio τ_c (= t_c/t_0) and the relative plate length to brace diameter ratio l_c/d_1.

As shown in figure 9.3 the strengthening effect further depends on the loading, i.e. compression, tension, in-plane bending or out-of-plane bending. For detailed information, reference is given to the publications by Choo et al. (2004, 2005).

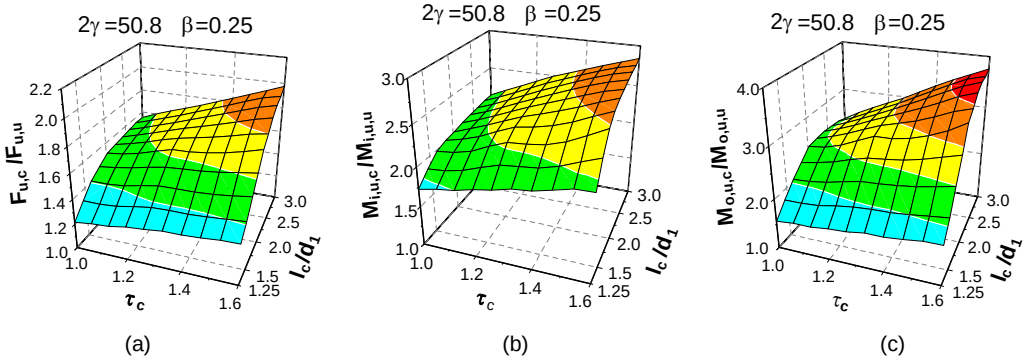

Figure 9.3 – Normalised strengths of X joints with collar plate reinforcement for (a) brace axial load, (b) in-plane bending, and (c) out-of-plane bending

9.1.3 Grouted joints

Grouting of joints was initially used for increasing the static capacity of existing joints or to reduce the stress concentration factors and thus to enhance the fatigue life. Grouting technology has been considerably improved since the first investigations in the seventies and nowadays it is also used for new designs. As shown in figure 9.4, grouting can be used in two ways, i.e. the chord can be fully grouted or the annulus between the chord and an internal member (e.g. a pile in a jacket) can be grouted. In the last case, a double-skin joint occurs.

Figure 9.4 – Grouted chords

In the case of brace compression loading, in most cases the brace capacity will be governing, but for double-skin joints with thin-walled members, chord plastification may occur. API (2007) recommends the joint capacity to be calculated using an effective chord thickness t_e according to equation 9.1, where t_0 is the chord thickness and t_{in} is the thickness of the inner tube.

$$t_e = \sqrt{t_0^2 + t_{in}^2} \tag{9.1}$$

In the case of brace tension loading, in most cases punching shear, based on the chord thickness t_0 is the governing failure mode (Dier and Lalani, 1998; Morahan and Lalani, 2002) but the capacity is considerably lower than that according to equation 4.2 due to the fact that the full cross section is not effective. The recommended design capacity, including a $\gamma_M = 1.1$ to the defined characteristic capacity in API (2007), is given in equation 9.2:

$$N_i^* = 0.36\, f_{y0}\, \pi\, d_i\, t_0\, \frac{k_a}{\sin\theta_i} \tag{9.2}$$

with k_a according to equation 4.3

For bending in-plane and bending out-of-plane loading, API (2007) also follows the recommendation of the MSL study (Morahan and Lalani, 2002). Using again a $\gamma_M = 1.1$ to the defined characteristic (lower bound) capacity in API, the design capacity is about 18% higher than that according to equation 5.2. This may be caused due to the fact that punching shear occurs at the tension side and bearing occurs at the compression side which results in a shifted neutral axis at failure. Thus:

$$M_i^* = 0.68\, f_{y0}\, d_1^2\, t_0\, \frac{k_b}{\sin\theta_i} \tag{9.3}$$

with k_b according to equations 5.3 and 5.4.

Grouting of joints results in a considerable increase in joint rigidity and sometimes in a reduction of the rotation capacity. Therefore, it is recommended to design preferably in such a manner that the brace capacity is governing or that secondary moments are considered in the design.

Although brace grouting is not usual, if applied, consideration should be taken with regard to a possible shift of the neutral axis at the connection and the effect on the capacity equations.

9.2 Flattened and cropped-end CHS brace members to CHS chords

Especially for small sized and temporary tubular structures, or in those cases where the fabricator does not have proper equipment for end profile cutting, (partial) flattening of the ends of members can be used. As illustrated in figure 9.5, various types of flattening can be provided. In the case of full or partial flattening, the maximum taper from the tube to the flat should remain within 25% (or 1:4), as shown in figures 9.5(b) and 9.5(c). More detailed information regarding fabrication is given in Rondal (1990) and the CIDECT Design Guide No. 7 (Dutta et al., 1998).

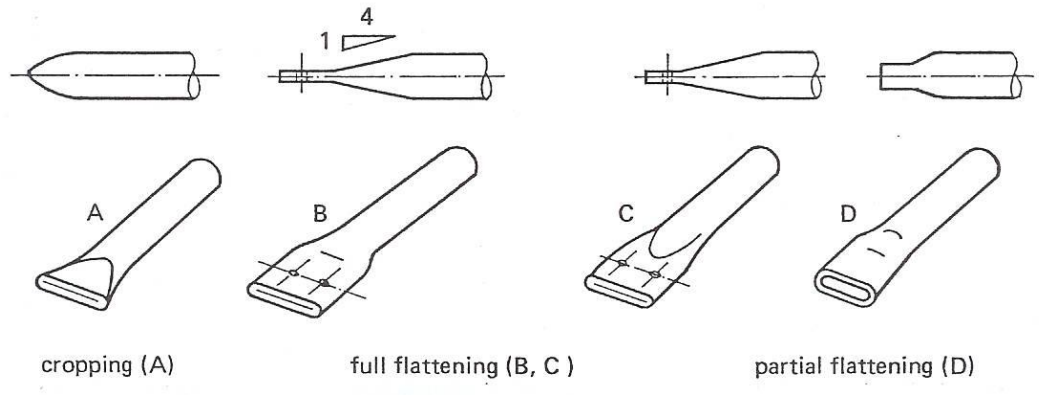

Figure 9.5 – Various types of flattening

For welded joints, the length of the flat part should be minimized for compression members to avoid local buckling. Especially for d_0/t_0 ratios exceeding 25, the flattening will reduce the compressive strength of the braces. Recommended design strength formulae for cropped-web N joints with overlap (Ciwko and Morris, 1981) are given in figure 9.6 with the range of validity in table 9.1.

Table 9.1 – Investigated dimensions and parameters (Ciwko and Morris, 1981)

Dimensions tested (mm)	**Parameters tested**
$114 \le d_0 \le 169$	$14 \le d_0/t_0 \le 50$
$42 \le d_1 \le 90$	$0.35 \le d_1/d_0 \le 0.8$
$3 \le t_0 \le 8$	$d_1/d_2 = 1.0$
$3 \le t_1 \le 4.6$	$t_1/t_2 = 1.0$
	$0\% \le Ov \le 75\%$
$f_{yi} \le 400$ N/mm^2	$\theta_1 = 90°$; $\theta_2 = 45°$

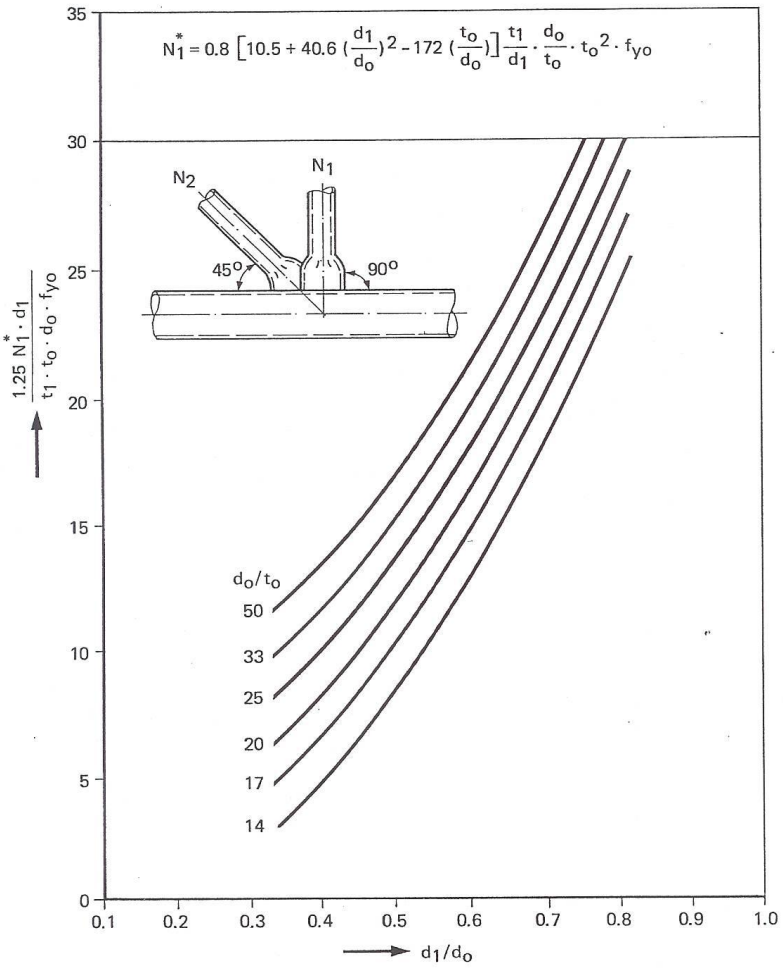

Figure 9.6 – Design diagram for cropped-end brace joints

Compared to the ultimate joint strength given in Ciwko and Morris (1981), for the vertical brace loaded in compression, a factor of 0.80 has been adopted to account for the transformation from ultimate strength to design strength.

Since the behaviour of this type of joint may be influenced by size effects, care should be taken in using these empirical formulae, and that is why the validity is restricted to the dimensional range tested, shown in table 9.1.

It is recommended that for chord compression and tension, the same Q_f functions are used as for profiled CHS gap joints (see table 4.1).

For trusses with flattened and cropped-end braces, an effective buckling length of 1.0 times the system length is recommended. The flattened part should be as short as possible to avoid a negative effect on the buckling behaviour.

Joints with partially-flattened end braces, as shown in figure 9.7 have been investigated in CIDECT program 5AP (Rondal, 1990).

These joints can be designed with the same joint strength formulae as for normal CHS joints provided that the following modifications are adopted:

T, Y and X joints: Replace in the formula for N_1^*: d_1 by $d_{1,min.}$

K joints with gap: Replace in the formula for N_1^*: d_1 by $(d_1+d_{1,min.})/2$

As a result, the joint strength of T and X joints is reduced since d_1 has to be replaced by $d_{1,min}$ in the joint strength formula. For K joints, the joint strength is decreased due to the replacement of d_1 by $(d_1+d_{1,min.})/2$. However, because of the flattening, the gap size is decreased resulting in an increase in joint strength. Since these effects partly compensate each other, the actual joint strength may not deviate considerably from that of a joint with profiled braces.

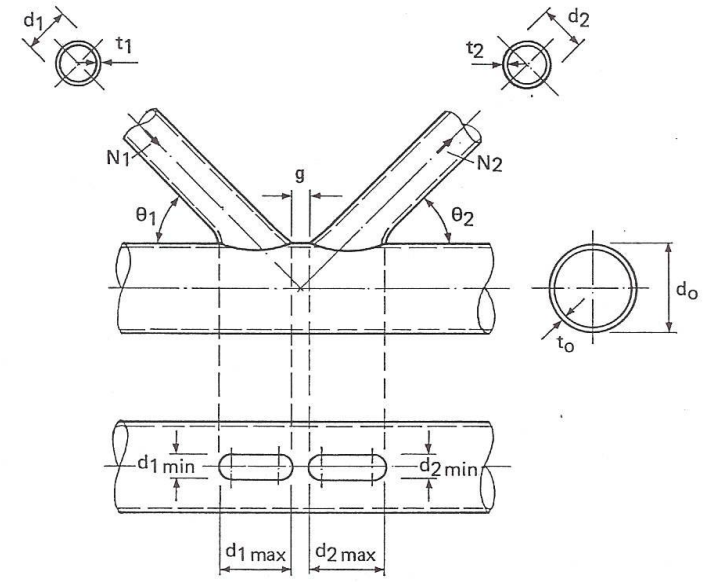

Figure 9.7 – K joint with partially-flattened end braces

10 Design strengths according to the 1st edition of Design Guide No. 1 and also incorporated in Eurocode 3

The recommendations in this chapter are those given in the 1st edition of this Design Guide (Wardenier et al., 1991) which are based on the 1989 version of the IIW-XV-E recommendations (IIW, 1989) and incorporated in various national and international codes, e.g. Eurocode 3 (CEN, 2005a, 2005b). Therefore, these recommendations are still included here, because designers may have to meet the requirements in these codes.

The previous design recommendations, in limit state terms, are given in tables 10.1 to 10.4 with a brief explanation about the background, since the general philosophy for design is given in the previous chapters.

For designers, efficiency diagrams with examples are given in sections 10.5, 10.6 and in chapter 11, all based on the design strength formulae of sections 10.1 to 10.4 (Reusink and Wardenier, 1989).

10.1 Previous design recommendations for axially loaded uniplanar joints

The design strength formulae for uniplanar T, X and K joints are originally based on the formulae of Kurobane (1981) and, after simplification and evaluation to design rules (Wardenier, 1982), incorporated in the IIW (1989) recommendations.

In principle, two criteria have to be checked: a chord plastification criterion and a punching shear criterion.

In the previous design recommendations, one chord plastification criterion is given for K joints, covering both gap and overlap joints although the behaviour is different. Hence, in the new recommended design formulae presented in chapter 4, separate criteria are given.

A further important difference with the new formulae in chapter 4 is that here in chapter 10, the chord stress function is still based on the prestress of the chord (see figures 10.1 and 10.2) instead of the maximum chord stress; thus excluding the stress due to the horizontal brace load components. Since this approach differs from the procedure for RHS joints, for which the maximum chord stress is used, it caused misinterpretation in practice. Hence, in the new recommendations in chapter 4, the chord stress function is related to the maximum chord stress.

The previous gap function used for K joints, shown in figure 10.3, also differs from the newly proposed, simplified expression in chapter 4.

In the previous design recommendations, the strength of special types of uniplanar joints shown in table 4.4, is also related to the capacity of the basic types of joints, i.e. the equations given in table 10.1.

In section 10.5, the joint capacity equations are given in efficiency diagrams in which the joint capacity is divided by the brace yield load, as described in section 4.7, but here for the capacity equations of tables 10.1 and 10.2.

In the previous version of this Design Guide, the validity of the joint design equations was limited to steel with a design yield stress of 355 N/mm^2. In the Eurocode 3, this is also extended to steel with a design yield stress of 460 N/mm^2, also under the conditions mentioned in section 1.2.1.

Table 10.1 – Previous design recommendations for axially loaded uniplanar joints

Type of joint	**Design strength**
T and Y joints	**Chord plastification**
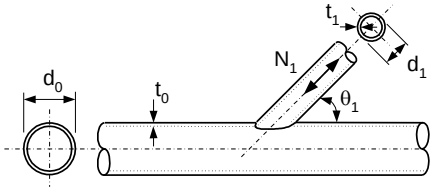	$N_1^* = \frac{f_{y0}\, t_0^2}{\sin\theta_1}\left(2.8+14.2\beta^2\right)\gamma^{0.2}\, f(n')$ eq. 10.1
X joints	**Chord plastification**
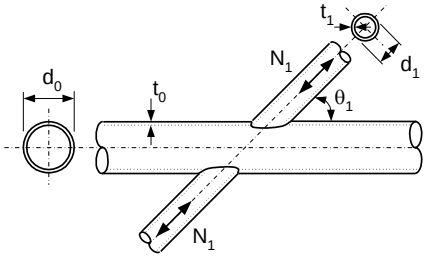	$N_1^* = \frac{f_{y0}\, t_0^2}{\sin\theta_1}\left(\frac{5.2}{1-0.81\beta}\right) f(n')$ eq. 10.2
K and N gap and overlap joints	**Chord plastification**
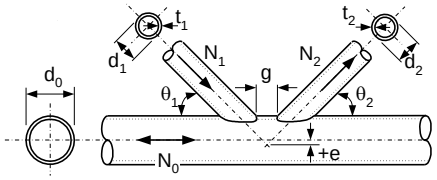	$N_1^* = \frac{f_{y0}\, t_0^2}{\sin\theta_1}\left(1.8+10.2\frac{d_1}{d_0}\right) f(\gamma, g')\, f(n')$ eq. 10.3 $N_2^* = \frac{\sin\theta_1}{\sin\theta_2} N_1^*$ eq. 10.4
General for T, Y, X, K and N gap joints	**Punching shear failure**
Punching shear check for $d_i \le d_0 - 2t_0$	$N_i^* = 0.58 f_{y0}\, t_0\, \pi\, d_i \frac{1+\sin\theta_i}{2\sin^2\theta_i}$ eq. 10.5
Functions	
f(n') = 1.0 for n' ≥ 0 (tension) f(n') = 1+0.3n'-0.3n'^{2} for n' < 0 (compression) n' = f_{op}/f_{y0} eq. 10.6	$f(\gamma, g') = \gamma^{0.2}\left[1+\frac{0.024\,\gamma^{1.2}}{\exp(0.5g'-1.33)+1}\right]$ eq. 10.7

Range of validity

$0.2 \le \frac{d_i}{d_0} \le 1.0$	Braces: class 1 or 2 and $\frac{d_i}{t_i} \le 50$	$30° \le \theta_i \le 90°$ $-0.55 \le \frac{e}{d_0} \le 0.25$	Chords: class 1 or 2 and $10 \le 2\gamma \le 50$ $10 \le 2\gamma \le 40$ (X joints)	Ov ≥ 25% $g \ge t_1 + t_2$

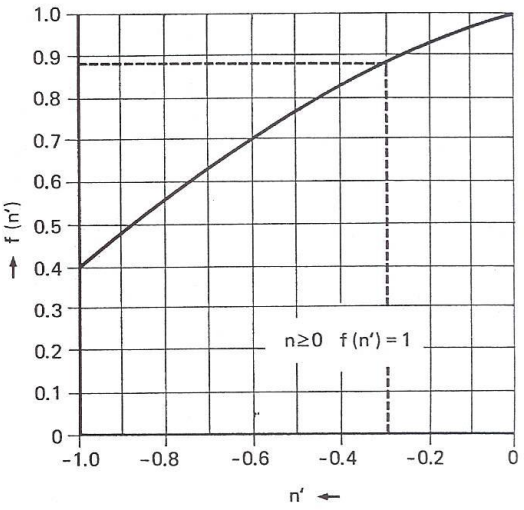

Figure 10.1 – Chord prestress function f(n')

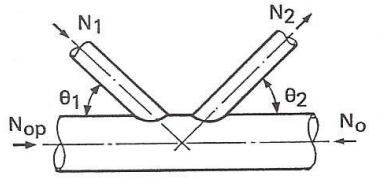

$$N_o = N_1 \cos\theta_1 + N_2 \cos\theta_2 + N_{op}$$

$$n' = \frac{N_{op}}{A_0 f_{y0}}$$

Figure 10.2 – Chord preload N_{op}

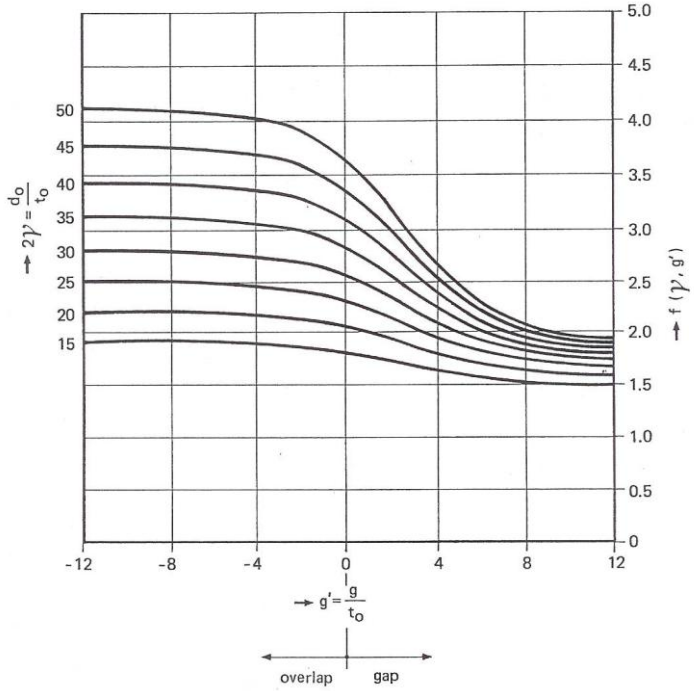

Figure 10.3 – Gap function

10.2 Previous design recommendations for joints under moment loading

The design recommendations for joints under in-plane bending moment loading are based on a modified function of Gibstein (1976) and for out-of-plane bending moments on a relation with axially loaded X joints, see Wardenier (1982). A correction to the constant in the formula for out-of-plane bending is applied based on a reanalysis for Eurocode 3 (Sedlacek et al., 1991).

Table 10.2 – Previous design recommendations for joints loaded by primary bending moments

<table>
<tr><th colspan="2">Type of joint</th><th colspan="2">Design capacity</th></tr>
<tr><td colspan="2">T, Y, X joints
 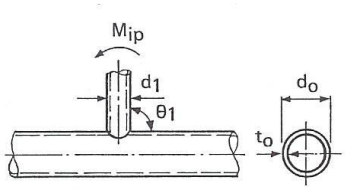
</td><td colspan="2">Chord plastification
$M_{ip}^{*} = 4.85\, f_{y0}\, t_0^2\, \gamma^{0.5}\, \beta\, d_1\, \frac{f(n')}{\sin\theta_1}$ eq. 10.8</td></tr>
<tr><td colspan="2">T, Y, X joints
 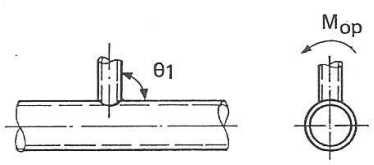
</td><td colspan="2">Chord plastification
$M_{op}^{*} = f_{y0}\, t_0^2\, \frac{2.7}{1-0.81\beta}\, d_1\, \frac{f(n')}{\sin\theta_1}$ eq. 10.9</td></tr>
<tr><td colspan="2">General</td><td colspan="2">Punching shear failure</td></tr>
<tr><td colspan="2">Punching shear check for
$d_1 \le d_0 - 2t_0$</td><td colspan="2">$M_{ip}^{*} = 0.58 f_{y0}\, t_0\, d_1^2\, \frac{1+3\sin\theta_1}{4\sin^2\theta_1}$ eq. 10.10
$M_{op}^{*} = 0.58 f_{y0}\, t_0\, d_1^2\, \frac{3+\sin\theta_1}{4\sin^2\theta_1}$ eq. 10.11</td></tr>
<tr><td colspan="4">Functions</td></tr>
<tr><td colspan="2"></td><td colspan="2">f(n') = 1.0 for n' ≥ 0
f(n') = 1+0.3n'-0.3n'^{2} for n' < 0
n' = f_{op}/f_{y0} eq. 10.6</td></tr>
<tr><td colspan="4">Range of validity</td></tr>
<tr><td>$0.2 \le \frac{d_1}{d_0} \le 1.0$</td><td>Braces: class 1 or 2
and $\frac{d_1}{t_1} \le 50$</td><td>$30° \le \theta_1 \le 90°$</td><td>Chords: class 1 or 2
and $10 \le 2\gamma \le 50$
$10 \le 2\gamma \le 40$ (X joints)</td></tr>
</table>

10.3 Previous design recommendations for axially loaded multiplanar joints

The correction factors for T and X joints are based on the work of Mitri et al. (1987), Paul et al. (1989) and initial work by van der Vegte (1995). The recommended reduction factor for multiplanar K joints is based on a simplification of the recommended function by Makino et al. (1984).

Since for large β ratios, the shear in the gap may result in a chord shear failure, an additional shear criterion is added for the gap location in gapped K joints.

In principle, the previous correction factors to the uniplanar design strength functions are the same as those given in chapter 6, only the reduction factor for K gap joints is here 0.9. In chapter 6, a factor of 1.0 is used, because the reduction due to the higher maximum chord loads in multiplanar joints is automatically included in the new chord stress function.

Table 10.3 – Previous correction factors for multiplanar joints

Type of joint	**Correction factor μ to uniplanar joint strength**
TT joints 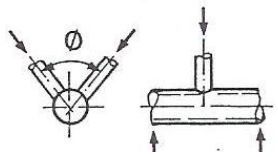	μ = 1.0
XX joints 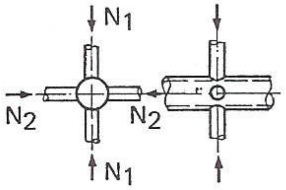	$\mu = 1 + 0.33\frac{N_2}{N_1}$ eq. 10.12 Note: Take account of the sign of N_2 and N_1 ($N_1 \geq N_2$)
KK gap joints 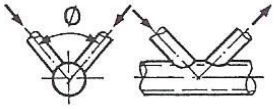	μ = 0.9 Note: In a gap joint, the cross section in the gap has to be checked for shear failure: $\left(\frac{N_{gap,0}}{N_{pl,0}}\right)^2 + \left(\frac{V_{gap,0}}{V_{pl,0}}\right)^2 \leq 1.0$ eq. 6.2 where: $N_{gap,0}$ = axial force in gap $N_{pl,0} = A_0 f_{y0}$ $V_{gap,0}$ = shear force in gap $V_{pl,0} = 0.58 f_{y0} \frac{2A_0}{\pi}$
Range of validity	Limits according to table 10.1 $60° \leq \phi \leq 90°$

10.4 Previous design recommendations for joints between plate, I, H or RHS braces and CHS chords

The design recommendations given in the 1st edition of this Design Guide for plate, I, H or RHS section to CHS joints are presented in table 10.4.

A distinction is made between TP joints (plate to CHS T joints) and XP joints (plate to CHS X joints), with the former having a plate on one side of the tube and the latter having plates on both sides of the tube.

In the 1st edition of the Design Guide, for simplicity, the same design strength is given for TP and XP joints. However, it was mentioned that for TP joints the function:

$$f(\beta) = 4+20\beta^2 \qquad 10.13$$

provides a better fit with the test results than the (lower) function:

$$f(\beta) = \frac{5.0}{1-0.81\beta} \qquad 10.14$$

which is based on the X joint test results. In Eurocode 3, separate functions for TP and XP joints are adopted.

The XP-3/TP-3 joint is a combination of XP-1/XP-2 or TP-1/TP-2 and is not given in table 10.4. Since the stiffness of a longitudinal plate parallel to the chord axis is considerably smaller than that perpendicular to the chord axis, the capacity of such a joint is equal to that of the XP-1 or TP-1 joint.

Jib with CHS quadrangular boom

Table 10.4 – Previous design recommendations for joints between plate, I, H or RHS braces and CHS chord

Design strength for XP and TP joints (in Eurocode 3, different functions for TP joints; see text)						
Type of joint	**Brace axial loading** $N_1^* = f(\beta)\,f(\eta)\,f(n')\,f_{y0}\,t_0^2$				**Brace in-plane bending** $M_{ip,1}^*$	**Brace out-of-plane bending** $M_{op,1}^*$
	$f(\beta)$	$f(\eta)$	$f(n')$	$f_{y0}\,t_0^2$		
XP-1/TP-1 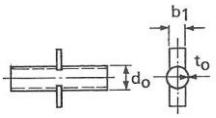	$\frac{5.0}{1-0.81\beta}$	1	$f(n')$	$f_{y0}\,t_0^2$	--	$0.5\,b_1\,N^*_{(XP-1)}$
XP-2/TP-2 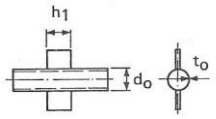	5.0	$1+0.25\eta$ $\eta \le 4$	$f(n')$	$f_{y0}\,t_0^2$	$h_1\,N^*_{(XP-2)}$	--
XP-4/TP-4 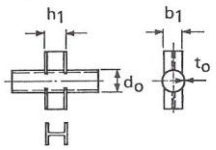	$\frac{5.0}{1-0.81\beta}$	$1+0.25\eta$ $\eta \le 4$	$f(n')$	$f_{y0}\,t_0^2$	$h_1\,N^*_{(XP-1)}$	$0.5\,b_1\,N^*_{(XP-4)}$
XP-5/TP-5 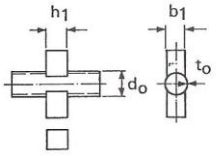	$\frac{5.0}{1-0.81\beta}$	$1+0.25\eta$ $\eta \le 2$	$f(n')$	$f_{y0}\,t_0^2$	$h_1\,N^*_{(XP-5)}$ $\eta \le 2$	$0.5\,b_1\,N^*_{(XP-5)}$
General	**Punching shear check**					
Punching shear check for $b_1 \le d_0 - 2t_0$	For XP-1/TP-1, XP-2/TP-2 (general) and for XP-4/TP-4 (in-plane bending only): $\frac{N_1}{A_1} + \frac{M_{ip,1}}{W_{el,ip,1}} + \frac{M_{op,1}}{W_{el,op,1}} \le 1.16 f_{y0} \frac{t_0}{t_1}$ For other cases: $\frac{N_1}{A_1} + \frac{M_{ip,1}}{W_{el,ip,1}} + \frac{M_{op,1}}{W_{el,op,1}} \le 0.58 f_{y0} \frac{t_0}{t_1}$					
Functions						
	$f(n') = 1.0$ for $n' \ge 0$; $f(n') = 1+0.3n'-0.3n'^2$ for $n' < 0$				$n' = \frac{f_{op}}{f_{y0}}$	
Range of validity						
$\beta \ge 0.4$	$\theta_1 = 90°$	$10 \le 2\gamma \le 40$			class 1 or 2	

10.5 Graphical design charts for axially loaded joints

10.5.1 Design chart for axially loaded T and Y joints

Table 10.5 – Efficiency design chart for CHS T and Y joints

<table>
<tr><th colspan="2">T and Y joints of circular hollow sections</th></tr>
<tr><th>Symbols</th><th>Geometric range of validity</th></tr>
<tr><td>$\beta = \frac{d_1}{d_0}$ $2\gamma = \frac{d_0}{t_0}$ $n' = \frac{f_{op}}{f_{y0}}$
 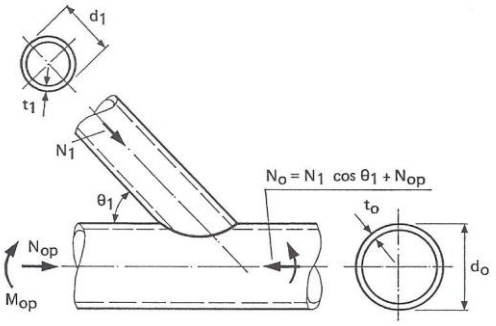

f_{op} = chord stress as a result of additional axial force or bending moment</td><td>$0.2 \le \beta \le 1.0$
$10 \le 2\gamma \le 50$
$d_1/t_1 \le 50$
$30° \le \theta_1 \le 90°$</td></tr>
<tr><th colspan="2">Design chart</th></tr>
<tr><td colspan="2"> 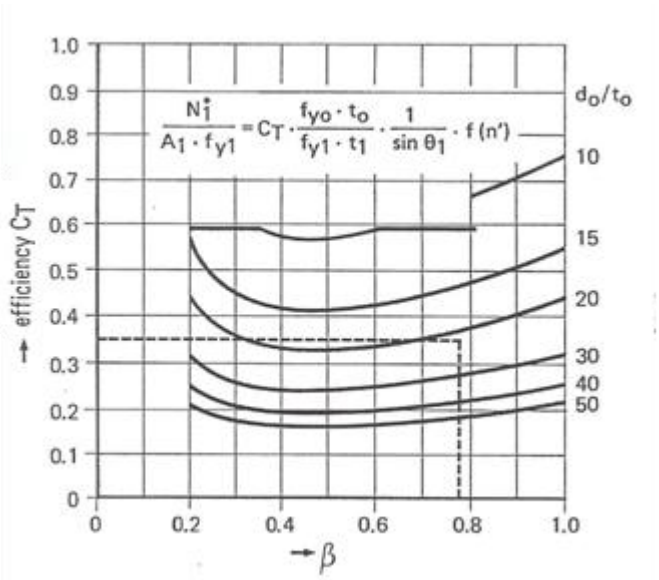
</td></tr>
</table>

Table 10.5 – Efficiency design chart for CHS T and Y joints (continued)

Calculation example for T and Y joints		
chord: Φ 219.1 x 10.0 brace: Φ 168.3 x 4.5	$d_0/t_0 = 21.9$ $d_1/t_1 = 37.4$	$f_{y0} = f_{y1}$
	$\beta = \frac{d_1}{d_0} = \frac{168.3}{219.1} = 0.77$	**C_T = 0.35**
$\theta_1 = 90°$ $f_{op} = -0.48 f_{y0}$	$\sin \theta_1 = 1.0$ f(n') = 0.79 (see figure 10.1)	
$\frac{N_1^*}{A_1 f_{y1}} = 0.35 \times \frac{10}{4.5} \times 0.79 = 0.61$		

The “London Eye” Wheel

10.5.2 Design chart for axially loaded X joints

Table 10.6 – Efficiency design chart for CHS X joints

<table>
<tr><th colspan="2">X joints of circular hollow sections</th></tr>
<tr><th>Symbols</th><th>Geometric range of validity</th></tr>
<tr><td>$\beta = \frac{d_1}{d_0}$ $2\gamma = \frac{d_0}{t_0}$ $n' = \frac{f_{op}}{f_{y0}}$
 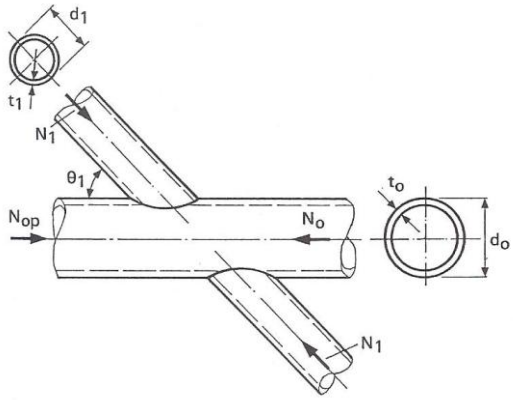

f_{op} = chord stress as a result of additional axial force or bending moment</td><td>$0.2 \le \beta \le 1.0$
$10 \le 2\gamma \le 40$
$d_1/t_1 \le 50$
$30° \le \theta_1 \le 90°$</td></tr>
<tr><th colspan="2">Design chart</th></tr>
<tr><td colspan="2"> 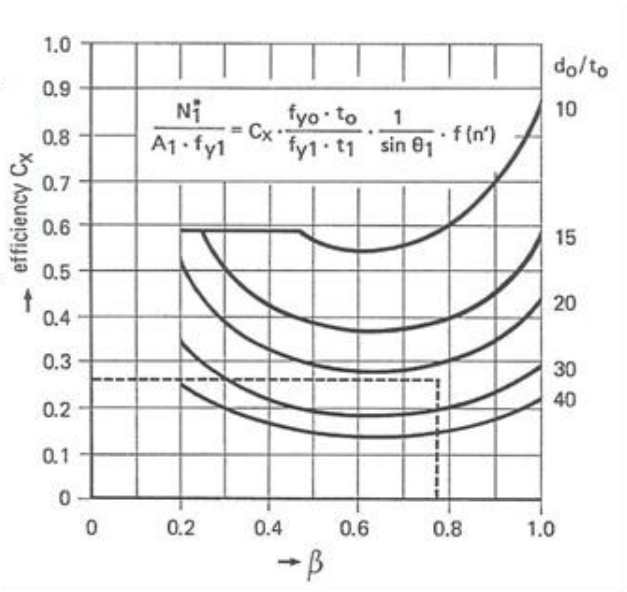
</td></tr>
</table>

Table 10.6 – Efficiency design chart for CHS X joints (continued)

Calculation example for X joints		
chord: Φ 219.1 x 10.0 brace: Φ 168.3 x 5.6	$d_0/t_0 = 21.9$ $d_1/t_1 = 30.0$	$f_{y0} = f_{y1}$
	$\beta = \frac{d_1}{d_0} = \frac{168.3}{219.1} = 0.77$	**C_X = 0.26**
$\theta_1 = 90°$ $f_{op} = -0.48 f_{y0}$	$\sin \theta_1 = 1.0$ f(n') = 0.79 (see figure 10.1)	
$\frac{N_1^*}{A_1 f_{y1}} = 0.26 \times \frac{10}{5.6} \times 0.79 = 0.37$		

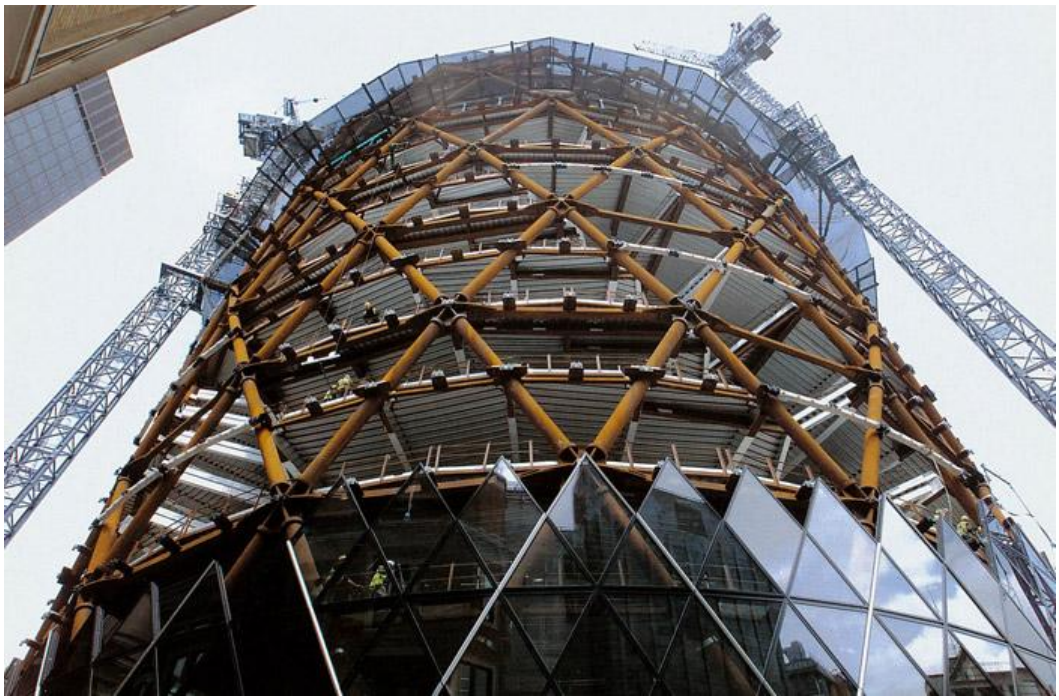

Building with CHS members and bolted joints

10.5.3 Design charts for axially loaded K and N gap joints

Table 10.7 – Efficiency design charts for CHS K and N gap joints

<table>
<tr><th colspan="2">K and N gap joints of circular hollow sections</th></tr>
<tr><th>Symbols</th><th>Geometric range of validity</th></tr>
<tr><td>$2\gamma = \frac{d_0}{t_0}$ $\quad n' = \frac{f_{op}}{f_{y0}}$ $\quad g' = \frac{g}{t_0}$
 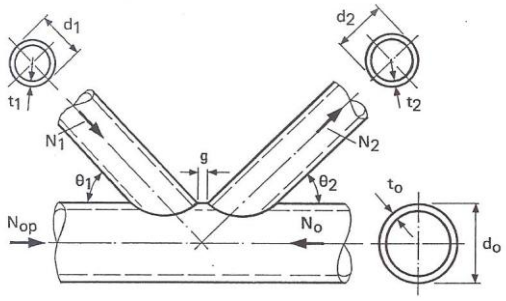

f_{op} = chord stress as a result of additional axial force or bending moment</td><td>$0.2 \le \frac{d_i}{d_0} \le 1.0$
$10 \le 2\gamma \le 50$
$d_i/t_i \le 50$
$g \ge t_1 + t_2$
$30° \le \theta_i \le 90°$
$-0.55 \le \frac{e}{d_0} \le 0.25$</td></tr>
<tr><th colspan="2">Design charts</th></tr>
<tr><td colspan="2"> 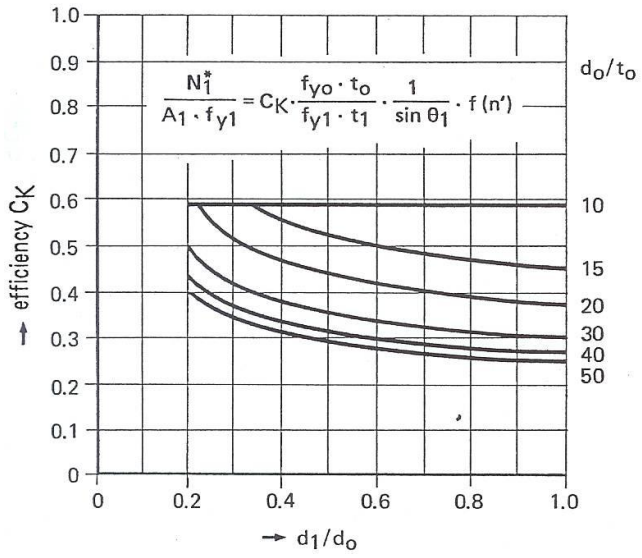

for g'= 2</td></tr>
</table>

Table 10.7 – Efficiency design charts for CHS K and N gap joints (continued)

Design charts
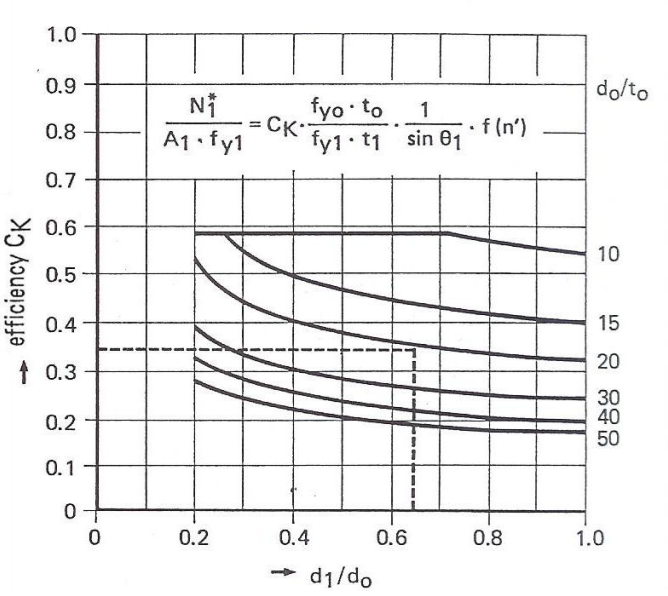 **for g'= 6** 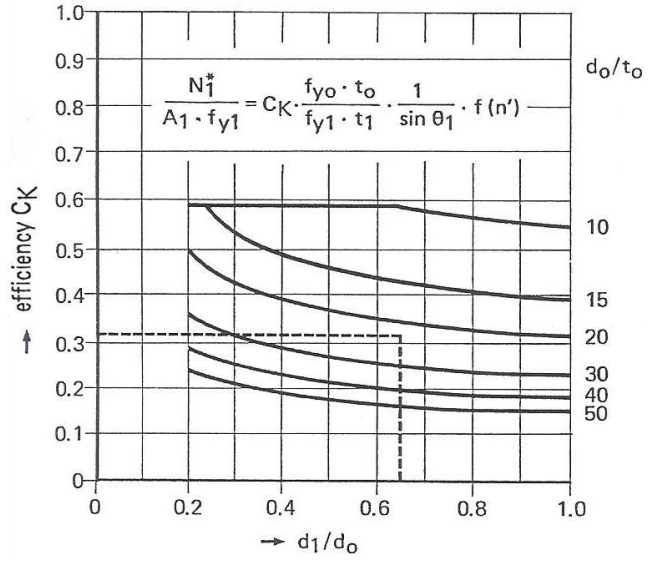 **for g'= 10**

Table 10.7 – Efficiency design charts for CHS K and N gap joints (continued)

Calculation example		
chord : Φ 219.1 x 10.0 brace 1: Φ 139.7 x 6.3	$d_0/t_0 = 21.9$ $d_1/t_1 = 22.2$	$f_{y0} = f_{y1} = f_{y2}$
brace 2: Φ 114.5 x 5.0	$d_2/t_2 = 22.9$	g = 85 mm, thus $g' = \frac{85}{10} = 8.5$
	$\frac{d_1}{d_0} = \frac{139.7}{219.1} = 0.64$	**C_K = 0.33**
$\theta_1 = \theta_2 = 40°$ $f_{op} = -0.3f_{y0}$	$\sin\theta_1 = 0.643$ f(n') = 0.88 (see figure 10.1)	
$\frac{N_1^*}{A_1 f_{y1}} = 0.33 \times \frac{10}{6.3} \times \frac{1}{0.643} \times 0.88 = 0.72$		
$\frac{N_2^*}{A_2 f_{y2}} = \frac{N_1^*}{A_1 f_{y1}} \frac{A_1 f_{y1}}{A_2 f_{y2}} \frac{\sin\theta_1}{\sin\theta_2} = 1.10 > 1.0$		

Tubular roof structure with arch for railway hall

10.5.4 Design chart for axially loaded K and N overlap joints

Table 10.8 – Efficiency design chart for CHS K and N overlap joints

<table>
<tr><th colspan="2">K and N overlap joints of circular hollow sections</th></tr>
<tr><th>Symbols</th><th>Geometric range of validity</th></tr>
<tr><td>$2\gamma = \frac{d_0}{t_0}$ $\quad n' = \frac{f_{op}}{f_{y0}}$
 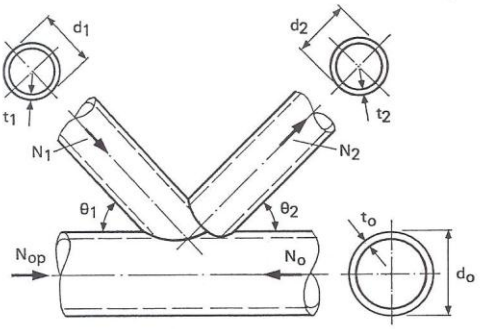

f_{op} = chord stress as a result of additional axial force or bending moment</td><td>$0.2 \le \frac{d_i}{d_0} \le 1.0$
$10 \le 2\gamma \le 50$
$d_i/t_i \le 50$
$30° \le \theta_i \le 90°$
$-0.55 \le \frac{e}{d_0} \le 0.25$</td></tr>
<tr><th colspan="2">Design chart</th></tr>
<tr><td colspan="2"> 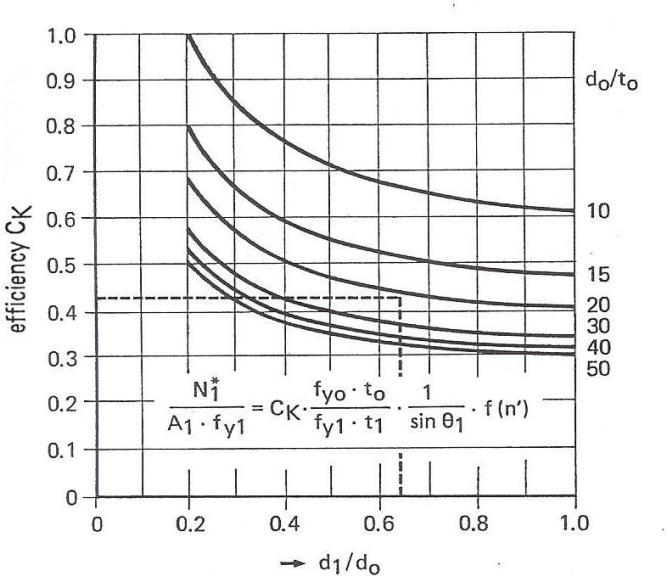
</td></tr>
</table>

Table 10.8 – Efficiency design chart for CHS K and N overlap joints (continued)

Calculation example		
chord : Φ 219.1 x 10.0 brace 1: Φ 139.7 x 6.3 brace 2: Φ 114.5 x 5.0	$d_0/t_0 = 21.9$ $d_1/t_1 = 22.2$ $d_2/t_2 = 22.9$	$f_{y0} = f_{y1} = f_{y2}$ Ov > 25%
	$\frac{d_1}{d_0} = \frac{139.7}{219.1} = 0.64$	**C_K = 0.44**
$\theta_1 = \theta_2 = 40°$ $f_{op} = -0.3f_{y0}$	$\sin\theta_1 = 0.643$ f(n') = 0.88 (see figure 10.1)	
$\frac{N_1^*}{A_1 f_{y1}} = 0.44 \times \frac{10}{6.3} \times \frac{1}{0.643} \times 0.88 = 0.95$		
$\frac{N_2^*}{A_2 f_{y2}} = \frac{N_1^*}{A_1 f_{y1}} \frac{A_1 f_{y1}}{A_2 f_{y2}} \frac{\sin\theta_1}{\sin\theta_2} = 1.46 > 1.0$		

Roof structure for a football stadium

10.6 Graphical design charts for joints loaded under brace bending moment

10.6.1 Design chart for joints loaded by brace in-plane bending moment

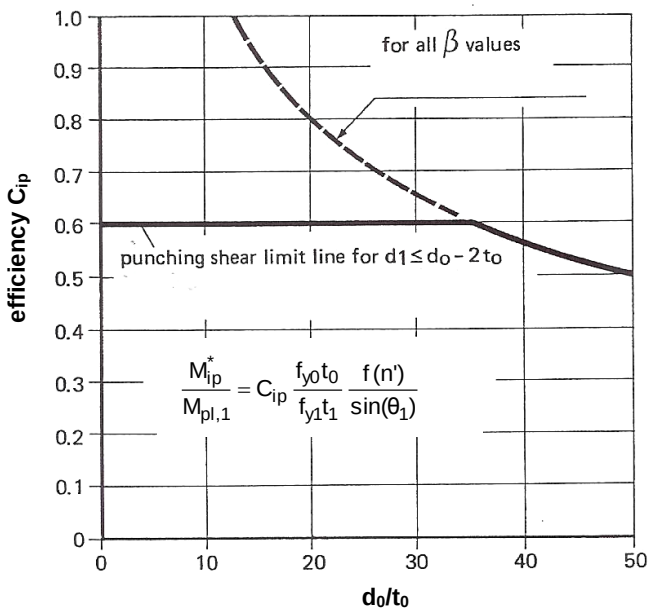

Figure 10.4 – Efficiency design chart for joints loaded by brace in-plane bending moment

10.6.2 Design chart for joints loaded by brace out-of-plane bending moment

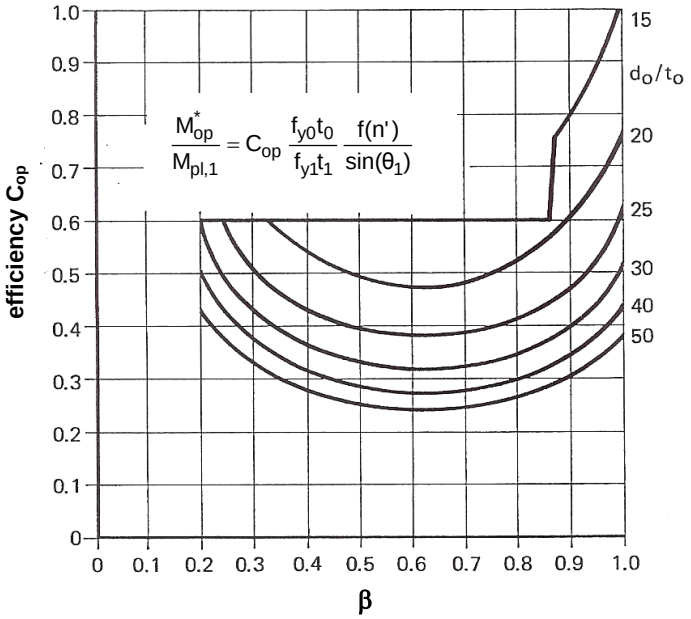

Figure 10.5 – Efficiency design chart for joints loaded by brace out-of-plane bending moment

11 Truss design examples based on the design strengths of the new IIW (2008) recommendations

In this section, design examples are presented which are based on the new IIW (2008) design equations for CHS to CHS joints, described in this 2nd edition of Design Guide No. 1.

11.1 Uniplanar truss

• Truss lay-out:

The following dimensions are assumed:

Trusses with span = 36 m and centre-to-centre = 12 m; purlins with centre-to-centre = 6 m

Truss depth ≈ (1/15) x span = 2.40 m (considering overall costs, e.g. costs of all cladding of the building, deflections, etc. 1/15 ℓ is generally an economical depth)

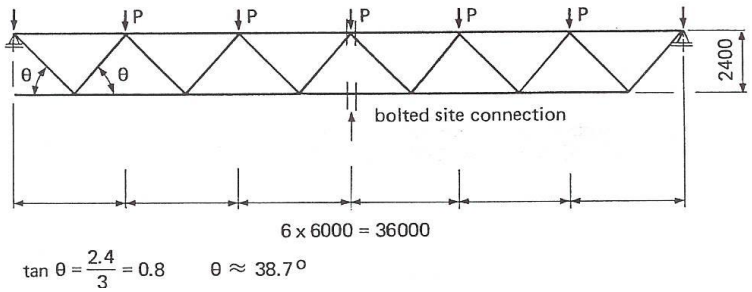

Figure 11.1 – Truss lay-out

A Warren type truss with K joints is chosen to limit the number of joints. The factored design load P from the purlins including the weight of the truss have been calculated as P = 108 kN.

• Member loads (kN)

A pin-jointed analysis of the truss gives the following member forces:

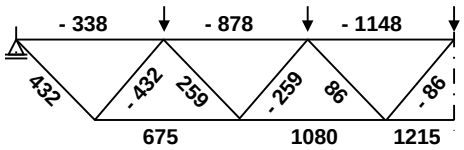

Figure 11.2 – Truss member axial loads

• Design of members

In this example, the chords will be made from steel with a yield stress of 355 N/mm^2 and the braces from steel with a yield stress of 275 N/mm^2.

For member selection, use either member resistance tables for the applicable effective length or the applicable buckling curve. Check the availability of the member sizes selected. Since the joints at the truss ends are generally decisive, the chords should not be too thin-walled. As a consequence, a continuous chord with the same wall thickness over the whole truss length is often the best choice.

Top chord

Use a continuous chord with an effective in-plane and out-of-plane length of:
ℓ_e = 0.9 x 6000 = 5400 mm, see chapter 3.3; N_0 = -1148 kN

Table 11.1 – Possible sections for top chord

f_{y0} (N/mm^2)	N_0 (kN)	ℓ_e (mm)	Possible sections (mm)	A_0 (mm^2)	d_0/t_0	$\bar{\lambda}$ (*)	χ (*)	$\chi f_{y0} A_0$ (kN)
355	-1148	5400	Ø 193.7 x 10.0	5771	19.4	1.09	0.61	1245
			Ø 219.1 x 7.1	4728	30.9	0.94	0.71	1189
			Ø 219.1 x 8.0	5305	27.4	0.95	0.71	1329
			Ø 244.5 x 5.6	4202	43.7	0.84	0.78	1159
			Ø 244.5 x 6.3	4714	38.8	0.84	0.78	1298

(*) Buckling curve “a” of Eurocode 3 (CEN, 2005a)

From a material point of view, the sections Ø 244.5 x 5.6 and Ø 219.1 x 7.1 are most efficient; however, these two dimensions are, for the supplier considered in this example, not available from stock (only to be delivered from factory). These dimensions can only be used if a large quantity is required, which is assumed in this example. Initially, Ø 219.1 x 7.1 is selected because the d_0/t_0 is lower, resulting in a higher joint strength.

Bottom chord

Table 11.2 – Possible sections for bottom chord

f_{y0} (N/mm^2)	N_0 (kN)	Possible sections (mm)	A_0 (mm^2)	d_0/t_0	$f_{y0} A_0$ (kN)
355	1215	Ø 168.3 x 7.1	3595	23.7	1276
		Ø 177.8 x 7.1	3807	25.0	1351
		Ø 193.7 x 6.3	3709	30.7	1317

Diagonals

Try to select members which satisfy $\frac{f_{y0}\ t_0}{f_{yi}\ t_i} \geq 2.0$; i.e.

$\frac{355 \times 7.1}{275 \times t_i} \geq 2.0$ or $t_i \leq 4.5$ mm

Use for the braces loaded in compression an initial effective length of 0.75 ℓ
= $0.75\sqrt{2.4^2 + 3.0^2} = 2.88$ m, see chapter 3.3.

Compression diagonals

Table 11.3 – Possible sections for compression diagonals

f_{yi} (N/mm^2)	N_i (kN)	ℓ_e (m)	Possible sections (mm)	A_i (mm^2)	$\bar{\lambda}$ (*)	χ (*)	$\chi f_{yi} A_i$ (kN)
275	-432	2.881	Ø 168.3 x 3.6	1862	0.57	0.90	462
			Ø 139.7 x 4.5	1911	0.69	0.85	448
	-259	2.881	Ø 114.6 x 3.6	1252	0.85	0.77	266
	-86	2.881	Ø 88.9 x 2.0 (**)	546	1.08	0.61	92

(*) Buckling curve “a” of Eurocode 3 (CEN, 2005a)
(**) The wall thickness is rather small for welding

Tension diagonals

Table 11.4 – Possible sections for tension diagonals

f_{yi} (N/mm^2)	N_i (kN)	Possible sections (mm)	A_i (mm^2)	$f_{yi} A_i$ (kN)
275	432	Ø 133.3 x 4.0	1621	445
	259	Ø 88.9 x 3.6	964	265
	86	Ø 48.3 x 2.3	332	91

Member selection

The number of sectional dimensions depends on the total tonnage to be ordered. In this example, for the braces only two different dimensions will be selected.

Comparison of the members suitable for the tension members and those suitable for the compression members shows that the following sections are most convenient:

- braces: Ø 139.7 x 4.5
  Ø 88.9 x 3.6

- top chord: Ø 219.1 x 7.1

- bottom chord: Ø 193.7 x 6.3

These chord sizes allow gap joints; no eccentricities are required.

It is recognized that the d_0/t_0 ratios of the chords selected are high. This may give joint strength problems in joints 2 and 5.

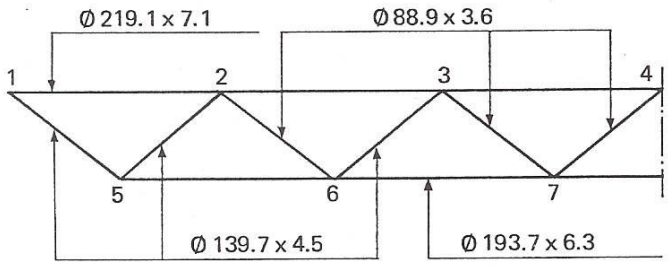

Figure 11.3 – Member dimensions

• Joint strength checks, commentary and revision

General

In table 11.5, all joints are treated as K joints, initially neglecting the additional X joint action in the joints 2, 3 and 4. In this case, there should be a larger margin between the design and the acting efficiency as will be shown in the more detailed accurate evaluation given below.

Joint 1

If in joint 1, a gap not exceeding g = $2t_0$ is chosen between the cap plate and the brace, nearly no eccentricity exists for the bolted joint of the cap plate. This joint is checked as a K(N) joint (see table 11.5) because the load transfer is similar as in an N joint (the reaction in the cap plate is upwards and the diagonal loading is downwards). In the example, β is conservatively based on the diameter of the brace.

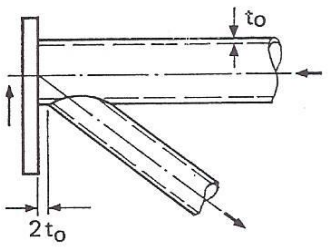

Figure 11.4 – Joint 1

Joint 2

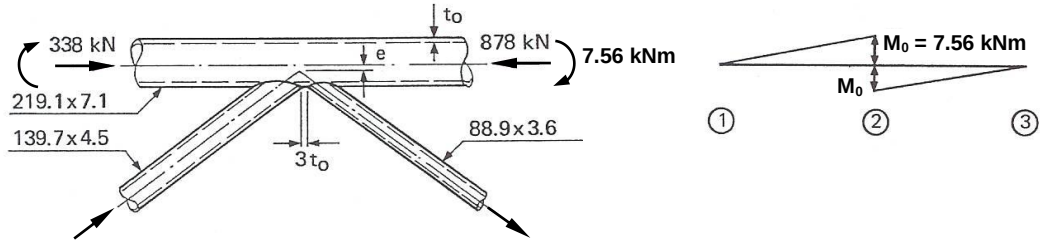

Figure 11.5 – Joint 2

Table 11.5 shows that the strength of joint 2 with g = $12.8t_0$ (and eccentricity e = 0 mm) is not sufficient. The easiest way to obtain adequate joint strength will be to decrease the gap from $12.8t_0$ to $3t_0$, resulting in a larger C_K = 0.39 and a slightly lower Q_f. However, this means that a (negative) eccentricity of e = 28 mm is introduced resulting in an eccentricity moment of: M = (878 - 338) x 28 x 10^{-3} = 15.12 kNm.

Since the length and the stiffness EI of the top chord members between joints 1-2 and 2-3 are the same (see figure 11.3), this moment can be equally distributed over both members, i.e. both members have to be designed additionally for M_0 = 7.56 kNm.

Including the chord bending moment effect gives the following values for the chord stress parameter n in the connecting face at the left and right side of the joint:

Left side: $$n = \frac{N_0}{A_0 f_{y0}} + \frac{M_0}{M_{pl,0}} = \frac{-338}{4728 \times 0.355} + \frac{7.56}{113.3} = -0.20 + 0.067 = -0.13$$

Right side: $$n = \frac{N_0}{A_0 f_{y0}} + \frac{M_0}{M_{pl,0}} = \frac{-878}{4728 \times 0.355} + \frac{-7.56}{113.3} = -0.52 - 0.067 = -0.59$$

Table 11.5 – Joint strength check, assuming K joint action only

Member sizes			Joint parameters				Actual efficiency	Joint strength efficiency						Check
Joint	Chord (mm)	Braces (mm)	β	d_0/t_0	g/t_0	n	$\frac{N_i}{A_i f_{yi}}$	C_K	$\frac{f_{y0}\, t_0}{f_{yi}\, t_i}$	Q_f	$\frac{1}{\sin\theta_i}$	$\frac{d_1 + d_2}{2d_i}$	$\frac{N_i^*}{A_i f_{yi}}$	$N_i^* \geq N_i$
1	Ø 219.1 x 7.1	plate Ø 139.7 x 4.5	0.64	30.9	2.0	-0.20	-- **0.82**	0.41	- 2.04	0.95	1.60	> 1.0	> 1.0	o.k.
2	Ø 219.1 x 7.1	Ø 139.7 x 4.5 Ø 88.9 x 3.6	0.52	30.9	12.8	-0.52	**0.82** **0.98**	0.34	2.04 2.55	0.83	1.60	0.82 1.29	0.76 > 1.0	not o.k. o.k.
2	Additional analysis of joint 2 with g/t_0 = 3.0 and e = -28 mm		0.52	30.9	3.0	-0.59	**0.82** **0.98**	0.39	2.04 2.55	0.80	1.60	0.82 1.29	0.84 > 1.0	o.k. o.k.
3	Ø 219.1 x 7.1	Ø 139.7 x 4.5 Ø 88.9 x 3.6	0.52	30.9	12.8	-0.68	**0.49** **0.32**	0.34	2.04 2.55	0.75	1.60	0.82 1.29	0.68 > 1.0	o.k. o.k.
4	Ø 219.1 x 7.1	Ø 88.9 x 3.6 Ø 88.9 x 3.6	0.41	30.9	7.1	-0.68	**0.32** **0.32**	0.35	2.55 2.55	0.75	1.60	1.0 1.0	> 1.0 > 1.0	o.k. o.k.
5	Ø 193.7 x 6.3	Ø 139.7 x 4.5 Ø 139.7 x 4.5	0.72	30.7	2.9	0.51	**0.82** **0.82**	0.41	1.81 1.81	0.87	1.60	1.0 1.0	> 1.0 > 1.0	o.k. o.k.
6	Ø 193.7 x 6.3	Ø 88.9 x 3.6 Ø 139.7 x 4.5	0.59	30.7	9.4	0.82	**0.98** **0.49**	0.37	2.26 1.81	0.71	1.60	1.29 0.82	> 1.0 0.62	o.k. o.k.
7	Ø 193.7 x 6.3	Ø 88.9 x 3.6 Ø 88.9 x 3.6	0.46	30.7	15.8	0.92	**0.32** **0.32**	0.32	2.26 2.26	0.60	1.60	1.0 1.0	0.69 0.69	o.k. o.k.

Note: Joints 1-4 discussed in detail in text

The right side with n = -0.59 is decisive, resulting in $Q_f = 0.80$. In combination with C_K, this gives a joint strength efficiency (see table 11.5):

$$\frac{N_1^*}{A_1 f_{y1}} = 0.84 > \frac{N_1}{A_1 f_{y1}} = 0.82 \rightarrow \text{o.k.}$$

The chord members between joints 1-2 and 2-3, which are in compression, should also be checked as a beam-column for buckling. From these, the chord member 2-3 is most critical. This check depends on the national code to be used. In general, the criterion to be verified has the following format:

$$\frac{N_0}{\chi\, A_0 f_{y0}} + k \frac{M_0}{M_{pl,0}} \leq 1.0$$

where:

χ = reduction factor for column buckling (see table 11.1 for the values of χ for the possible chord sections)

k = amplification factor for second order effects depending on slenderness, section classification and moment diagram (in this case use triangle)

$M_{pl,0}$ = plastic resistance ($W_{pl,0} f_{y0}$) of the chord (class 1 or 2 sections)

$$\frac{N_0}{\chi\, A_0 f_{y0}} + k \frac{M_0}{M_{pl,0}} = \frac{878}{1189} + k \frac{7.56}{113.3} = 0.74 + 0.067k < 1.0$$

Independent of the code used, this will not be critical.

More accurate calculation based on combined K and X joint actions.

As already mentioned, actually this joint has a combination of K joint and X joint actions and can be substituted by a K joint and an X joint, see chapter 4.1.

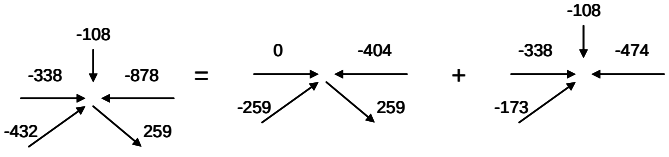

Joint 2 – K joint action:

$n = \frac{N_0}{A_0 f_{y0}} = \frac{-404}{4728 \times 0.355} = -0.24$ compression; thus $Q_f = 0.93$ (see figure 4.8)

For the modified configuration with $g = 3t_0$, $\beta = 0.52$ and $2\gamma = 30.9$: $C_K = 0.39$ (see table 4.7)

For brace 1: $\frac{N_1^*}{A_1 f_{y1}} = 0.39 \times 2.04 \times \frac{0.93}{0.625} \times 0.82 = 0.97$

Due to acting load: $\frac{N_1}{A_1 f_{y1}} = \frac{259}{525.5} = 0.49$

Hence, the utilization ratio for K joint action is $\frac{N_1}{N_1^*} = \frac{0.49}{0.97} = 0.50$

For brace 2: $\frac{N_2^*}{A_2 f_{y2}} = 0.39 \times 2.55 \times \frac{0.93}{0.625} \times 1.29 > 1.0$

thus the actual efficiency $\frac{N_2}{A_2 f_{y2}} = 0.98 < 1.0 \rightarrow$ o.k.

Joint 2 – X joint action:

$n = \frac{N_0}{A_0 f_{y0}} = \frac{-474}{4728 \times 0.355} = -0.28$ compression; including the above mentioned chord bending moment M_0 gives: n = -0.28 - 0.067 = -0.35, thus Q_f = 0.88 (see figure 4.6)

For $\frac{d_1}{d_0} = \frac{139.7}{219.1} = 0.64$ and 2γ = 30.9: C_X = 0.20 (see table 4.6)

$$\frac{N_1^*}{A_1 f_{y1}} = 0.20 \times 2.04 \times \frac{0.88}{0.625} = 0.57$$

Due to acting load: $\frac{N_1}{A_1 f_{y1}} = \frac{173}{525.5} = 0.33$

Hence, the utilization ratio for X joint action is $\frac{N_1}{N_1^*} = \frac{0.33}{0.57} = 0.58$

The combined acting efficiencies for brace 1 due to K joint and X joint action are:
0.50 + 0.58 = 1.08 > 1.0, thus the joint is still not o.k.

Note: Based on the check as a K joint only (see table 11.5 for the evaluation of joint 2 with g/t_0 = 3.0), this utilization ratio was $\frac{N_1}{N_1^*} = \frac{0.82}{0.84} = 0.98$, which would have been about 10% over-optimistic.

Further decreasing the gap will not help because the design efficiency as a K joint is already close to 1.0. Hence, the effect of the X joint action should be decreased. This can be done as follows:

- By using a section for brace 1 with about the same cross sectional area but a lower thickness (e.g. Ø 168.3 x 3.6), which increases the design efficiency. However, this increases the number of section types for the braces to three.
- By increasing the thickness of the top chord and choosing Ø 219.1 x 8.0

An additional type of section can increase the costs, but increasing the chord thickness also increases material costs. The choice will be made after checking the other joints.

Joint 3

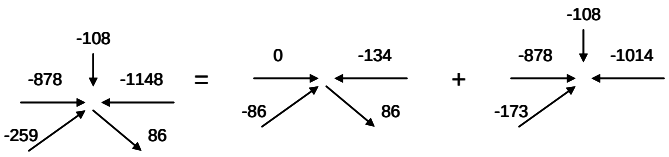

Joint 3 – K joint action:

$n = \frac{N_0}{A_0 f_{y0}} = \frac{-134}{4728 \times 0.355} = -0.08$ compression; thus Q_f = 0.98 (see figure 4.8)

For $g = 12.8t_0$ with β = 0.52 and 2γ = 30.9: C_K = 0.34 (see table 4.7)

$$\frac{N_1^*}{A_1 f_{y1}} = 0.34 \times 2.04 \times \frac{0.98}{0.625} \times 0.82 = 0.89$$

Due to acting load: $\frac{N_1}{A_1 f_{y1}} = \frac{86}{525.5} = 0.16$

Hence, the utilization ratio for K joint action is $\frac{N_1}{N_1^*} = \frac{0.16}{0.89} = 0.18$

For brace 2: $\frac{N_2^*}{A_2 f_{y2}} = 0.34 \times 2.55 \times \frac{0.98}{0.625} \times 1.29 > 1.0$

thus the actual efficiency $\frac{N_2}{A_2 f_{y2}} = 0.32 < 1.0 \rightarrow$ o.k.

Joint 3 – X joint action:

$n = \frac{N_0}{A_0 f_{y0}} = \frac{-1014}{4728 \times 0.355} = -0.60$ compression; thus Q_f = 0.77 (see figure 4.6)

For $\frac{d_1}{d_0} = \frac{139.7}{219.1} = 0.64$ and 2γ = 30.9: C_X = 0.20 (see table 4.6)

$\frac{N_1^*}{A_1 f_{y1}} = 0.20 \times 2.04 \times \frac{0.77}{0.625} = 0.50$

Due to acting load: $\frac{N_1}{A_1 f_{y1}} = \frac{173}{525.5} = 0.33$

Hence, the utilization ratio for X joint action is $\frac{N_1}{N_1^*} = \frac{0.33}{0.50} = 0.66$

The combined acting efficiencies due to K joint and X joint action are 0.18 + 0.66 = 0.84 < 1.0 and the criteria are satisfied.

Note: Based on the check as a K joint only (see table 11.5 for the evaluation of joint 3), this utilization ratio was $\frac{N_1}{N_1^*} = \frac{0.49}{0.68} = 0.72$ *, which would have been about 14% over-optimistic.*

Joint 4

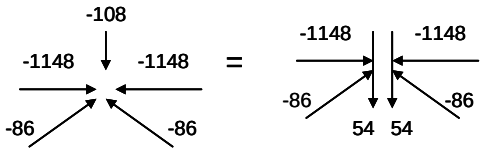

At joint 4, a site joint will be made consisting of two plates which also transfer the purlin load to the chord. This means that joint 4 behaves as two N joints. Assuming no eccentricity at the bolted joint and cap plates of 15 mm, the gap between the toe of the brace and the cap plate will be (see equation 1.1):

$$g = 0.5\left(\frac{219.1}{2}\frac{\sin(2 \times 38.7)}{\sin^2 38.7} - \frac{88.9}{\sin 38.7}\right) - 15 = 50.6\,\text{mm} = 7.1 t_0$$

The check in table 11.5 shows that the joint is o.k.

Evaluation

The joint checks showed that joint 2 is not o.k. Considering the options mentioned, in this example, the chord section will be changed from Ø 219.1 x 7.1 into Ø 219.1 x 8.0. Recalculating the joint for e = 0 (with g = $12.8t_0$), gives a utilization ratio of 0.49 for K joint action and 0.45 for X joint action, thus combined 0.94 < 1.0.

Compared to the selected members in figure 11.3, only the top chord is changed into Ø 219.1 x 8.0 and all joints can be made without any eccentricity.

• Purlin joints

Depending on the type of purlins, various purlin joints are possible. If corrosion will not occur, a cut-out of a channel section welded on top of the chord at the purlin support location and provided with bolt stubs gives an easy support, see figure 11.7. Table 7.1 provides evidence for the design of plate to tube joints. The joints in table 7.1 are not exactly similar to that between the open U section and a CHS chord but the capacity may be based on equation 7.6 for an RHS to CHS joint. Since no cross plates are present, only the sides are effective; therefore a very conservative reduction factor to be applied is $h_1/(h_1+b_1)$.

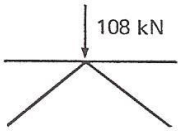

Figure 11.6 – Purlin load

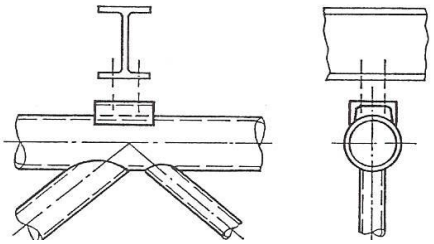

Figure 11.7 – Purlin joint

For the purlin joint at the centre, in figure 11.8 another alternative is given to allow the site bolted joint of the truss.

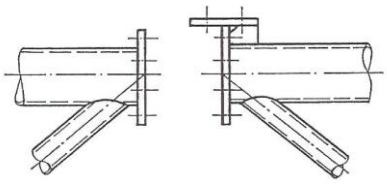

Figure 11.8 – Purlin support at the site joint of the truss

The top chord can also be provided with cap plates only. In that case, a T stub for purlin support has to be fitted in between the cap plates.

• Bolted site flange joints

Bottom tensile chord joint

According to table 8.1, 8 bolts Ø 22 - 10.9 are required for a full strength connection (i.e. $A_0\, f_{y0}$) of Ø 190.7 x 5.3 with f_{y0} = 235 N/mm^2. In this example, the cross section area and the yield stresses of the chord section Ø 193.7 x 6.3 are different from those in table 8.1, whereas the bolt strength is the same. This means that the number of bolts has to be determined taking account of these effects. Therefore, a slightly larger section Ø 216.3 x 8.2 with about the same capacity is taken as reference. For the chord section Ø 193.7 x 6.3 with f_{y0} = 355 N/mm^2 and the same bolt strength, the number of bolts can be estimated to be:

$$\frac{\pi(193.7-6.3)\times 6.3}{\pi(216.3-8.2)\times 8.2}\times\frac{355}{235}\times 12 = 13\,\text{bolts}$$

As a first estimate, the cap plate thickness for 13 bolts Ø 22 - 10.9 can be taken slightly smaller than 25 mm (due to f_{yp} = 355 N/mm^2) and the edge distances e_1 = 40 mm and e_2 = 35 mm. Based on equation 8.1 and rounded off, a plate thickness of 20 mm can be used.

Considering the centre-to-centre distance of the bolts, this option is possible.

Top compression chord joint

For the top chord joint, the compression loading is transferred through contact pressure. The number of bolts required depends on the erection loads which can be in tension, and the national code requirements with regard to the minimum strength related to the member tensile strength. In order to determine the number of bolts for the compression flange joint, one could design for the design force in the member, being 1148 kN, which results in:

$$\frac{1148}{\pi(216.3-8.2)\times 8.2\times 0.235}\times 12 \approx 11 \text{ bolts Ø 22 - 10.9}$$

Then, 11 bolts Ø 22 - 10.9 are needed with a practical cap plate thickness of 16 mm (f_y = 355 N/mm^2) and edge distances e_1 = 40 mm and e_2 = 35 mm.

The end support joint can be made as shown in figure 8.2.

Note: Using the IIW (1989) design recommendations gives the same brace and bottom chord dimensions as presented in this example; however the top chord in this example will be marginally thicker, i.e. 8 mm instead of 7.1 mm.

11.2 Vierendeel truss

• Truss lay-out and design of members

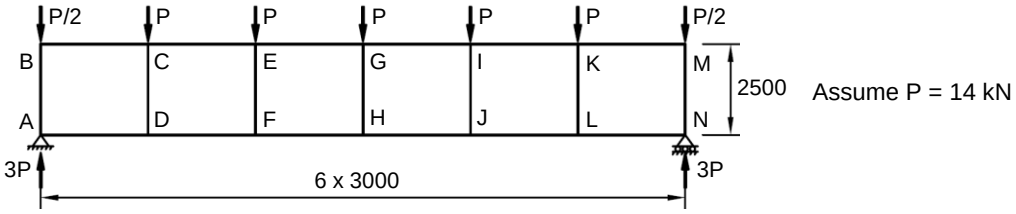

Figure 11.9 – Vierendeel truss

For Vierendeel trusses with top and bottom chords having the same bending stiffness $\frac{EI}{\ell}$, initially a simplified design calculation can be used, if:

- the loads act at the joints
- the joints are rigid
- the longitudinal displacements of the chords can be disregarded

Under these conditions, the moments will be zero at the centres of the chord members between the joints and the load and moment distribution can be determined easily, see figures 11.10 and 11.11.

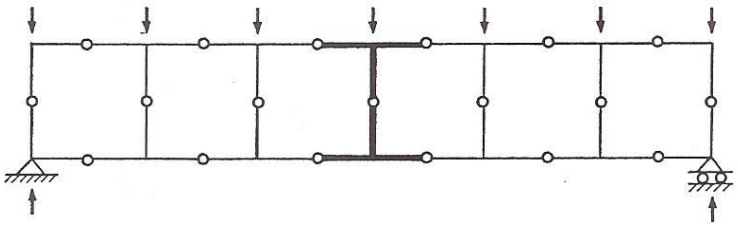

Figure 11.10 – Simplified modelling

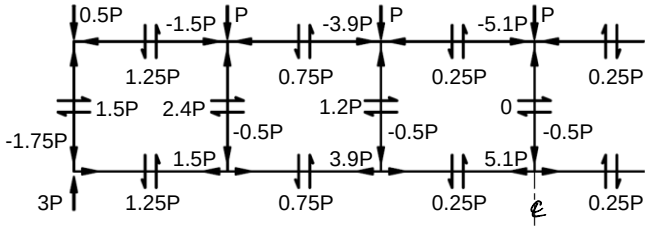

(a) Member axial forces and shear forces

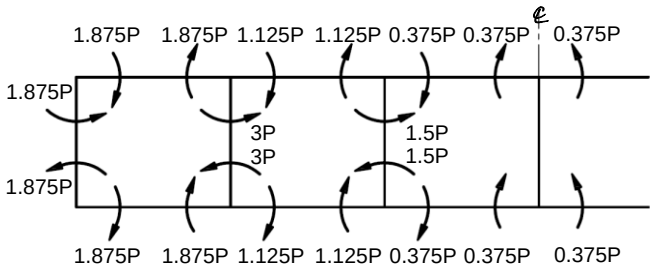

(b) Bending moments

Figure 11.11 – Forces and moments within Vierendeel truss (shown applied at the nodes)

Chord members

As shown in figure 11.11, the chord member loaded in compression has to be designed as a beam-column (for buckling) for the following conditions (P in kN):

N_0 = -1.5 P kN and M_0 = 1.875 P kNm (1.25 P kN shear)
N_0 = -3.9 P kN and M_0 = 1.125 P kNm (0.75 P kN shear)
N_0 = -5.1 P kN and M_0 = 0.375 P kNm (0.25 P kN shear)

The first case with the highest moment will be decisive. In this example, no further member checks are given.

Braces

The braces have to be checked (not given in this example) for the moments, axial and shear loads. As shown, the second brace (member C-D) is decisive with:

M_1 = 3.0 P kNm, N_1 = -0.5 P kN and 2.4 P kN shear load.

Joint loads

The joints of the second brace (C-D) have the largest moment loading. The moments in the chords are in equilibrium with the moment in the brace. Since the bottom chord is loaded in tension, in general, the joints with the top chords are decisive if the top and bottom chords have the same dimensions. For the chord sections, the moments are most critical.

For Vierendeel trusses the rotational stiffness of the joints is very important. This requires joints with diameter ratios β close to 1.0, see chapter 5.

Evaluation

As mentioned above, the second brace is the heaviest loaded member in the Vierendeel truss. The diameter is limited by the chord members and an increase in brace wall thickness does not increase the joint strength, see figure 5.2. Consequently, if all truss members are made from the same dimension, this results in over-design of the other braces and chord members if lateral buckling is prevented.

• Joint strength check

In this example, it is assumed that all members are made from the same circular hollow sections Ø 193.7 x 6.3 with f_y = 355 N/mm^2, A = 3709 mm^2, W_{pl} = 221.3 x 10^3 mm^3, N_{pl} = 1317 kN and M_{pl} = 78.6 kNm.

According to table 5.1 the design resistance (punching shear not applicable) is given by:

$$M^*_{ip,1} = 4.3\, f_{y0}\, t_0^2\, \gamma^{0.5}\, \beta\, d_1 \frac{Q_f}{\sin\theta_1}$$

$$M^*_{ip,1} = 4.3 \times 355 \times 6.3^2 \times \left(\frac{193.7}{2 \times 6.3}\right)^{0.5} \times 1.0 \times 193.7 \times Q_f$$

$$M^*_{ip,1} = 46.0\, Q_f \text{ kNm} \le W_{pl,1} f_{y1} = 78.6 \text{ kNm}$$

For 2γ = 30.7 and β = 1.0 (see efficiency diagram in table 4.5):

$$N^*_1 = 0.38 A_1 f_{y1} Q_f = 500\, Q_f \text{ kN}$$

Note: The shear force of 2.4 P need not be considered for the joint strength.

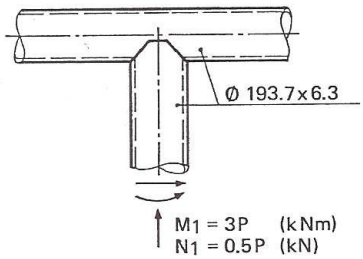

Figure 11.12 – Brace loading

In the braces, the largest moment occurs in member C-D. For Q_f the decisive combination of chord loading has to be considered, which is the most punitive of the chord stresses at either side of the joint in the connecting face. For P = 14 kN, table 11.6 lists the values of Q_f obtained for joints C and D.

Table 11.6 – Determination of Q_f

Joint	Axial compression (kN)	Bending moment (*) (kNm)	$n = \frac{N_0}{N_{pl,0}} + \frac{M_0}{M_{pl,0}}$	Q_f
Top chord				
C_{left}	-21.0	26.3	0.32	0.93
C_{right}	-54.6	-15.8	-0.24	0.95
Bottom chord				
D_{left}	21.0	-26.3	-0.32	0.93
D_{right}	54.6	15.8	0.24	0.95

(*) Bending moments giving tensile stress in the chord connecting face are taken as positive

From table 11.6 follows that the chord section at the left side of joint D is critical (i.e. lowest Q_f) with $Q_f = 0.93$, thus:

$M^*_{ip,1} = 46.0\ Q_f = 42.8$ kNm $\qquad \frac{M_1}{M^*_{ip,1}} = \frac{3 \times 14}{42.8} = 0.98$

$N^*_1 = 500\ Q_f = 465$ kN $\qquad \frac{N_1}{N^*_1} = \frac{0.5 \times 14}{465} = 0.02$

With the interaction equation 5.7:

$$\frac{N_1}{N^*_1} + \left(\frac{M_1}{M^*_{ip,1}} \right)^2 = 0.02 + (0.98)^2 = 0.98 \le 1.0 \rightarrow \text{o.k.}$$

This calculation confirms that axial forces have a minor effect in Vierendeel trusses.

As shown in figure 11.13, the joints at the end of the girder can be made in various ways. The use of type (a) is in accordance with the previous calculations. The end cap compensates for the fact that the chord is not continuous. Type (b) can only be used for very low loads since the diagonal reaction forces in the corner cannot be transferred satisfactorily. Type (c) with a fill-in plate provides an adequate load transfer.

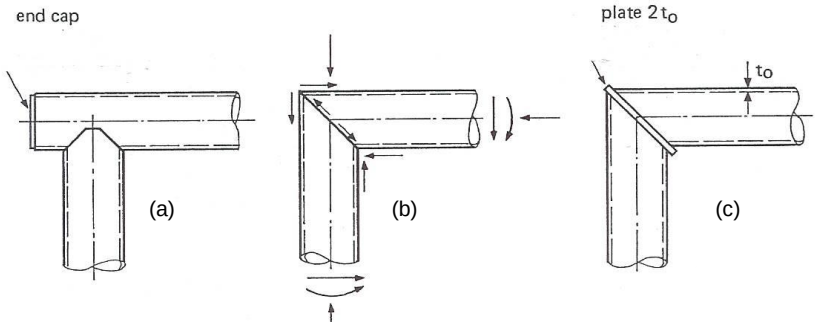

Figure 11.13 – Vierendeel end corner joints

• Remarks

Especially if thin-walled sections are used or if the joint stiffness has to be taken into account (β < 1.0), a more precise semi-rigid frame analysis by computer has to be carried out to determine the moment distribution and the deflections.

• Plastic design of Vierendeel trusses

If all of the sections selected are class 1 (plastic design) sections, and also meet the criteria for rigid joint behaviour, such as β = 1.0 in the foregoing example, a more favourable distribution of bending moments may be obtained in the truss by the use of “Plastic Moment Distribution” (i.e. a set of moments which is in equilibrium with the applied loads, by the Lower Bound Theorem).

Note: Using the IIW (1989) design recommendations gives for the same chord and brace dimensions a larger capacity, i.e. P = 17 kN instead of P = 14 kN.

11.3 Multiplanar truss (triangular girder)

• Truss lay-out

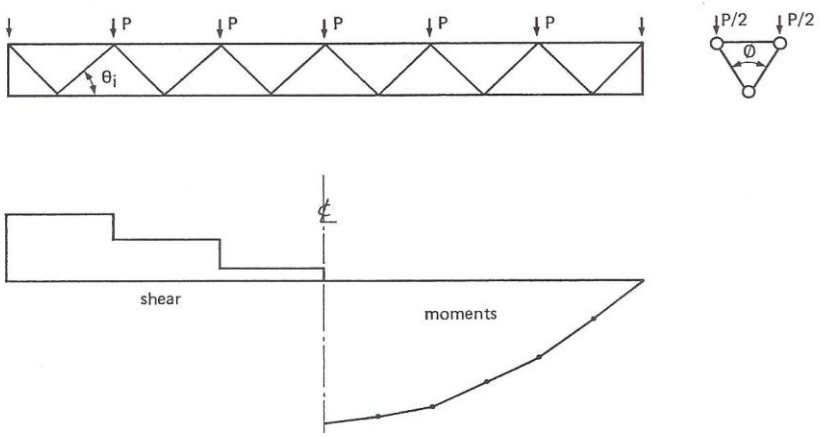

$\phi = 60°$

P = 187 kN

Figure 11.14 – Triangular truss

• Member loads

The member loads will be determined in a similar way as for the uniplanar truss, assuming pin ended members.

The load in the bottom chord follows by dividing the relevant moment by the girder depth. Since two top chords are used, the load at the top has to be divided by 2. The loads in the braces follow from the shear forces V in the girder, see figure 11.15.

The top chords should be connected in the top plane for equilibrium of loading, see figure 11.16. This can be achieved by a bracing system which connects the loading points. Connection of the loading points only, results in a triangular truss which has no torsional rigidity. Combination with diagonals gives torsional resistance.

Now the loads in one plane are known, and the design can be treated in a similar way as for uniplanar trusses.

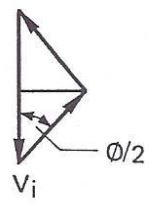

Figure 11.15

Figure 11.16

• Joints

The joints can also be treated in a similar way as for uniplanar joints, however, taking account of the larger chord loads. This means a larger Q_f reduction factor for the joints with the bottom chord. From a fabrication point of view, it is better to avoid overlaps of the intersecting braces from both planes. Sometimes this may result in an eccentricity in the two planes, also called offset.

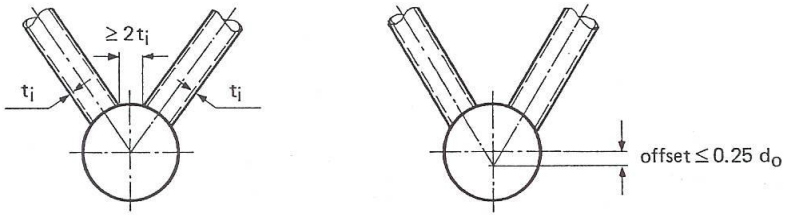

Figure 11.17 – Gap and offset

The offset has to be incorporated in member design and joint capacity verification. For the chords, the moments due to this offset have to be distributed over the chord members, affecting the chord stress function Q_f and hence, the joint capacity.

• Design calculation

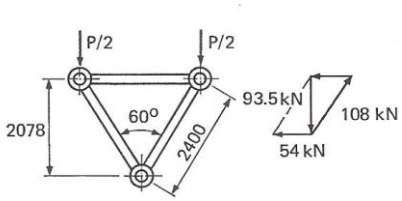

Assume P = 187 kN (limit state)

This means that the loads acting in the side planes of the triangular truss are:

$$\frac{P}{2\cos 30°} = 108\,\text{kN}$$

Figure 11.18 – Cross section of the triangular truss

This is equal to the purlin loads used in the design example for the uniplanar truss in chapter 11.1. As a consequence, the top chord and the diagonals can be the same to those for the uniplanar truss provided the same steel grades are used.

Only for the bottom chord, the required cross section should be twice that required for the uniplanar truss, i.e. Ø 219.1 x 11.0 with A_0 = 7191 mm^2 and $W_{pl,0}$ = 476.8 x 10^3 mm^3. (This section may have a longer delivery time.)

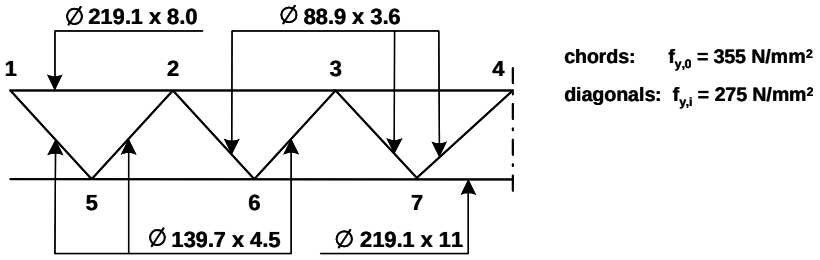

Figure 11.19 – Member dimensions and steel grades

The detailed check of the members is already given in section 11.1 and is the same here. However, the eccentricity moment should be taken into account both for member design and joint strength verification (i.e. effect of the chord moment on the chord stress factor Q_f).

The braces between the top chords are determined by the horizontal loads of 54 kN at each purlin support or by loads resulting from not equally distributed loading of the roof. Since transport is simpler for V-trusses than for triangular trusses, it is also possible to use the purlins as connection between the top chords. A simple bolted joint as given in figure 11.7 can easily transfer the shear load of 54 kN. However, in this way the truss has no torsional rigidity and cannot act as horizontal wind bracing of the roof. If this is required, braces between the top chords should be used.

• Joint strength check

As mentioned, the initial difference with the joint strength checks for the uniplanar truss in section 11.1 is that the effect of noding eccentricity has to be incorporated. A joint without any eccentricity would result in an overlap of the braces in the two planes, see figure 11.20(a). To allow welding, an out-of-plane gap of 22.5 mm is chosen which results in an eccentricity of 50 mm (in-plane 43 mm). As a consequence, the in-plane gap increases, resulting in slightly lower C_K values.

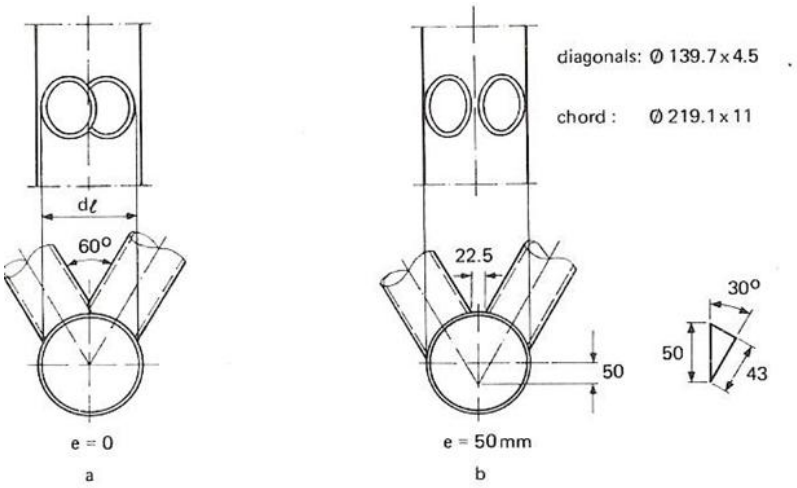

Figure 11.20 – Joint between diagonals and bottom chord

Besides the joint capacity checks carried out in section 11.1, the multiplanar joint has to be checked for chord shear, see table 6.1. The joint with maximum shear *in the gap* is joint 5 with:

$V_{gap,0}$ = 2.5 P = 2.5 x 187 = 467.5 kN

Further:

$N_{gap,0}$ = 0.5 x (2 x 675) = 675 kN (see figure 11.2) and $M_{gap,0}$ = 675 x 0.05 = 33.75 kNm

$$N_{pl,0} = A_0 f_{y0} = 7191 \times 0.355 = 2552\,\text{kN} \qquad \frac{N_{gap,0}}{N_{pl,0}} = \frac{675}{2552} = 0.26$$

$$V_{pl,0} = 0.58 f_{y0} \frac{2A_0}{\pi} = 0.58 \times 0.355 \times \frac{2 \times 7191}{\pi} = 943\,\text{kN} \qquad \frac{V_{gap,0}}{V_{pl,0}} = \frac{467.5}{943} = 0.50$$

$$M_{pl,0} = W_{pl,0} f_{y0} = 476.8 \times 10^3 \times 0.355 \times 10^{-3} = 169.3\,\text{kNm} \qquad \frac{M_{gap,0}}{M_{pl,0}} = \frac{33.75}{169.3} = 0.20$$

A conservative, linear interaction gives:

$$\frac{N_{gap,0}}{N_{pl,0}} + \frac{V_{gap,0}}{V_{pl,0}} + \frac{M_{gap,0}}{M_{pl,0}} = 0.26 + 0.50 + 0.20 = 0.96 \le 1.0$$

The exact interaction is more complicated (Wardenier, 1982), because for a CHS, the interaction between M and N is different from the (quadratic) interaction between N and V (see equation 6.2).

Note: In general, this chord shear check becomes critical for larger β ratios.

The end support joint can be dealt with in a similar way as described in chapter 11.1.

If only horizontal braces are used between the top chords to transfer the relatively small 54 kN tension forces, then the effect on the capacity of the joints in the side planes will be marginal and the T joints in the horizontal plane (with no chord bending but with high chord loads) can be calculated independently from the K joints in the side planes. If a K bracing system is used, the joints can be dealt with as multiplanar joints (see chapter 6.2), considering the effects indicated in table 4.4. Detailed theoretical background information about multiplanar effects is given in van der Vegte (1995).

11.4 Truss with semi-flattened end braces

To avoid overlaps in triangular trusses, it is also possible to use semi-flattened end bracings, as shown in figure 9.7.

The design of members is similar to that discussed in chapter 11.1, with the exception of the braces loaded in compression, for which an out-of-plane effective length factor of 1.0 instead of 0.75 has to be taken into account. As shown in chapter 9.2, the joint strength is decreased due to the reduction in β but increased due to the reduction in gap size. The above mentioned effects may partly compensate each other and the actual joint strength may not deviate considerably from that of a joint with profiled braces.

Full flattening, for which design information is given in figure 9.6, is only recommended for small sized secondary structures.

Girder with flattened-end braces

12 List of symbols and abbreviations

12.1 Abbreviations of organisations

AIJ Architectural Institute of Japan
AISC American Institute of Steel Construction
API American Petroleum Institute
ASTM American Society for Testing and Materials
AWS American Welding Society
CEN European Committee for Standardization
IIW International Institute of Welding
ISO International Organization for Standardization

12.2 Other abbreviations

CHS circular hollow section
FE finite element
RHS rectangular or square hollow section

12.3 General symbols

A cross-sectional area; chord stress parameter in API function
A_g gross cross-sectional area of CHS
A_{gv} gross area in shear for block failure
A_i cross-sectional area of member i
A_n net cross-sectional area of CHS
A_{nt} net area in tension for block failure
C_e, C_T, C_X, C_K efficiency coefficients
C, C_{ip}, C_{op} rotational stiffness coefficients for in-plane and out-of-plane bending
C_1, C_2, C_3 coefficients in chord stress functions
E modulus of elasticity
$F_{u,c}$ ultimate axial load capacity of a collar plate reinforced joint
$F_{u,u}$ ultimate axial load capacity of a comparable unreinforced joint
I moment of inertia
K effective length factor
L distance between chord panel points
L_w weld length
M^* moment or flexural resistance of a joint, expressed as a moment in the brace
M_c resulting chord bending moment
$M_{el,i}$ elastic moment capacity of member i
$M_{gap,0}$ chord bending moment in gap
M_i bending moment applied to member i (i = 0, 1, 2)
$M_{i,u,c}$ ultimate in-plane bending moment capacity of a collar plate reinforced joint
$M_{i,u,u}$ ultimate in-plane bending moment capacity of comparable unreinforced joint
$M_{ip,i}$ in-plane bending moment applied to member i
$M_{o,u,c}$ ultimate out-of-plane bending moment capacity of a collar plate reinforced joint
$M_{o,u,u}$ ultimate out-of-plane bending moment capacity of a comparable unreinforced joint
$M_{op,i}$ out-of-plane bending moment applied to member i
$M_{pl,i}$ plastic moment capacity of member i
N axial force
N^*_{can} joint resistance based on can thickness
$N_{gap,0}$ chord axial force in gap
N_i axial force applied to member i (i = 0, 1, 2)
N^*_i joint resistance, expressed as an axial force in member i

N_{op} chord load excluding the effect of the horizontal brace load components
$N_{pl,i}$ axial yield capacity of member i
Ov overlap Ov = q/p x 100%
P factored design load
Q_f chord stress function (in the new formulae of chapters 4 and 5)
Q_u, Q_{ub} functions in design strength equations accounting for the effect of geometric parameters
Q_{uk} characteristic Q_u value; equal to Q_u in API (2007) equations and equal to $1.1Q_u$ in IIW (2008) equations
T_u ultimate tensile resistance of a bolt
V shear force
$V_{gap,0}$ chord shear force in gap
$V_{pl,0}$ shear yield capacity of the chord
$W_{el,i}$ elastic section modulus of member i
$W_{pl,i}$ plastic section modulus of member i

a throat thickness
b_i external width of an RHS brace or plate branch or I section member i (90º to plane of truss)
b_0 external width of an RHS chord or I section chord
c_s variable used in strength equations for K and N overlap joints (see table 4.3)
d diameter; bolt diameter
d_{ei}, d_{ej}, $d_{e,ov}$ functions used to describe the strength of K and N overlap joints (see table 4.3)
d_i, d_j external diameter of a CHS member i (i = 0, 1, 2) or j (overlapped brace)
$d_{i,min.}$ minimum diameter at flattened or cropped-end of brace i (see figure 9.7)
$d_{i,max.}$ maximum diameter at flattened or cropped-end of brace i (see figure 9.7)
e noding eccentricity for a joint – positive being towards the outside of the truss (see figures 1.1 and 1.2); edge distance
f_{op} prestress in chord
f_u ultimate tensile stress
f_{ui}, f_{uj} ultimate tensile stress of overlapping brace i or overlapped brace j in an overlap joint
f_y yield stress
f_{yi}, f_{yj} yield stress of member i (i = 0, 1, 2) or j
f_{yp} yield stress of a plate
f(n') chord prestress function in IIW (1989) recommendations
f_1, f_2, f_3 functions; parameters for a bolted flange joint
g gap between the brace members (ignoring welds) of a K or N joint, at the face of the chord (see figure 1.2)
g' gap divided by chord wall thickness
h_i external depth of an RHS brace or plate branch or I section member i (in plane of truss)
h_0 external depth of an RHS chord or I section chord
k factor in beam-column equation
k_a, k_b functions in punching shear equation
l (member) length
l_c length of a collar plate
l_{can} can length
l_d length of a doubler plate
l_e effective length
n stress ratio in CHS chord; number of bolts
n' prestress ratio in CHS chord, i.e. based on the chord load excluding the effect of the horizontal brace load components
p length of projected contact area between the overlapping brace member and the chord, without the presence of the overlapped member (see figure 1.1)
q length of overlap between brace members of a K or N joint at chord face (see figure 1.1)
r ratio between actual can length and the can length at which the joint resistance can be based on the can thickness; radius between flange and web in an I section
r_o external corner radius of an RHS
r_1, r_2 parameters for a bolted flange joint
s edge distance of a cap plate (diameter cap plate minus diameter connected CHS)

t, t_i, t_j thickness of hollow section member i or flange thickness of I section member i (i = 0, 1, 2) or j (overlapped brace)

t_c thickness of a collar plate

t_{can} thickness of a joint can

t_d thickness of a doubler plate

t_f thickness of flange plate

t_{in} thickness of inner tube

t_p thickness of plate

t_w thickness of web

w distance between the welds, measured from plate face-to-plate face, around the perimeter of the CHS; $w = 0.5\pi d_i - t_p$

α chord length parameter ($\alpha = 2l_0 / d_0$); stress reduction factor for Knee joints

β width ratio between brace/branch member(s) and the chord
$= d_1 / d_0$, b_1 / d_0 (for T, Y, X)
$= (d_1 + d_2)/2d_0$ (for K, N)

χ reduction factor for (column) buckling

ε parameter used to define section class limitations

ϕ joint resistance (or capacity) factor (approximate inverse of γ_M); angle between two planes

γ half diameter to thickness ratio of the chord ($\gamma = d_0 / 2t_0$)

γ_M partial safety factor for joint resistance (approximate inverse of ϕ)

η brace depth h_1 to chord diameter d_0 ratio

$\bar{\lambda}$ non-dimensional slenderness

μ correction factor accounting for multiplanar effect to be applied to uniplanar joint strength

θ_i included angle between brace/branch member i (i = 1, 2) and the chord

τ brace wall-to-chord wall thickness ratio ($\tau = t_1/t_0$)

12.4 Subscripts

M material

c collar plate

d doubler plate

e effective

el elastic

i subscript used to denote the member of a hollow section joint. Subscript i = 0 designates the chord (or “through member”); i = 1 refers in general to the brace for T, Y and X joints, or it refers to the compression brace member for K and N joints; i = 2 refers to the tension brace member for K and N joints. For K and N overlap joints, the subscript i is used to denote the overlapping brace member (see figure 1.1)

in inner tube

ip in-plane bending

j subscript used to denote the overlapped brace member for K and N overlap joints

op out-of-plane bending; prestress

p plate

pl plastic

u ultimate

w web

y yield

12.5 Superscripts

* resistance or capacity

Symbols not shown here are specifically defined at the location where they are used.

In all calculations, the nominal (guaranteed minimum) mechanical properties should be used.

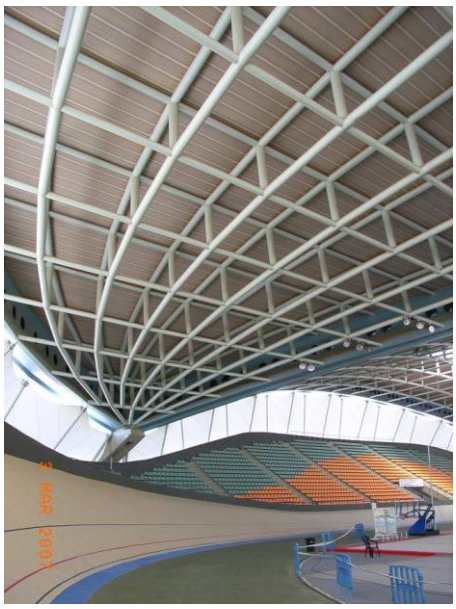

Vierendeel trusses for a curved roof

13 References

AIJ, 2002: Recommendations for the design and fabrication of tubular truss structures in steel. Architectural Institute of Japan, (in Japanese).

AISC, 2005: Specification for structural steel buildings. ANSI/AISC 360-05, American Institute of Steel Construction, Chicago, Ill., USA.

API, 2007: Recommended practice for planning, designing and constructing fixed offshore platforms – Working stress design. API RP 2A, 21st Edition, Suppl. 3, American Petroleum Institute, Dallas, USA.

ASTM, 2007a: Standard specification for cold-formed welded and seamless carbon steel structural tubing in rounds and shapes. ASTM A500/A500M-07, ASTM International, West Conshohocken, PA, USA.

ASTM, 2007b: Standard specification for hot-formed welded and seamless carbon steel structural tubing. ASTM A501-07, ASTM International, West Conshohocken, PA, USA.

AWS D1.1, 2006: Structural welding code – Steel. American Welding Society, Miami, USA.

Buitrago, J., Healy, B.E., and Chang, T.Y., 1993: Local joint flexibility of tubular joints. Proceedings 12th International Conference on Offshore Mechanics and Arctic Engineering, Glasgow, UK, Vol. I.

Canadian Standards Association, 2004: General requirements for rolled or welded structural quality steel/structural quality steel. CAN/CSA G40.20-04/G40.21-04, Toronto, ON, Canada.

CEN, 2005a: Eurocode 3: Design of steel structures − Part 1-1: General rules and rules for buildings. EN 1993-1-1:2005, European Committee for Standardization, Brussels, Belgium.

CEN, 2005b: Eurocode 3: Design of steel structures − Part 1-8: Design of joints. EN 1993-1-8:2005, European Committee for Standardization, Brussels, Belgium.

CEN, 2006a: Hot-finished structural hollow sections of non-alloy and fine grain steels – Part 2: Tolerances, dimensions and sectional properties. EN 10210-2:2006(E), European Committee for Standardization, Brussels, Belgium.

CEN, 2006b: Cold-formed welded structural hollow sections of non-alloy and fine grain steels – Part 2: Tolerances, dimensions and sectional properties. EN 10219-2:2006(E), European Committee for Standardization, Brussels, Belgium.

Choo, Y.S., Liang, J.X., and Vegte, G.J. van der, 2004: An effective external reinforcement scheme for circular hollow section joints. Proceedings ECCS-AISC Workshop 'Connections in Steel Structures V', Bouwen met Staal, Zoetermeer, The Netherlands, pp. 423-432.

Choo, Y.S., Vegte, G.J. van der, Zettlemoyer, N., Li, B.H., and Liew, J.Y.R., 2005: Static strength of T joints reinforced with doubler or collar plates – I: Experimental investigations. Journal of Structural Engineering, American Society of Civil Engineers, USA, Vol. 131, No. 1, pp. 119-128.

Ciwko, J.B., and Morris, C.A., 1981: Static behaviour of cropped web joints for trusses with round tubular members. CIDECT Report 5K-81/9.

Dexter, E.M., and Lee, M.M.K., 1996: Effects of can length and overlap on the strength of K-joints in CHS tubular members. Proceedings 7th International Symposium on Tubular Structures, Miskolc, Hungary, Tubular Structures VII, Balkema, Rotterdam, The Netherlands, pp. 131-138.

Dexter, E.M., and Lee, M.M.K., 1998: Effect of overlap on the behaviour of axially loaded CHS K-joints. Proceedings 8th International Symposium on Tubular Structures, Singapore, Tubular Structures VIII, Balkema, Rotterdam, The Netherlands, pp. 249-258.

Dier, A.F., and Lalani, M., 1995: Strength and stiffness of tubular joints for assessment/design purposes. Proceedings Offshore Technology Conference, OTC 7799, Houston, USA.

Dier, A.F., and Lalani, M., 1998: Guidelines on strengthening and repair of offshore structures. Proceedings 8th International Conference on Behaviour of Offshore Structures, Delft, The Netherlands.

Dier, A.F., 2005: Tubular joint technology for offshore structures. Steel Structures 5, UK.

Dutta, D., Wardenier, J., Yeomans, N., Sakae, K., Bucak, Ö., and Packer, J.A., 1998: Design guide for fabrication, assembly and erection of hollow section structures. CIDECT series 'Construction with hollow sections' No. 7, TÜV-Verlag, Köln, Germany.

Dutta, D., 2002: Structures with hollow sections. Ernst & Sohn, Berlin, Germany.

Eekhout, M., 1996: Tubular structures in architecture. CIDECT.

Efthymiou, M., 1985: Local rotational stiffness of unstiffened tubular joints. Report RKER 85.199, KSEPL, Shell, The Netherlands.

Galambos, T.V., (Ed.) 1998: Guide to stability design criteria for metal structures. 5th Edition, Structural Stability Research Council, John Wiley & Sons, New York.

Gibstein, M.B., 1976: The static strength of T joints subjected to in-plane bending. Det Norske Veritas, Report No. 76/137, Oslo, Norway.

Hoadley, P.W., and Yura, J.A., 1985: Ultimate strength of tubular joints subjected to combined loads. Proceedings Offshore Technology Conference, OTC 4854, Houston, USA.

Igarashi, S., Wakiyama, K., lnoue, K., Matsumoto, T., and Murase, Y., 1985: Limit design of high strength bolted tube flange joint, Part 1 and 2. Journal of Structural and Construction Engineering, Transactions of AIJ, Department of Architecture Reports, Osaka University, Japan.

IIW, 1989: Design recommendations for hollow section joints - Predominantly statically loaded. 2nd Edition, International Institute of Welding, Commission XV, IIW Doc. XV-701-89.

IIW, 2008: Static design procedure for welded hollow section joints - Recommendations. 3rd Edition, International Institute of Welding, Commission XV, IIW Doc. XV-1281r1-08 and IIW Doc. XV-E-08-391.

ISO 19902, 2001: Offshore structures, Part 2: Fixed steel structures. ISO/CD 19902 (Draft E), International Organization for Standardization.

Karcher, D., and Puthli, R.S., 2001: The static design of stiffened and unstiffened CHS L-joints. Proceedings 9th International Symposium on Tubular Structures, Düsseldorf, Germany, Swets & Zeitlinger, Lisse, The Netherlands, pp. 221-228.

Kato, B., and Hirose, A., 1984: Bolted tension flanges joining circular hollow section members. CIDECT Report 8C-84/24-E.

Kitipornchai, S., and Traves, W.H., 1989: Welded tee end connections for circular hollow tubes. Journal of Structural Engineering, American Society of Civil Engineers, USA, Vol. 115, No. 12, pp. 3155-3170.

Kurobane, Y., 1981: New developments and practices in tubular joint design (+ Addendum). International Institute of Welding, Annual Assembly, Oporto, IIW Doc. XV-488-81.

Kurobane, Y., Packer, J.A., Wardenier, J., and Yeomans, N., 2004: Design guide for structural hollow section column connections. CIDECT series 'Construction with hollow sections' No. 9, TÜV-Verlag, Köln, Germany.

Lee, M.M.K., and Llewelyn-Parry, A., 1998: Ultimate strength of ring stiffened T-joints – A theoretical model. Proceedings 8th International Symposium on Tubular Structures, Singapore, Tubular Structures VIII, Balkema, Rotterdam, The Netherlands, pp. 147-156.

Ling, T.W., Zhao, X.-L., Al-Mahaidi, R., and Packer, J.A., 2007a: Investigation of shear lag failure in gusset-plate welded structural steel hollow section connections. Journal of Constructional Steel Research, Vol. 63, No. 3, pp. 293-304.

Ling, T.W., Zhao, X.-L., Al-Mahaidi, R., and Packer, J.A., 2007b: Investigation of block shear tear-out failure in gusset-plate welded connections in structural steel hollow sections and very high strength tubes. Engineering Structures, Vol. 29, No. 4, pp. 469-482.

Liu, D.K., and Wardenier, J., 2004: Effect of the yield strength on the static strength of uniplanar K-joints in RHS (steel grades S460, S355 and S235). IIW Doc. XV-E-04-293.

Lu, L.H., Winkel, G.D. de, Yu, Y., and Wardenier, J., 1994: Deformation limit for the ultimate strength of hollow section joints. Proceedings 6th International Symposium on Tubular Structures, Melbourne, Australia, Tubular Structures VI, Balkema, Rotterdam, The Netherlands, pp. 341-347.

Makino, Y., Kurobane, Y., and Ochi, K., 1984: Ultimate capacity of tubular double K-joints. Proceedings IIW Conference on Welding of Tubular Structures, Boston, USA, Pergamon Press, pp. 451-458.

Makino, Y., Kurobane, Y., Paul, J.C., Orita, Y., and Hiraishi, K., 1991: Ultimate capacity of gusset plate-to-tube joints under axial and in plane bending loads. Proceedings 4th International Symposium on Tubular Structures, Delft, The Netherlands, Delft University Press, Delft, The Netherlands, pp. 424-434.

Makino, Y., Kurobane, Y., Ochi, K., Vegte, G.J. van der, and Wilmshurst, S.R., 1996: Database of test and numerical analysis results for unstiffened tubular joints. IIW Doc. XV-E-96-220.

Mang, F., Herion, S., and Karcher, D., 1997: L-joints made of circular hollow sections. Revised Final Report of CIDECT Project 5BE, University of Karlsruhe, Karlsruhe, Germany.

Marshall, P.W., 1986: Design of internally stiffened tubular joints. Proceedings International Meeting on Safety Criteria in Design of Tubular Structures, Tokyo, Japan, pp. 381-390.

Marshall, P.W., 1992: Design of welded tubular connections. Elsevier, Amsterdam, The Netherlands.

Marshall, P.W., 2004: Review of tubular joint criteria. Proceedings ECCS-AISC Workshop 'Connections in Steel Structures V', Bouwen met Staal, Zoetermeer, The Netherlands, pp. 457-467.

Marshall, P.W., 2006: Punching shear and hot spot stress - Back to the future? Kurobane Lecture, Proceedings 11th International Symposium on Tubular Structures, Quebec City, Canada, Tubular Structures XI, Taylor & Francis Group, London, UK, pp. 287-299.

Martinez Saucedo, G., and Packer, J.A., 2006: Slotted end connections to hollow sections. CIDECT Final Report 8G-10/4, University of Toronto, Toronto, Canada.

Mitri, H.S., Scola, S., and Redwood, R.G., 1987: Experimental investigation into the behaviour of axially loaded tubular V-joints. Proceedings CSCE Centennial Conference, Montreal, Canada, pp. 397-410.

Morahan, D., and Lalani, M., 2002: Fatigue and ultimate limit state of grouted tubular joints. Proceedings 21st Offshore Mechanics and Arctic Engineering Conference, Oslo, Norway.

Mouty, J., (Ed.) 1981: Effective lengths of lattice girder members. CIDECT Monograph No. 4, CIDECT.

Packer, J.A., Wardenier, J., Kurobane, Y., Dutta, D., and Yeomans, N., 1992: Design guide for rectangular hollow section (RHS) joints under predominantly static loading. 1st Edition, CIDECT series 'Construction with hollow sections' No. 3, TÜV-Verlag, Köln, Germany.

Packer, J.A., 1996: Nailed tubular connections under axial loading. Journal of Structural Engineering, American Society of Civil Engineers, Vol. 122. No. 8, pp. 458-467.

Packer, J.A., and Henderson, J.E., 1997: Hollow structural section connections and trusses – A design guide. 2nd Edition, Canadian Institute of Steel Construction, Toronto, Canada.

Packer, J.A., 2006: Tubular brace member connections in braced steel frames. Houdremont Lecture, Proceedings 11th International Symposium on Tubular Structures, Quebec City, Canada, Tubular Structures XI, Taylor & Francis Group, London, UK, pp. 3-14.

Packer, J.A., 2007: Design with hollow structural sections – A report on recent developments in the USA. Proceedings 5th International Conference on Advances in Steel Structures, Singapore, Vol. II, pp. 228-237.

Paul, J.C., Valk, C.A.C. van der, and Wardenier, J., 1989: The static strength of circular multi-planar X joints. Proceedings 3rd International Symposium on Tubular Structures, Lappeenranta, Finland, Elsevier, Amsterdam, The Netherlands, pp. 73-80.

Paul, J.C., 1992: The ultimate behaviour of multiplanar TT and KK joints made of circular hollow sections. Ph.D. Thesis, Kumamoto University, Japan.

Pecknold, D.A., Ha, C.C., and Mohr, W.C., 2000: Ultimate strength of DT tubular joints with chord preloads. Proceedings 19th International Conference on Offshore Mechanics and Arctic Engineering, New Orleans, USA.

Pecknold, D.A., Park, J.B., and Koppenhoefer, K.C., 2001: Ultimate strength of gap K tubular joints with chord preloads. Proceedings 20th International Conference on Offshore Mechanics and Arctic Engineering, Rio de Janeiro, Brazil.

Pecknold, D.A., Marshall, P.W., and Bucknell, J., 2007: New API RP2A tubular joint strength design provisions. Journal of Energy Resources Technology, American Society of Mechanical Engineers, USA, Vol. 129, No. 3, pp. 177-189.

Puthli, R.S., 1998: Hohlprofilkonstruktionen aus Stahl nach DIN V ENV 1993 (EC3) und DIN 18800 (11.90). Werner Verlag GmbH & Co. KG., Düsseldorf, Germany.

Qian, X.D., 2005: Static strength of thick-walled CHS joints and global frame behaviour. Ph.D. Thesis, National University of Singapore, Singapore.

Qian, X.D., Wardenier, J., and Choo, Y.S., 2007: A uniform approach for the design of CHS 100% overlap joints. Proceedings 5th International Conference on Advances in Steel Structures, Singapore, Vol. II, pp. 172-182.

Qian, X.D., Choo, Y.S., Vegte, G.J. van der, and Wardenier, J., 2008: Evaluation of the new IIW CHS strength formulae for thick-walled joints. Proceedings 12th International Symposium on Tubular Structures, Shanghai, China, Tubular Structures XII, Taylor & Francis Group, London, UK, pp. 271-279.

Rautaruukki, 1998: Design handbook for structural hollow sections. Hämeenlinna, Finland.

Reusink, J.H., and Wardenier, J., 1989: Simplified design charts for axially loaded joints of circular hollow sections. Proceedings 3rd International Symposium on Tubular Structures, Lappeenranta, Finland, Elsevier, Amsterdam, The Netherlands, pp. 154-161.

Rondal, J., 1990: Study of maximum permissible weld gaps in connections with plane end cuttings (5AH2); Simplification of circular hollow section welded joints (5AP). CIDECT Report 5AH2/5AP-90/20.

Rondal, J., Würker, K.-G., Dutta, D., Wardenier, J., and Yeomans, N., 1996: Structural stability of hollow sections. 2nd Printing, CIDECT series 'Construction with hollow sections' No. 2, TÜV-Verlag, Köln, Germany.

Sedlacek, G., Wardenier, J., Dutta, D., and Grotmann, D., 1991: Evaluation of test results on hollow section lattice girder connections. Background Report to Eurocode 3 'Common unified rules for steel structures', Document 5.07, Eurocode 3 Editorial Group.

Sedlacek, G., Völling, B., Pak, D., and Feldmann, M., 2006: Local buckling behaviour of cold-formed RHS made from S1100. Proceedings 11th International Symposium on Tubular Structures, Quebec City, Canada, Tubular Structures XI, Taylor & Francis Group, London, UK, pp. 147-152.

Sherman, D.R., 1996: Designing with structural tubing. Engineering Journal, American Institute of Steel Construction, USA, Vol. 33, No. 3, pp. 101-109.

Standards Australia, 1991: Structural steel hollow sections. Australian Standard AS 1163, Standards Australia, Sydney.

Stol, H.G.A., Puthli, R.S., and Bijlaard, F.S.K., 1985: Experimental research on tubular T joints under proportionally applied combined static loading. Proceedings 4th International Conference on Behaviour of Offshore Structures, Delft, The Netherlands, Elsevier, Amsterdam, The Netherlands, pp. 441-452.

Syam, A.A., and Chapman, B.G., 1996: Design of structural steel hollow section connections. 1st Edition, Australian Institute of Steel Construction, Sydney, Australia.

Togo, T., 1967: Experimental study on mechanical behaviour of tubular joints. Ph.D. Thesis, Osaka University, Japan, (in Japanese).

Vegte, G.J. van der, 1995: The static strength of uniplanar and multiplanar tubular T and X joints. Ph.D. Thesis, Delft University of Technology, Delft, The Netherlands.

Vegte, G.J. van der, and Makino, Y., 2006: Ultimate strength formulation for axially loaded CHS uniplanar T-joints. International Journal of Offshore and Polar Engineering, ISOPE, Vol. 16, No. 4, pp. 305-312.

Vegte, G.J. van der, Makino, Y., and Wardenier, J., 2007: New ultimate strength formulation for axially loaded CHS K-joints. Proceedings 5th International Conference on Advances in Steel Structures, Singapore, Vol. II, pp. 218-227.

Vegte, G.J. van der, Wardenier, J., Qian, X.D., and Choo, Y.S., 2008a: Reanalysis of the moment capacity of CHS joints. Proceedings 12th International Symposium on Tubular Structures, Shanghai, China, Tubular Structures XII, Taylor & Francis Group, London, UK, pp. 579-588.

Vegte, G.J. van der, Wardenier, J., Zhao, X.-L., and Packer, J.A., 2008b: Evaluation of new CHS strength formulae to design strengths. Proceedings 12th International Symposium on Tubular Structures, Shanghai, China, Tubular Structures XII, Taylor & Francis Group, London, UK, pp. 313-322.

Wardenier, J., 1982: Hollow section joints. Delft University Press, Delft, The Netherlands.

Wardenier, J., Kurobane, Y., Packer, J.A., Dutta, D., and Yeomans, N., 1991: Design guide for circular hollow section (CHS) joints under predominantly static loading. 1st Edition, CIDECT series 'Construction with hollow sections' No. 1, TÜV-Verlag, Köln, Germany.

Wardenier, J., 2002: Hollow sections in structural applications. Bouwen met Staal, Zoetermeer, The Netherlands.

Wardenier, J., 2007: A uniform effective width approach for the design of CHS overlap joints. Proceedings 5th International Conference on Advances in Steel Structures, Singapore, Vol. II, pp. 155-165.

Wardenier, J., Vegte, G.J. van der, Makino, Y., and Marshall, P.W., 2008a: Comparison of the new IIW (2008) CHS joint strength formulae with those of the previous IIW (1989) and the new API (2007). Proceedings 12th International Symposium on Tubular Structures, Shanghai, China, Tubular Structures XII, Taylor & Francis Group, London, UK, pp. 281-291.

Wardenier, J., Vegte, G.J. van der, and Makino, Y., 2008b: Joints between plates or I sections and a circular hollow section chord. Proceedings 18th International Offshore and Polar Engineering Conference, Vancouver, Canada, Vol. IV, pp. 319-326.

Willibald, S., 2001: The static strength of ring-stiffened tubular T- and Y-joints. CIDECT Student Prize Paper, Proceedings 9th International Symposium on Tubular Structures, Düsseldorf, Germany, Swets & Zeitlinger, Lisse, The Netherlands, pp. 581-588.

Winkel, G.D. de, 1998: The static strength of I-beam to circular hollow section column connections. Ph.D. Thesis, Delft University of Technology, Delft, The Netherlands.

Yura, J.A., Zettlemoyer, N., and Edwards, I.E., 1980: Ultimate capacity equations for tubular joints. Proceedings Offshore Technology Conference, OTC 3690, USA.

Zhao, X.-L., Wardenier, J., Packer, J.A., and Vegte, G.J. van der, 2008: New IIW (2008) static design recommendations for hollow section joints. Proceedings 12th International Symposium on Tubular Structures, Shanghai, China, Tubular Structures XII, Taylor & Francis Group, London, UK, pp. 261-269.

Appendix A: Comparison between the new IIW (2008) design equations and the previous recommendations of IIW (1989) and/or CIDECT Design Guide No. 1 (1991)

In this Appendix, the new IIW (2008) design equations for CHS to CHS joints, presented in chapters 4 and 5 of this 2nd edition of Design Guide No. 1, are compared with the previous IIW (1989) equations incorporated in the 1st edition of this Design Guide (Wardenier et al., 1991). The latter were also implemented in Eurocode 3 and other national and international codes (see Wardenier et al., 2008a). The previous formulations are summarized in chapter 10 of this 2nd edition of the Design Guide.

A1 Q_u factors for CHS to CHS joints

The Q_u functions for CHS to CHS joints included in the new equations (chapters 4 and 5) and those (indirectly) included in the equations of the previous recommendations (chapter 10) are summarised in table A1. For K gap joints, the expressions are further worked out in table A2 for four relative gap values g/t_0.

Considering complexity, the new formula for X joints is marginally more complicated than the previous one whereas for T joints the format is comparable. The new K gap joint formula is significantly simpler than the previous expression due to the simpler gap function.

Table A1 – Comparison of Q_u functions for CHS joints

	New IIW (2008) formulae (chapters 4 and 5)	**Previous IIW (1989) and CIDECT (1991) formulae (chapter 10)**
Q_u	$Q_u = \frac{N_i^* \sin\theta_i}{f_{y0}\, t_0^2\, Q_f}$ and	$Q_u = \frac{M_i^* \sin\theta_i}{f_{y0}\, t_0^2\, d_1\, Q_f}$
X joints	$Q_u = 2.6\left(\frac{1+\beta}{1-0.7\beta}\right)\gamma^{0.15}$	$Q_u = \frac{5.2}{1-0.81\beta}$
T joints	$Q_u = 2.6\left(1+6.8\beta^2\right)\gamma^{0.2}$	$Q_u = 2.8\left(1+5.1\beta^2\right)\gamma^{0.2}$ (*)
K gap joints	$Q_u = 1.65\left(1+8\beta^{1.6}\right)\gamma^{0.3}[1+\frac{1}{1.2+(\frac{g}{t_0})^{0.8}}]$	$Q_u = 1.8\left(1+5.67\frac{d_1}{d_0}\right)\gamma^{0.2}[1+\frac{0.024\gamma^{1.2}}{\exp\left(0.5\frac{g}{t_0}-1.33\right)+1}]$
Brace in-plane bending	$Q_u = 4.3\beta\gamma^{0.5}$	$Q_u = 4.85\beta\gamma^{0.5}$
Brace out-of-plane bending	$Q_u = 1.3\left(\frac{1+\beta}{1-0.7\beta}\right)\gamma^{0.15}$	$Q_u = \frac{2.7}{1-0.81\beta}$

(*) chord bending effect included

The equations for brace in-plane bending and out-of-plane bending moments in the new IIW (2008) design recommendations are based on the same principles as in the previous edition of CIDECT Design Guide No. 1.

For brace in-plane bending, only the constant has been changed resulting in about 11% lower strength. This reduction is a result of newly derived data with larger dimensions and relatively smaller welds.

For brace out-of-plane bending, the capacity is similar to the previous recommendations, and again related to the axial load capacity of X joints using a factor of $0.5d_1$. In general, the capacity of the new equation gives slightly lower strengths than the previous formulation.

Table A2 – Comparison of Q_u functions for CHS K gap joints

	New IIW (2008) (chapters 4 and 5)	**Previous IIW (1989) formulae (chapter 10)**
K gap joints	$Q_u = 1.65\left(1+8\beta^{1.6}\right)\gamma^{0.3}\left[1+\frac{1}{1.2+\left(\frac{g}{t_0}\right)^{0.8}}\right]$	$Q_u = 1.8\left(1+5.67\frac{d_1}{d_0}\right)\gamma^{0.2}\left[1+\frac{0.024\gamma^{1.2}}{\exp\left(0.5\frac{g}{t_0}-1.33\right)+1}\right]$
g = 0	$Q_u = 3\left(1+8\beta^{1.6}\right)\gamma^{0.3}$	$Q_u = 1.8\left(1+5.67\frac{d_1}{d_0}\right)\gamma^{0.2}\left[1+0.019\gamma^{1.2}\right]$
g = 2t₀	$Q_u = 2.2\left(1+8\beta^{1.6}\right)\gamma^{0.3}$	$Q_u = 1.8\left(1+5.67\frac{d_1}{d_0}\right)\gamma^{0.2}\left[1+0.014\gamma^{1.2}\right]$
g = 10t₀	$Q_u = 1.87\left(1+8\beta^{1.6}\right)\gamma^{0.3}$	$Q_u = 1.8\left(1+5.67\frac{d_1}{d_0}\right)\gamma^{0.2}\left[1+0.0006\gamma^{1.2}\right]$
g = ∞	$Q_u = 1.65\left(1+8\beta^{1.6}\right)\gamma^{0.3}$	$Q_u = 1.8\left(1+5.67\frac{d_1}{d_0}\right)\gamma^{0.2}$

A2 Q_f factors

The expressions for Q_f of chapter 4 and the f(n') functions of chapter 10 are recorded in table A3.

Table A3 – Comparison of functions for Q_f and f(n')

Function Q_f		
(chapter 4)	$Q_f = \left(1-\lvert n\rvert\right)^{C_1}$ with $n = \frac{N_0}{N_{pl,0}} + \frac{M_0}{M_{pl,0}}$ in connecting face	
	Chord compression stress (n < 0)	**Chord tension stress (n ≥ 0)**
T, Y, X joints	$C_1 = 0.45 - 0.25\beta$	$C_1 = 0.20$
K gap joints	$C_1 = 0.25$	

Function f(n')		
(chapter 10)	$n' = \frac{N_{op}}{A_0 f_{y0}} + \frac{M_0}{W_{el,0} f_{y0}}$	
	Chord compression prestress (n' < 0)	**Chord tension prestress (n' ≥ 0)**
T, Y, X and K gap joints	$f(n') = 1+0.3n'-0.3n'^2$	$f(n') = 1.0$

In the previous formulae, the effect of the brace load components in the chord was included in the joint capacity, while only the so-called compression preload N_{op} had to be considered in the chord stress function f(n'). In the new recommendations, for both compression loading and tension loading, the maximum chord load has to be included in the chord load function Q_f. This means that for a proper comparison, the combined effect of the functions Q_u and Q_f should be taken into account.

For X joints, the new and previous chord stress functions are directly comparable. For a fair comparison for K gap joints, however, the curve for f(n') should be shifted to the left due to the effect of the brace load components. For T joints, the effect of chord in-plane bending as a result of the brace load was already included in the previous joint strength equation. The function f(n') only had to take into account the additional loading.

In practice, it is usual that designers consider the full chord loading. In the new equations, the chord stress function is based on the maximum chord load including chord bending due to brace load. Figure A1 shows comparisons between the Q_f and f(n') functions respectively as a function of n and n' on the horizontal axis.

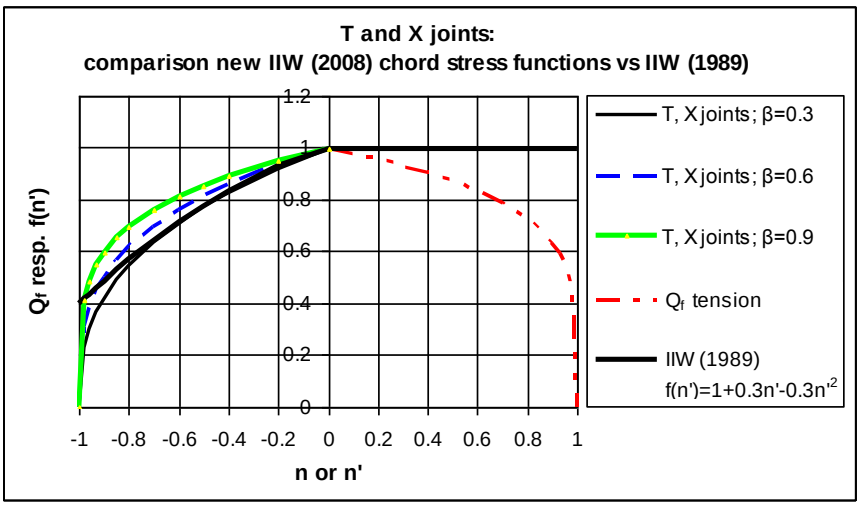

Figure A1(a) – CHS T and X joints: comparison of the Q_f and f(n') functions for chord axial loading

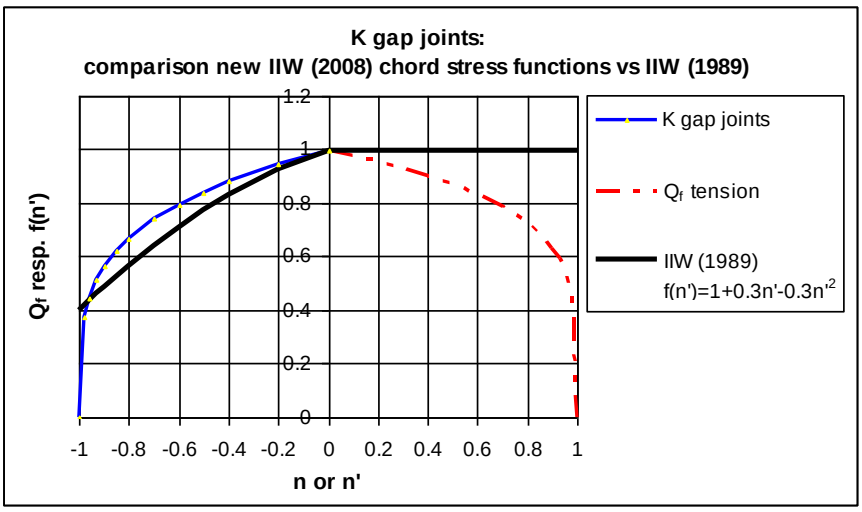

Figure A1(b) – CHS K gap joints: comparison of the Q_f and f(n') functions

This figure shows that the new formulae give for very high chord compression stress and chord tensile stress, a larger reduction in joint capacity. For chord compression stress up to 0.8 times the chord yield load, the reduction is now less for T and X joints. For K gap joints, the factors are about the same. However, considering the effect of the brace load components, for joints with a large β ratio, the new chord load function may result in a larger reduction.

A3 Axially loaded T and Y joints

The new and the previous Q_u equations for T and Y joints are compared in figure A2. For larger β ratios, the new Q_u function gives larger capacities than the previous equation, since in the previous equations, the effect of chord bending due to brace axial loading was included in the Q_u.

Considering both effects, the difference in capacity is small for compression loaded chords, but for tension loaded chords, the new formula gives lower capacities than the previous equation.

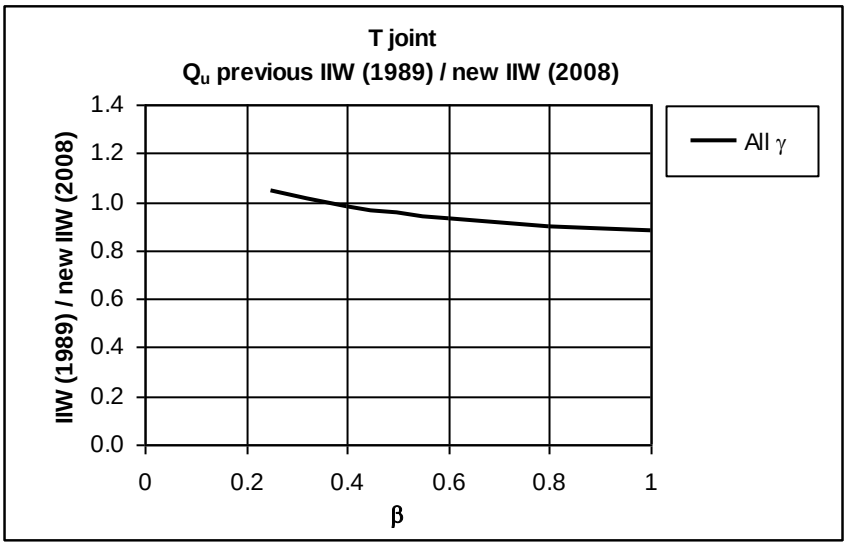

Figure A2 – CHS T joints: comparison of the previous (1989) with the new (2008) IIW equations*, excluding Q_f and f(n')*

A4 Axially loaded X joints

The new and the previous Q_u equations for X joints are compared in figure A3. The new design equations (chapter 4) give for low and large β ratios, a lower capacity if only Q_u is considered. A similar observation is made for X joints with low γ ratios.

It was known that the previous equation for X joints gave too high strength values for very low β values and had to be corrected. However, in general it can be concluded that the ratios are in reasonable agreement for medium β and γ values.

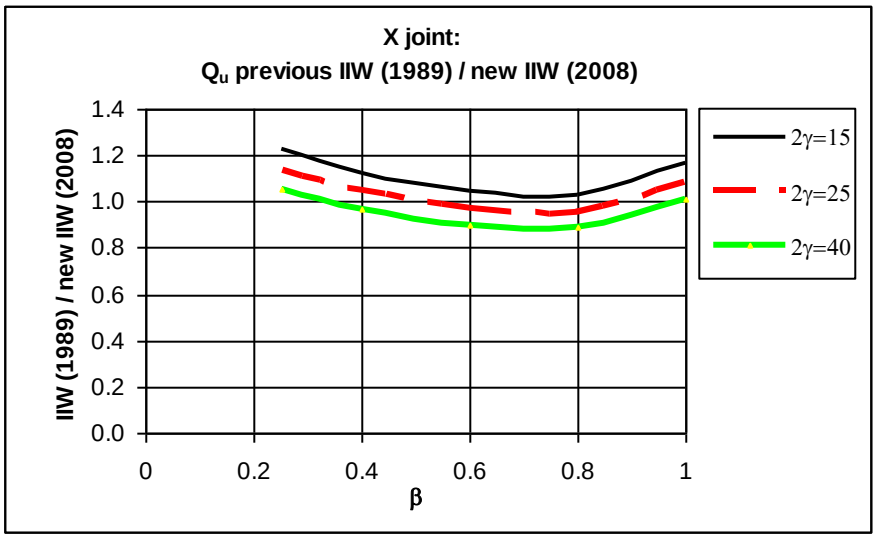

Figure A3 – CHS X joints: comparison of the previous (1989) with the new (2008) IIW equations

A5 Axially loaded K gap joints

The new and the previous combined $Q_u Q_f$ capacities for K gap joints (with $\theta_i = 45°$ and $f_{yi} = f_{y0}$) are compared in figure A4. The new design equations (chapter 4) give for low γ values, lower strengths than the previous equations (chapter 10), which agrees with the work by Qian et al. (2008) on joints with thick-walled sections. Further, for low β values, the new functions give lower capacities. The database used previously included many small scale specimens with low β ratios and relatively large welds, which increased the mean ultimate strength value of joints with low β values with small gaps. The new strength equations are based on sections with larger dimensions.

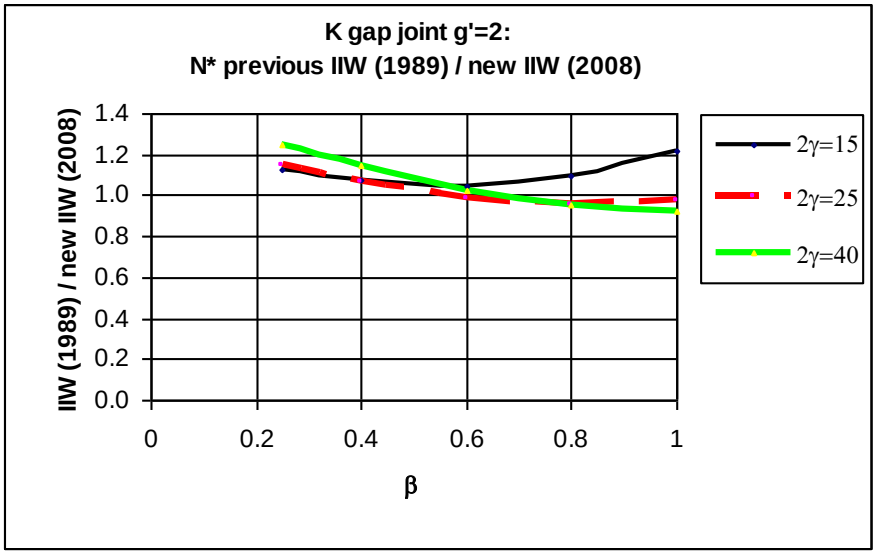

Figure A4(a) – CHS K gap joints ($g' = g/t_0 = 2$): comparison of the previous (1989) with the new (2008) IIW equations

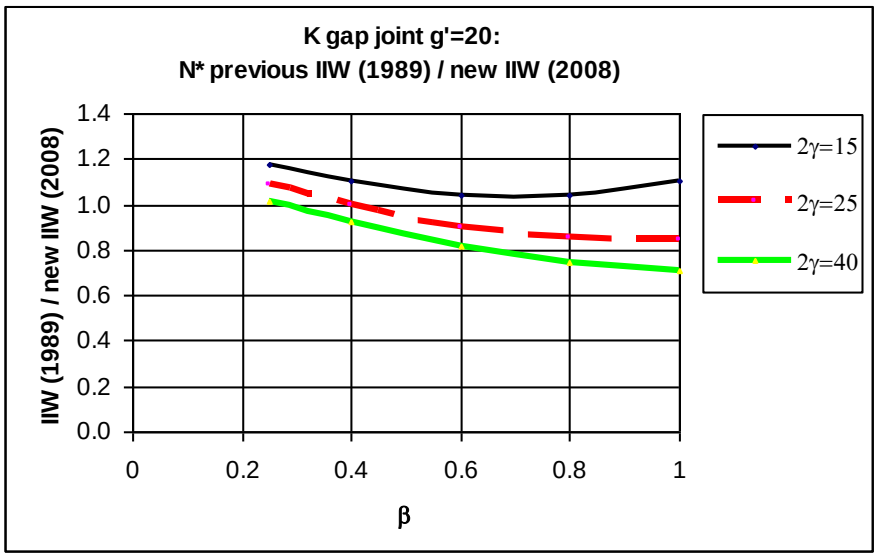

Figure A4(b) – CHS K gap joints (g' = g/t_0 = 20): comparison of the previous (1989) with the new (2008) IIW equations

For large gaps with a medium to high γ value, the new Q_u Q_f functions give larger capacities than the previous recommendations. Due to the strong influence of the gap function for this case, the strength was slightly under-predicted by the previous equations.

In general, considering the Q_u with the Q_f functions, the new IIW formulae for K gap joints (chapter 4) will give slightly smaller or equal strength values as compared to the capacities of the current IIW recommendations (chapter 10). Only in selected cases (large gaps with medium to high γ ratios), the new recommendations will predict slightly larger capacities than the current IIW equations. Especially for K gap joints with tension loaded chords, the new recommendations give a considerably lower capacity due to the chord stress function.

A6 Joints loaded by brace in-plane bending moments

The new and the previous (1st edition of this Design Guide) Q_u equations for brace in-plane bending are compared in figure A5. For all β and γ ratios, the previous recommendations give a 13% larger capacity than the new IIW recommendation, since the new equation is based on FE data of specimens with relatively smaller welds. However, as shown in Appendix B, the new equations give considerably larger capacities than those of API (2007).

A7 Joints loaded by brace out-of-plane bending moments

The new and the previous Q_u equations for brace out-of-plane bending are compared in figure A6. It is observed that for medium β and γ ratios, the new equation gives about the same capacity, while for high and low β values and for low γ values, it gives slightly lower results.

A8 Welded plate, I, H or RHS to CHS chord joints

For welded plate, I, H, or RHS to CHS chord joints, the same remarks apply as for T and X joints with CHS braces and chords.

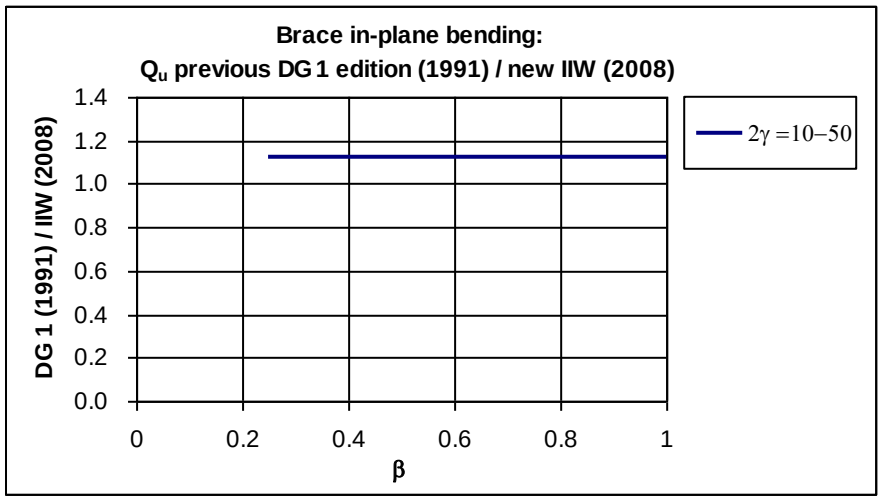

Figure A5 – CHS joints loaded by brace in-plane bending moments: comparison of the previous (1991) Design Guide No. 1 recommendations with the new (2008) IIW equations, *excluding Q_f and f(n')*

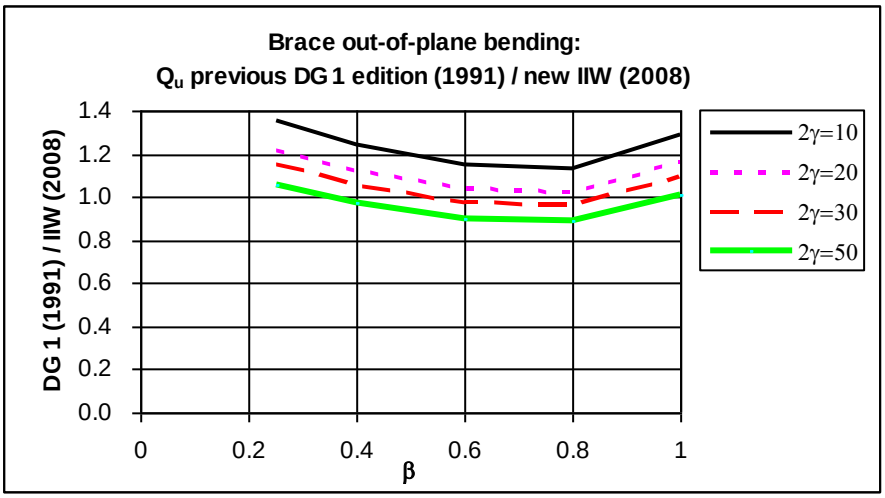

Figure A6 – CHS joints loaded by brace out-of-plane bending moments: comparison of the previous (1991) Design Guide No. 1 recommendations with the new (2008) IIW equations

A9 Further remarks

For joints with CHS chords, the validity range in the (2008) IIW recommendations and in the previous (1989) version differs. Previously the recommendations were given for steel grades with yield stresses up to 355 N/mm^2 whereas in the IIW (2008) version, steels with a nominal yield stress up to 460 N/mm^2 are included. This also affected the range of validity for the diameter to thickness ratio for compression members and flexural members, and their section classification.

The equations for K overlap joints have been changed completely. Although the current Eurocode 3 recommendations are based on the IIW (1989) and the previous version of this CIDECT Design Guide (1991), in the Corrigendum 2009 to Eurocode 3 (CEN, 2005b) it is mentioned that shear between the braces and the chord has to be checked for larger overlaps; i.e. larger than 60% or 80%, respectively (see section 4.4.2), depending on whether the hidden toe location of the overlapped brace is un-welded or welded to the chord.

Appendix B: Comparison between the new IIW (2008) design equations and those of the API (2007)

Recently the equations for the capacity of CHS joints in the API (2007), which are generally used for offshore structures, have been revised (Marshall, 2004). These new API equations are mainly based on numerical work carried out by Pecknold et al. (2000, 2001, 2007).

In this Appendix, the new IIW (2008) design equations for CHS to CHS joints, presented in chapters 4 and 5, are compared with the new API (2007) equations (see Wardenier et al., 2008a).

Dier (2005) states that the equations in the updated API 21st edition provide more accurate guidance than the equations in the ISO Draft (2001) for offshore structures. Hence, the API equations are here considered in the comparisons.

Since IIW and CIDECT give design values, while the API provides characteristic values, for comparison, all Q_u functions in the figures are changed to "characteristic", i.e. the equations of chapters 4 and 5 are multiplied by $\gamma_M = 1.1$.

B1 Q_u factors

The Q_u functions included in the new IIW (2008) equations (chapters 4 and 5) and those included in the new API (2007) are summarised in table B1. For K gap joints, the expressions are further worked out in table B2 for three relative gap values g/t_0.

Considering complexity, the IIW (2008) formulae included in chapters 4 and 5 are considerably simpler than those included in the API (2007); this especially applies to the equations for X and K gap joints.

Bridge with triangular CHS girders

Table B1 – Comparison of Q_u functions for CHS joints

	New IIW (2008) (chapters 4 and 5) – design strength	**API (2007) – characteristic strength**
Q_u	$Q_u = \frac{N_i^* \sin\theta_i}{f_{y0}\, t_0^2\, Q_f}$ and $Q_u = \frac{M_i^* \sin\theta_i}{f_{y0}\, t_0^2\, d_1\, Q_f}$	
X joints	$Q_u = 2.6\left(\frac{1+\beta}{1-0.7\beta}\right)\gamma^{0.15}$	$Q_u = \left[2.8+(12+0.1\gamma)\beta\right]Q_\beta$ (*)
T joints	$Q_u = 2.6\left(1+6.8\beta^2\right)\gamma^{0.2}$	$Q_u = 2.8+(20+0.8\gamma)\beta^{1.6}$ but $\le 2.8+36\beta^{1.6}$
K gap joints	$Q_u = 1.65\,(1+8\beta^{1.6})\gamma^{0.3}\,[1+\frac{1}{1.2+(\frac{g}{t_0})^{0.8}}]$	$Q_u = (16+1.2\gamma)\beta^{1.2}\,Q_g$ (**) but $\le 40\,\beta^{1.2}\,Q_g$
Brace in-plane bending	$Q_u = 4.3\,\beta\,\gamma^{0.5}$	$Q_u = (5+0.7\gamma)\beta^{1.2}$
Brace out-of-plane bending	$Q_u = 1.3\left(\frac{1+\beta}{1-0.7\beta}\right)\gamma^{0.15}$	$Q_u = 2.5+(4.5+0.2\gamma)\beta^{2.6}$

(*) $Q_\beta = \frac{0.3}{\beta\,(1-0.833\beta)}$ for $\beta > 0.6$ and $Q_\beta = 1.0$ for $\beta \le 0.6$

(**) $Q_g = 1+0.2\left(1-2.8\frac{g}{d_0}\right)^3$ for $\frac{g}{d_0} \ge 0.05$, but $Q_g \ge 1.0$; For $\frac{g}{d_0} < 0.05$ other functions apply

Table B2 – Comparison of Q_u functions for CHS K gap joints

	New IIW (2008) (chapters 4 and 5) – design strength	**API (2007) – characteristic strength**
K gap joints	$Q_u = 1.65\,(1+8\beta^{1.6})\,\gamma^{0.3}\,[1+\frac{1}{1.2+(\frac{g}{t_0})^{0.8}}]$	$Q_u = (16+1.2\gamma)\beta^{1.2}\,Q_g$ $\quad Q_g \ge 1.0$
g = 2t₀	$Q_u = 2.2\left(1+8\beta^{1.6}\right)\gamma^{0.3}$	$Q_u = (16+1.2\gamma)\beta^{1.2}\left[1+0.2\,(1-\frac{2.8}{\gamma})^3\right]$
g = 10t₀	$Q_u = 1.87\left(1+8\beta^{1.6}\right)\gamma^{0.3}$	$Q_u = (16+1.2\gamma)\beta^{1.2}\left[1+0.2\,(1-\frac{14}{\gamma})^3\right]$
g = ∞	$Q_u = 1.65\left(1+8\beta^{1.6}\right)\gamma^{0.3}$	$Q_u = (16+1.2\gamma)\beta^{1.2}$

B2 Q_f factors

The Q_f functions are recorded in table B3.

Table B3 – Comparison of Q_f functions

Function Q_f in the new IIW (2008) recommendations		
(chapter 4)	$Q_f = (1-\lvert n\rvert)^{C_1}$ with $n = \frac{N_0}{N_{pl,0}} + \frac{M_0}{M_{pl,0}}$ in connecting face	
	Chord compression stress (n < 0)	**Chord tension stress (n ≥ 0)**
T, Y, X joints	$C_1 = 0.45 - 0.25\beta$	$C_1 = 0.20$
K gap joints	$C_1 = 0.25$	

Function Q_f in the API (2007)			
	$Q_f = \left[1 + C_1\left(\frac{N_0}{N_{pl,0}}\right) - C_2\left(\frac{M_{ip}}{M_{pl,0}}\right) - C_3\ A^2\right]$ $A = \sqrt{\left(\frac{N_0}{N_{pl,0}}\right)^2 + \left(\frac{M_c}{M_{pl,0}}\right)^2}$ $M_c = \sqrt{M_{ip}^2 + M_{op}^2}$		
	C_1	**C_2**	**C_3**
T, Y joints	0.3	0	0.8
X joints (*) $\beta \le 0.9$ $\beta = 1.0$	0.2 -0.2	0 0	0.5 0.2
K gap joints	0.2	0.2	0.3
All brace moment loaded joints	0.2	0	0.4

(*) Linearly interpolated values for $0.9 < \beta < 1.0$

The Q_u and Q_f functions of the IIW (2008) and API (2007) are substantially different. Hence, for a proper comparison, the combined effect of the functions Q_u and Q_f has to be considered.

Figure B1 shows a comparison between the IIW (2008) Q_f functions of chapter 4 and the API (2007) functions for chord axial loading only, for which the API equations can be simplified to:

$$Q_f = 1 + 0.2\frac{N_0}{N_{pl,0}} - 0.5\left(\frac{N_0}{N_{pl,0}}\right)^2 \quad \text{for X joints with } \beta \le 0.9 \qquad \text{B1}$$

$$Q_f = 1 + 0.3\frac{N_0}{N_{pl,0}} - 0.8\left(\frac{N_0}{N_{pl,0}}\right)^2 \quad \text{for T joints} \qquad \text{B2}$$

$$Q_f = 1 + 0.2\frac{N_0}{N_{pl,0}} - 0.3\left(\frac{N_0}{N_{pl,0}}\right)^2 \quad \text{for K gap joints} \qquad \text{B3}$$

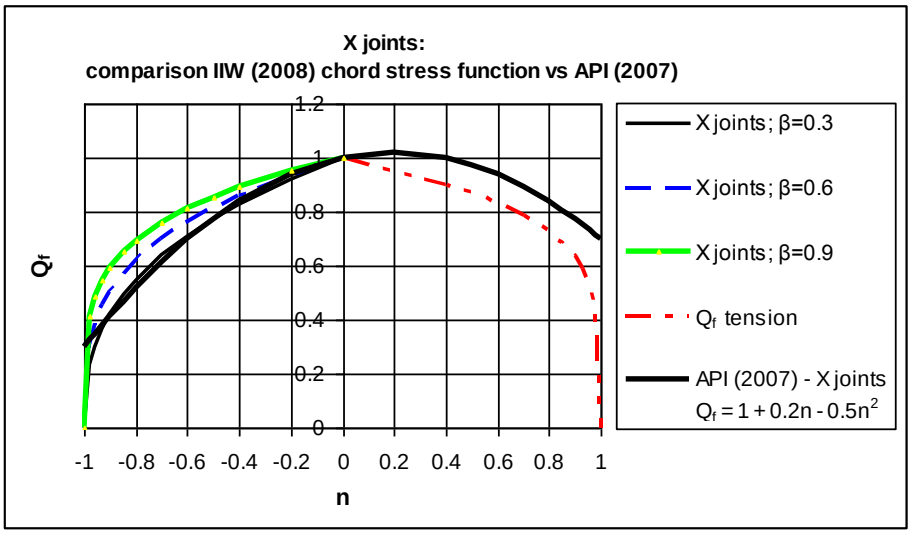

Figure B1(a) – Comparison of the IIW (2008) Q_f function for chord axial loading in X joints with that of the API (2007)

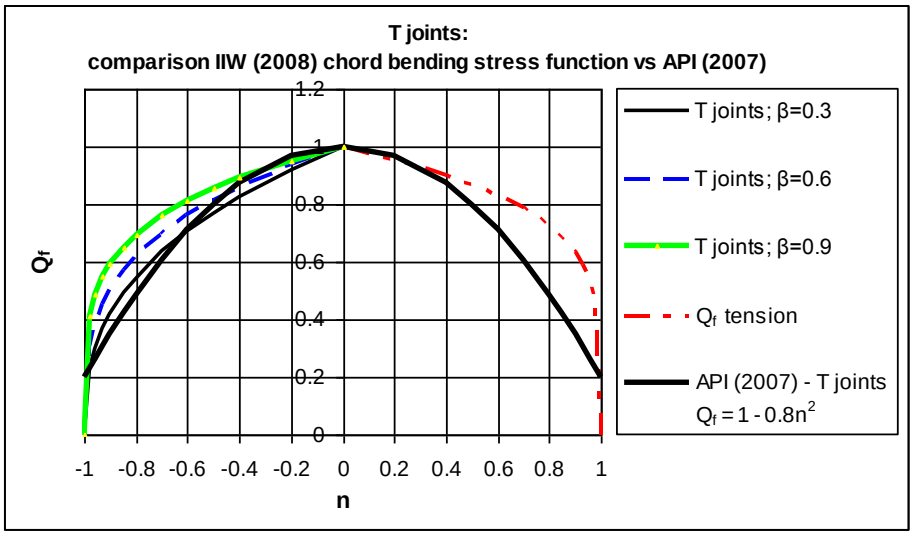

Figure B1(b) – Comparison of the IIW (2008) Q_f function for chord in-plane bending in axially loaded T joints with that of the API (2007)

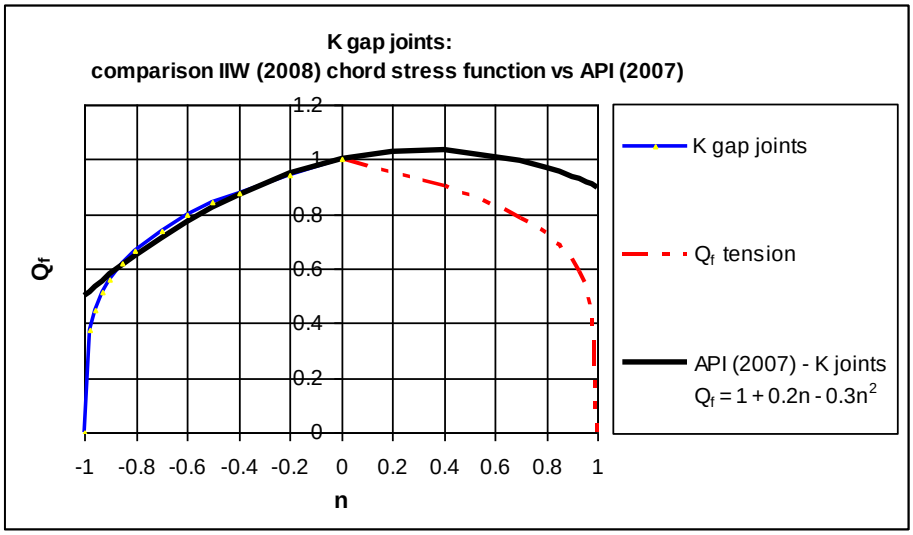

Figure B1(c) – Comparison of the IIW (2008) Q_f function for K gap joints with that of the API (2007)

Figure B1(a) shows that for X joints with compression loaded chords, the API (2007) gives a lower bound for the IIW (2008) Q_f function, whereas for tension loaded chords, the reduction in capacity is considerably less severe than that given by the new IIW equation. This is mainly caused by the limitation of $2\gamma \geq 20$ in the API recommendations; for lower 2γ values the effect is larger.

As shown in figure B1(b), the API chord bending stress function for T joints gives a considerably larger reduction than the IIW (2008) chord bending stress function. For chord axial compression loading, the API (2007) chord stress function is generally also more severe than that according to the IIW (2008).

For K gap joints, the Q_f function gives for compression loaded chords up to 90% of the chord yield load about the same reduction, whereas for tension loaded chords, the IIW (2008) function gives a considerably larger reduction than that according to the API (2007) which is, as mentioned, caused by the validity range of 2γ.

B3 Axially loaded T and Y joints

The new IIW (2008) equations (characteristic value) and the API (2007) Q_u equations for T and Y joints are compared in figure B2. The Q_u function in the API (2007) provides for low and high β ratios, a slightly lower capacity than the new IIW function. For medium β ratios, the capacity is equal to that of the IIW (2008) function.

Considering the combined Q_u and Q_f functions for T joints, the capacity of the IIW (2008) equations is about the same as that according to the API (2007).

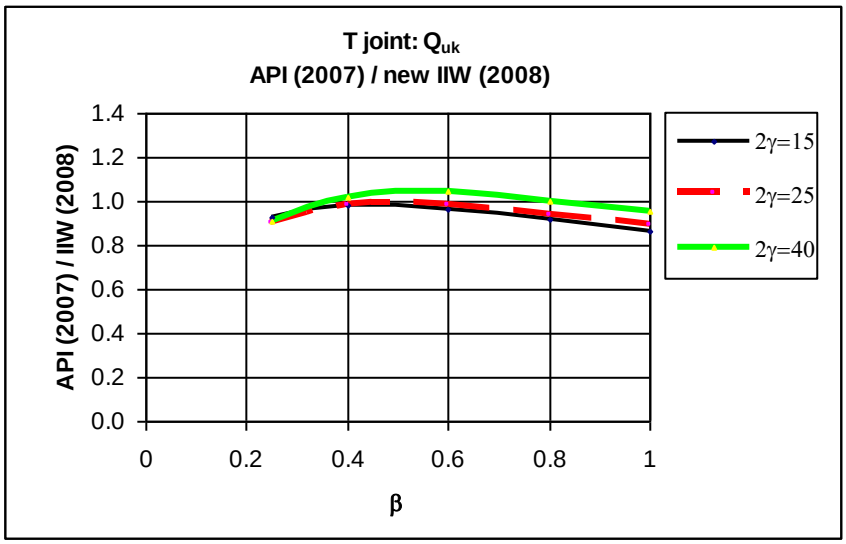

Figure B2 – Comparison of the IIW (2008) equation for T joints with that of the API (2007), *excluding* Q_f

B4 Axially loaded X joints

The new IIW (2008) equation (characteristic value) and the API (2007) Q_u equation for X joints are compared in figure B3. The Q_u function in the IIW (2008) design equation provides about the same values as that of the API. The Q_f of the IIW (2008) equation gives for compression loaded chords, a slightly smaller reduction than the API (2007), and for tension loaded chords a larger reduction. In general, it can be concluded that the capacities of the IIW (2008) equation and those of the API (2007) are in reasonable agreement.

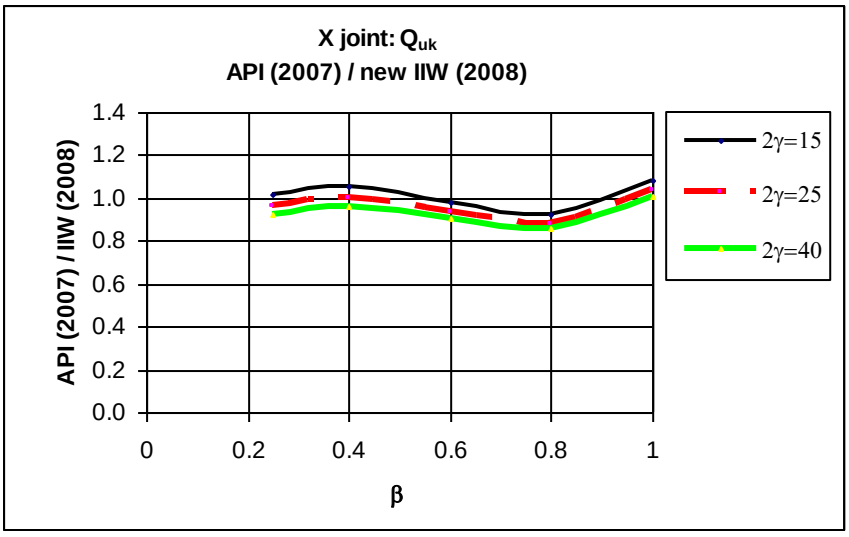

Figure B3 – Comparison of the IIW (2008) equation for X joints with that of the API (2007)

B5 Axially loaded K gap joints

The new IIW (2008) equation (characteristic value) and the API (2007) Q_u equation for K gap joints are compared in figures B4(a) and B4(b). Considering the combined Q_u and Q_f functions, the IIW (2008) strength functions (chapter 4) give for joints with medium β ratios, and for joints with a compression loaded chord, about the same capacity as the API (2007). For joints with low β ratios, the capacity according to the IIW (2008) equation is higher than that according to the API (2007). For large β ratios, the capacity according to the IIW (2008) equation is equal or slightly lower than the values obtained with the API (2007). As explained before, for joints with tension loaded chords, the IIW (2008) equation gives lower strengths than the values obtained with the API (2007).

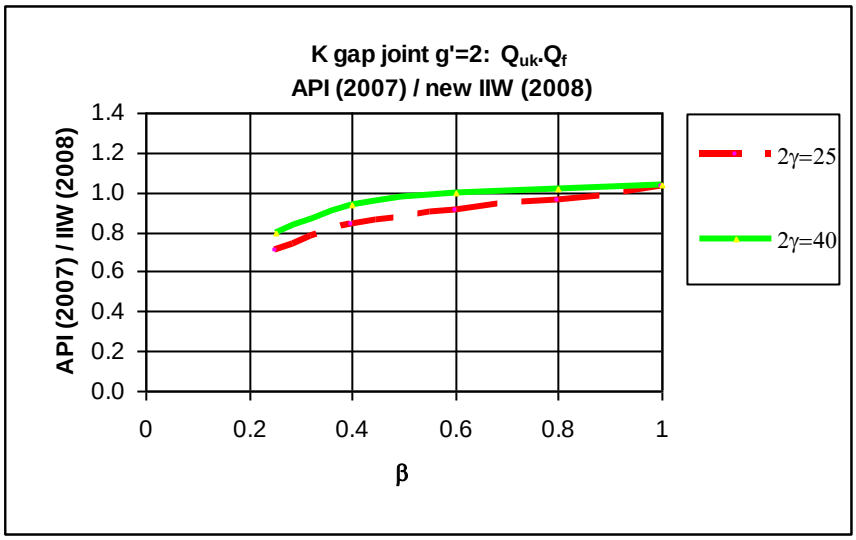

Figure B4(a) – Comparison of the IIW (2008) equation for K gap joints ($g' = g/t_0 = 2$, $\theta_i = 45°$ and $f_{yi} = f_{y0}$) with that of the API (2007)

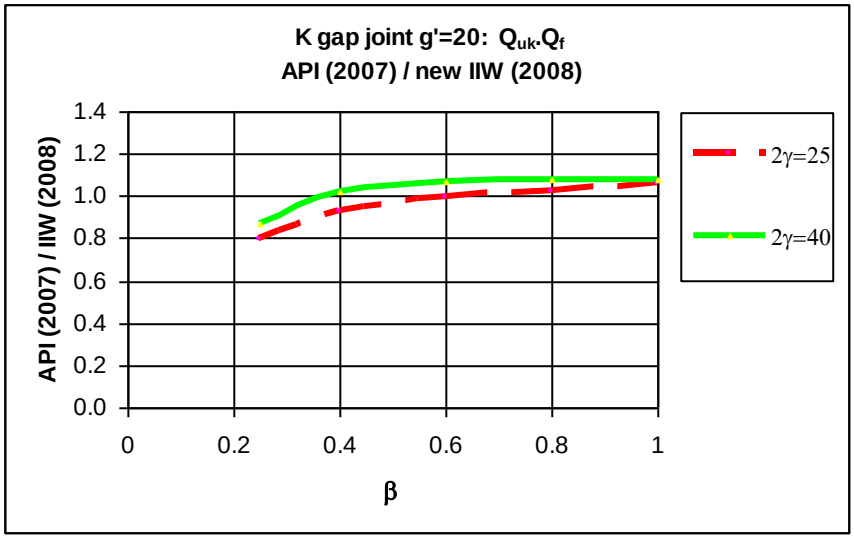

Figure B4(b) – Comparison of the IIW (2008) equation for K gap joints ($g' = g/t_0 = 20$, $\theta_i = 45°$, $f_{yi} = f_{y0}$) with that of the API (2007)

B6 Joints loaded by brace in-plane bending moments

The new IIW (2008) equation (characteristic value) and the API (2007) Q_u equation for brace in-plane bending moments are compared in figure B5. The Q_{uk} function in the API (2007) gives a considerably lower capacity than the IIW (2008) equation (chapter 5), especially for moderate to low β. The API strength function for in-plane bending was forced to be the same for all joint types, and was driven down by finite element results for symmetrical K joint bending, a common case for offshore jacket braces loaded by wave action. The resulting conservatism for other joint types is partially offset by a lesser penalty in Q_f, because the API chord stress function for brace(s) loaded in bending is less severe.

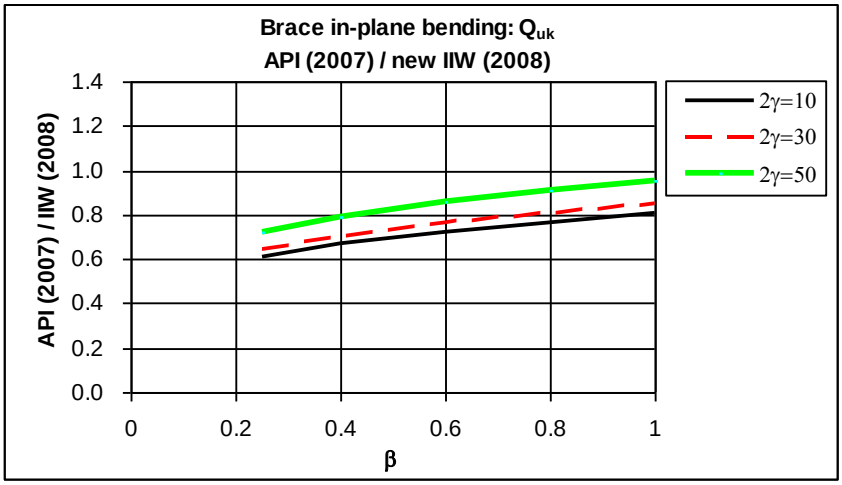

Figure B5 – Comparison of the IIW (2008) equation for brace in-plane bending with that of the API (2007), *excluding* Q_f

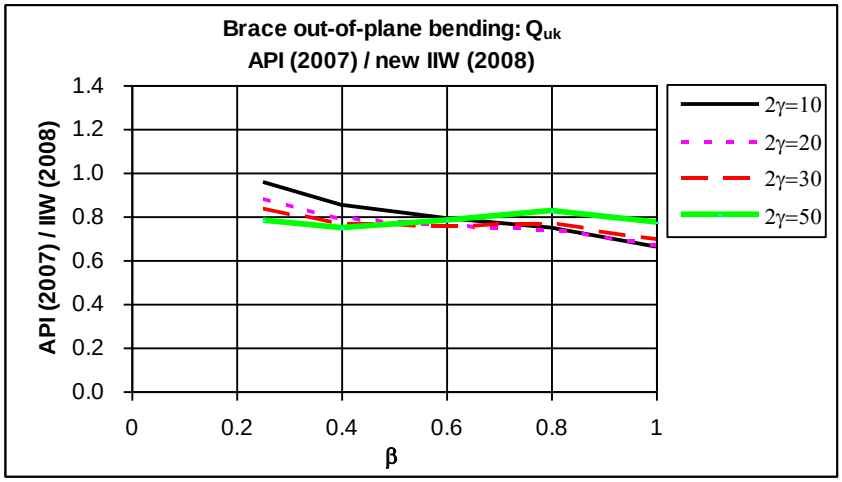

Figure B6 – Comparison of the IIW (2008) equation for brace out-of-plane bending with that of the API (2007)

B7 Joints loaded by brace out-of-plane bending moments

Comparing the IIW (2008) characteristic value (1.1 x M*) with the API (2007) equation for brace out-of-plane bending moments as illustrated in figure B6, shows that the API gives about 20% lower capacities. The new API equation also provides very low capacities compared to the previous API and to the experimental results.

Similar to the brace in-plane bending case (section B6), this is influenced by the symmetrical K joint loading case in offshore jackets. *(Note: $2\gamma = 10$ is outside the validity range of the API)*.

B8 Summary

In figures B7 to B11, the new IIW (2008) equations for axially loaded T, X, K gap joints, brace in-plane bending and brace out-of-plane bending are compared with those of the API (2007). In each of the figures, Q_{uk} or $Q_{uk}Q_f$ for K gap joints is plotted as a function of β.

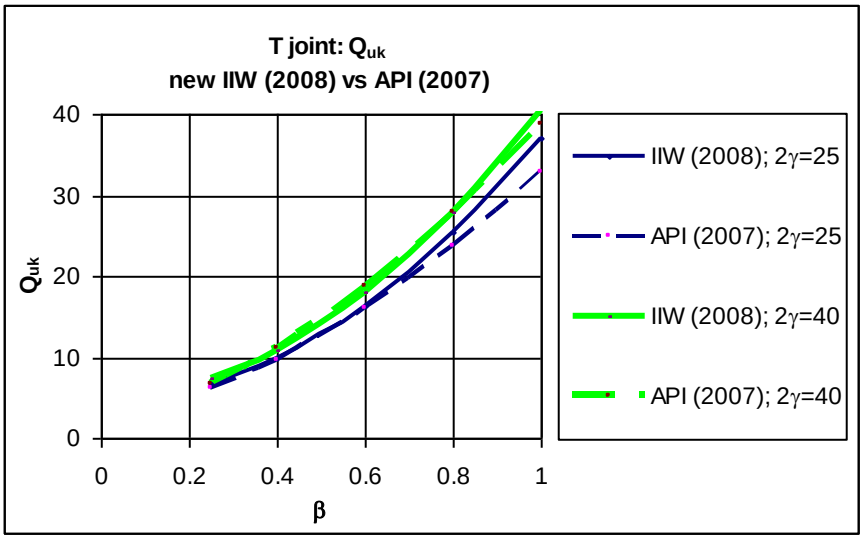

Figure B7 – Comparison of the IIW (2008) Q_u equation for T joints with that of the API (2007)

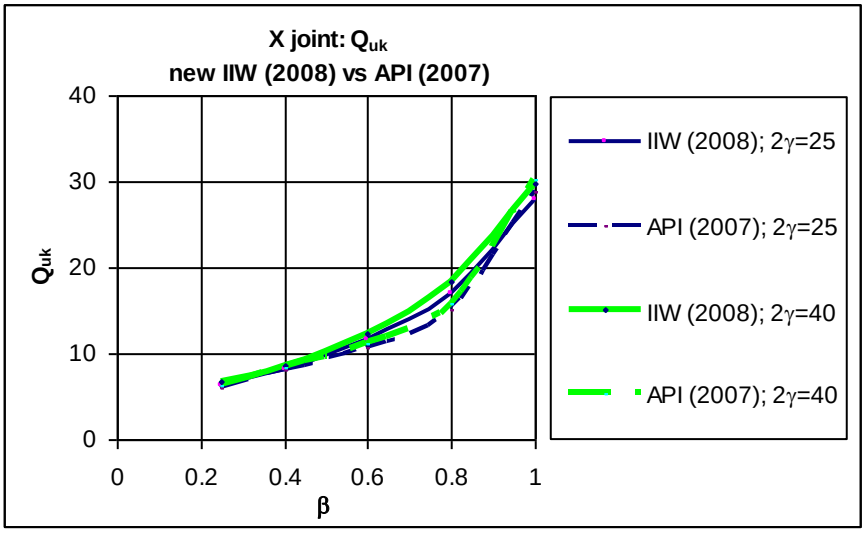

Figure B8 – Comparison of the IIW (2008) Q_u equation for X joints with that of the API (2007)

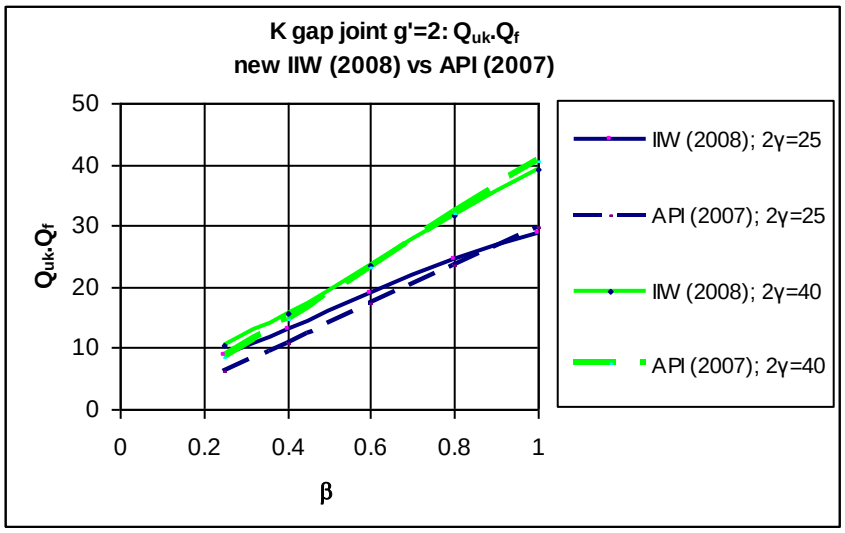

Figure B9(a) – Comparison of the IIW (2008) combined $Q_u Q_f$ equations for K gap joints (g' = 2) with those of the API (2007)

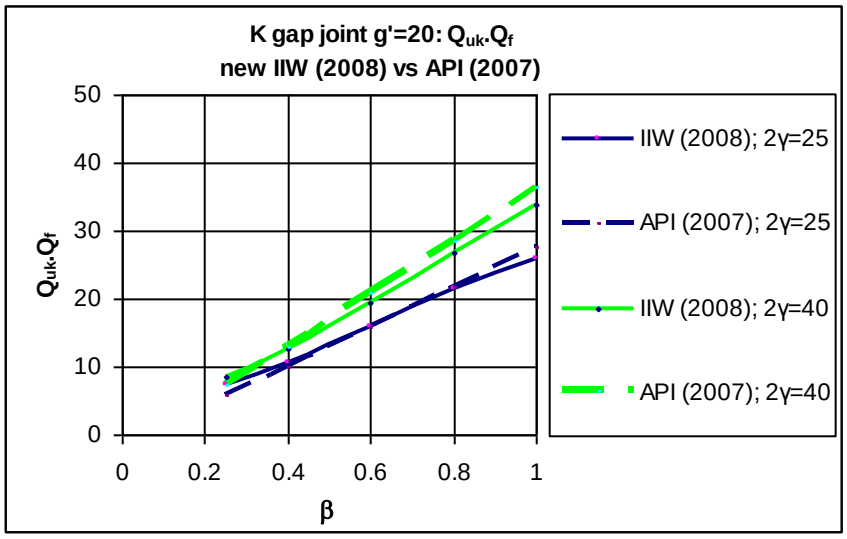

Figure B9(b) – Comparison of the IIW (2008) combined $Q_u Q_f$ equations for K gap joints (g' = 20) with those of the API (2007)

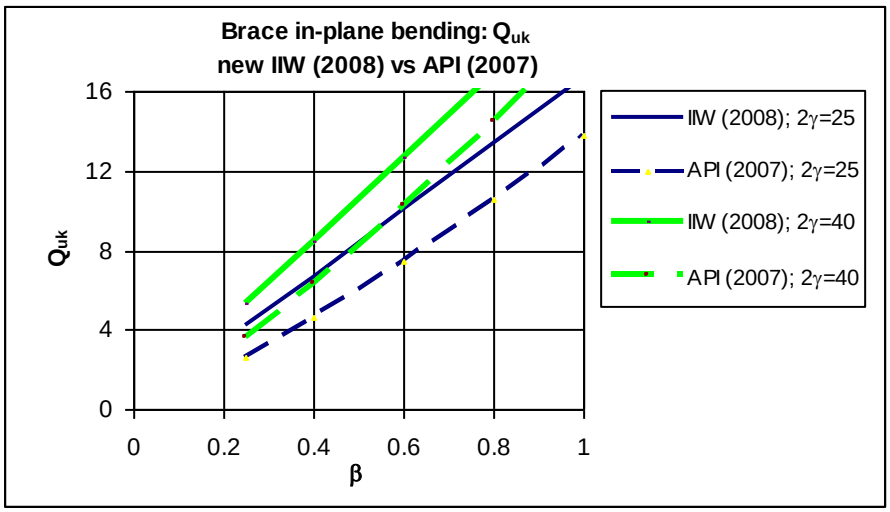

Figure B10 – Comparison of the IIW (2008) equation for brace in-plane bending with that of the API (2007)

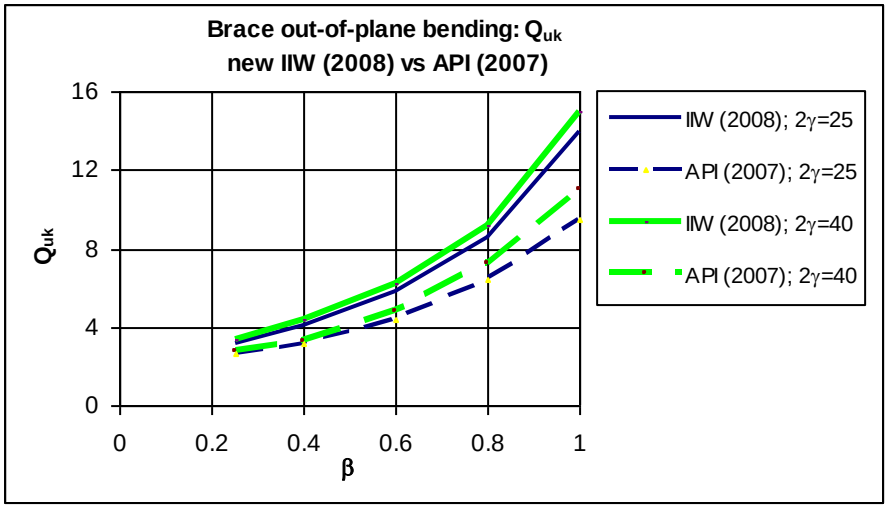

Figure B11 – Comparison of the IIW (2008) equation for brace out-of-plane bending with that of the API (2007)

Comité International pour le Développement et l'Etude de la Construction Tubulaire

International Committee for the Development and Study of Tubular Structures

CIDECT, founded in 1962 as an international association, joins together the research resources of the principal hollow steel section manufacturers to create a major force in the research and application of hollow steel sections world-wide.

The CIDECT website is www.cidect.com

The objectives of CIDECT are:

- to increase the knowledge of hollow steel sections and their potential application by initiating and participating in appropriate research and studies.
- to establish and maintain contacts and exchanges between producers of hollow steel sections and the ever increasing number of architects and engineers using hollow steel sections throughout the world.
- to promote hollow steel section usage wherever this makes good engineering practice and suitable architecture, in general by disseminating information, organising congresses, etc.
- to co-operate with organisations concerned with specifications, practical design recommendations, regulations or standards at national and international levels.

Technical activities

The technical activities of CIDECT have centred on the following research aspects of hollow steel section design:

- Buckling behavlour of empty and concrete filled columns
- Effective buckling lengths of members in trusses
- Fire resistance of concrete filled columns
- Static strength of welded and bolted joints
- Fatigue resistance of welded joints
- Aerodynamic properties
- Bending strength of hollow steel section beams
- Corrosion resistance
- Workshop fabrication, including section bending
- Material properties

The results of CIDECT research form the basis of many national and international design requirements for hollow steel sections.

CIDECT Publications

The current situation relating to CIDECT publications reflects the ever increasing emphasis on the dissemination of research results.

The list of CIDECT Design Guides, in the series “Construction with Hollow Steel Sections”, already published, is given below. These Design Guides are available in English, French, German and Spanish.

1. Design guide for circular hollow section (CHS) joints under predominantly static loading (1st edition 1991, 2nd edition 2008)
2. Structural stability of hollow sections (1992, reprinted 1996)
3. Design guide for rectangular hollow section (RHS) joints under predominantly static loading (1st edition 1992, 2nd edition 2009)
4. Design guide for structural hollow section columns exposed to fire (1995, reprinted 1996)
5. Design guide for concrete filled hollow section columns under static and seismic loading (1995)
6. Design guide for structural hollow sections in mechanical applications (1995)
7. Design guide for fabrication, assembly and erection of hollow section structures (1998)
8. Design guide for circular and rectangular hollow section welded joints under fatigue loading (2000)
9. Design guide for structural hollow section column connections (2004)

In addition, as a result of the ever increasing interest in steel hollow sections in internationally acclaimed structures, two books “Tubular Structures in Architecture” by Prof. Mick Eekhout (1996), sponsored by the European Community, and “Hollow Sections in Structural Applications” by Prof. Jaap Wardenier (2002) have been published.

Copies of the Design Guides, the architectural book and research papers may be obtained through the CIDECT website: http://www.cidect.com

“Hollow Sections in Structural Applications” by Prof. Jaap Wardenier (2002) is available from the publisher:

Bouwen met Staal
Boerhaavelaan 40
2713 HX Zoetermeer, The Netherlands
P.O. Box 190
2700 AD Zoetermeer, The Netherlands

Tel. +31(0)79 353 1277
Fax +31(0)79 353 1278
E-mail info@bouwenmetstaal.nl

CIDECT Organisation (2008)

- President: H-J. Westendorf, Vallourec & Mannesmann Tubes, Germany
- Treasurer/Secretary: R. Murmann, CIDECT, United Kingdom
- A General Assembly of all members meeting once a year and appointing an Executive Committee responsible for administration and execution of established policy.
- A Technical Commission and a Promotion Committee meeting at least once a year and directly responsible for the research work and technical promotion work.

Present members of CIDECT are:

- Atlas Tube, Canada
- Australian Tube Mills, Australia
- Borusan Mannesmann Boru, Turkey
- Corus Tubes, United Kingdom
- Grupo Condesa, Spain
- Industrias Unicon, Venezuela
- Rautaruukki Oyj, Finland
- Sidenor SA, Greece
- Tata Iron & Steel, India
- Vallourec & Mannesmann Tubes, Germany
- Voest-Alpine Krems, Austria

Acknowledgements for photographs:

The authors express their appreciation to the following additional persons and firms for making available some photographs used in this Design Guide:

Bouwdienst, Rijkswaterstaat, The Netherlands
Prof. Y.S. Choo, Singapore
CORUS Tubes, UK
Mr. D. Dutta, Germany
Mr. Félix Escrig, Spain
Mr. Juan Carlos Gómez de Cózar, Spain
Instituto para la Construcción Tubular (ICT), Spain
Prof. Y. Makino, Japan
Mr. José Sánchez, Spain
V & M, Germany

Disclaimer

Care has been taken to ensure that all data and information herein is factual and that numerical values are accurate. To the best of our knowledge, all information in this book is accurate at the time of publication.

CIDECT, its members and the authors assume no responsibility for errors or misinterpretations of information contained in this Design Guide or in its use.

This Design Guide is a revision and update of the 1st Design Guide in a series that CIDECT has published under the general series heading “Construction with Hollow Steel Sections”. The previously published Design Guides in the series, which are all available in English, French, German and Spanish, are:

1. Design guide for circular hollow section (CHS) joints under predominantly static loading (1st edition 1991, 2nd edition 2008)
2. Structural stability of hollow sections (1992, reprinted 1996)
3. Design guide for rectangular hollow section (RHS) joints under predominantly static loading (1st edition 1992, 2nd edition 2009)
4. Design guide for structural hollow section columns exposed to fire (1995, reprinted 1996)
5. Design guide for concrete filled hollow section columns under static and seismic loading (1995)
6. Design guide for structural hollow sections in mechanical applications (1995)
7. Design guide for fabrication, assembly and erection of hollow section structures (1998)
8. Design guide for circular and rectangular hollow section welded joints under fatigue loading (2000)
9. Design guide for structural hollow section column connections (2004)

ISBN 978-3-938817-03-2

This Design Guide is a revision and update of the 1st Design Guide in a series that CIDECT has published under the general series heading “Construction with Hollow Steel Sections”. The previously published Design Guides in the series, which are all available in English, French, German and Spanish, are:

1. Design guide for circular hollow section (CHS) joints under predominantly static loading (1st edition 1991, 2nd edition 2008)
2. Structural stability of hollow sections (1992, reprinted 1996)
3. Design guide for rectangular hollow section (RHS) joints under predominantly static loading (1st edition 1992, 2nd edition 2009)
4. Design guide for structural hollow section columns exposed to fire (1995, reprinted 1996)
5. Design guide for concrete filled hollow section columns under static and seismic loading (1995)
6. Design guide for structural hollow sections in mechanical applications (1995)
7. Design guide for fabrication, assembly and erection of hollow section structures (1998)
8. Design guide for circular and rectangular hollow section welded joints under fatigue loading (2000)
9. Design guide for structural hollow section column connections (2004)

ISBN 978-3-938817-03-2